SANDIA REPORT
SAND2020-10828
Printed October 2020

Sandia National Laboratories

Final Report on Hydrogen Plant Hazards and Risk Analysis Supporting Hydrogen Plant Siting near Nuclear Power Plants

Austin Glover, Austin Baird, Dusty Brooks

Prepared by
Sandia National Laboratories
Albuquerque, New Mexico
87185 and Livermore,
California 94550

Issued by Sandia National Laboratories, operated for the United States Department of Energy by National Technology & Engineering Solutions of Sandia, LLC.

Available to DOE and DOE contractors from
U.S. Department of Energy
Office of Scientific and Technical Information
P.O. Box 62
Oak Ridge, TN 37831

Telephone: (865) 576-8401
Facsimile: (865) 576-5728
E-Mail: reports@osti.gov
Online ordering: http://www.osti.gov/scitech

Available to the public from
U.S. Department of Commerce
National Technical Information Service
5301 Shawnee Rd
Alexandria, VA 22312

Telephone: (800) 553-6847
Facsimile: (703) 605-6900
E-Mail: orders@ntis.gov
Online order: https://classic.ntis.gov/help/order-methods/

ABSTRACT

Nuclear power plants (NPPs) are considering flexible plant operations to take advantage of excess thermal and electrical energy. One option for NPPs is to pursue hydrogen production through high temperature electrolysis as an alternate revenue stream to remain economically viable. The intent of this study is to investigate the risk of a high temperature steam electrolysis hydrogen production facility (HTEF) in close proximity to an NPP. This analysis evaluates a postulated HTEF located 1 km from an NPP, including the likelihood of an accident and the associated consequence to critical NPP targets. This analysis shows that although the likelihood of a leak in an HTEF is not negligible, the consequence to critical NPP targets is not expected to lead to a failure at a distance of 1 km. Furthermore, the minimum separation distance of the HTEF is calculated based on the target fragility criteria of 1 psi defined in Regulatory Guide 1.91.

ACKNOWLEDGEMENTS

The authors would like to thank Brian Ehrhart for reviewing this report and providing useful feedback and analysis.

CONTENTS

LIST OF FIGURES

LIST OF TABLES

This page left blank

ACRONYMS AND DEFINITIONS

Abbreviation	Definition
HTEF	high temperature steam electrolysis hydrogen production facility
HTSE	high temperature steam electrolysis
IPEE	individual plant examination of external events
IPF	intermediate processing facility
LNG	liquid natural gas
LOOP	loss of offsite power
LWR	light water reactor
MCA	maximum credible accident
MLE	maximum likelihood estimate
NPP	nuclear power plant
P&ID	pipe and instrumentation diagram
PEM	proton exchange membrane
PWR	pressurized water reactor
SOEC	solid oxide electrolyzer cell

1. INTRODUCTION

Nuclear power plants (NPPs) may use flexible plant operations and generation to take advantage of excess thermal and electrical energy. However, NPPs must show that the operation of such a system is safe and does not pose a significant threat to the high consequence NPP facilities and structures. Hydrogen production through high temperature electrolysis is a feasible option for NPPs because the excess thermal and electrical energy produced through normal operation can be used to produce a carbon-free, storable energy source. When compared to the other methods of hydrogen production (such as steam methane reforming and low temperature electrolysis), high temperature electrolysis offers a more efficient and economically stable option. Steam methane reforming uses natural gas in the hydrogen production process, which introduces economic instability because of its reliance on natural gas, which experiences dramatic price fluctuations. Renewable energy such as wind turbines or solar photovoltaics can be used to create hydrogen through low temperature electrolysis with electrical energy only [1]. However, this method is less efficient when compared to high temperature electrolysis and is less economically attractive because thermal energy is less expensive than electrical energy [2]. NPPs can pursue hydrogen production through high temperature electrolysis as an alternate revenue stream to remain an economically viable power production option.

The intent of this study is to investigate the risk of a high temperature steam electrolysis hydrogen production facility (HTEF) in close proximity to an NPP, from which thermal and electrical energy are supplied. In this analysis, a theoretical HTEF located 1 km from an NPP will be analyzed in terms of risk to normal plant operations. A facility component list was developed for a theoretical HTEF. Next, the associated leak frequencies for the individual components in the HTEF was evaluated to develop an overall facility leak frequency. The NPP site was evaluated for critical targets and the fragility of each was documented. Finally, the consequence of a hydrogen jet release in the HTEF was calculated and compared to the target fragility. Note that the consequence was evaluated at 1 km from the NPP and a deterministic separation distance calculation was also performed.

1.1. High-Temperature Steam Electrolysis Process

Water electrolysis is the process in which water is split into hydrogen and oxygen molecules through an electrochemical process. A typical system for water electrolysis includes an anode, cathode, electrolyte, and a power supply. The electrolyte can be constructed several ways: aqueous solution containing ions, a proton exchange membrane (PEM), or an oxygen ion exchange ceramic membrane. The system uses direct current, with the negative side on the cathode source, where hydrogen is produced. The anode side is connected to the positive side of the DC source [3]. High temperature steam electrolysis (HTSE) utilizes both heat and electricity to split water into hydrogen and oxygen in solid oxide electrolyzer cells (SOECs), which is essentially a solid oxide fuel cell operating in reverse [2]. This process splits water into oxygen and hydrogen by using steam at temperatures of ~600-850°C as well as electrical input. Note that although the ceramics used in the HTEF design require high temperatures to become ionically/electrically active, expensive catalysts (like platinum) that are used in PEM fuel cells/ electrolyzers can be avoided.

1.2. Overview of HTEF Design

General designs for an HTEF powered via steam production directly from a nuclear power plant and electrical production from the power plants turbines are given in the reports from INL by Vedros and Otani [4] as well as Frick et al. [2]. Figure 1-1 shows the high temperature electrolysis main process area flow diagram.

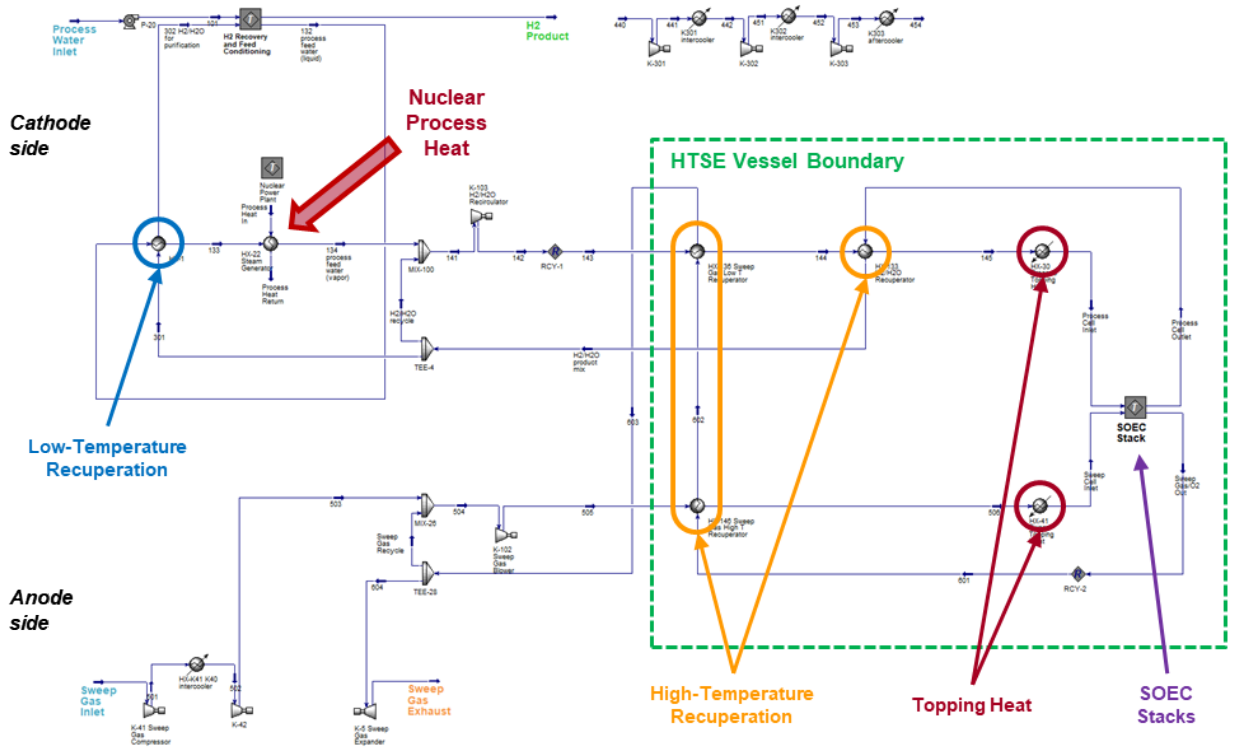

Figure 1-1: High Temperature Electrolysis Main Process Area Flow Diagram [2]

The two main systems of the HTEF design are summarized below [4]. Also, a general description of these systems are provided based on a review of the Pipe and Instrumentation Diagrams (P&IDs):

1. Heat Extraction System: Heat is extracted from the NPP and delivered to a tertiary heat exchanger to generate steam that is then used for the electrolysis process.

2. HTEF: The HTEF is located 1 km from the walls of the pressurized water reactor (PWR) reactor building and the HTSE units are designed to produce a total of 300 US tons (272,156 kg) of hydrogen daily. Piping leads to a hydrogen storage facility 5 km away that contains 30 spherical tanks holding a total of 20 US tons (18,144 kg) of hydrogen [4].

Using a SOEC requires the stack inlet to be heated to 700-800°C. A light water reactor (LWR) generates steam at temperatures around 300°C compared to the 700-800°C required [2]. Using electrical input in

addition to the thermal input can make up for this difference in temperature. The NPP is used in this analysis for both the electrical and thermal input for the HTSE process. Around 5% of the NPP coolant from secondary cooling loop exiting from the PWR is sent to the intermediate processing facility (IPF) 1 km away, through a tertiary loop which generates steam at 47 bar (680 psia) through 600 mm diameter schedule 30 pipe. The steam thermal input to the HTEF enters at 5 bar (75 psia) to be used in the HTSE process. Coolant exits the IPF and returns to the NPP steam generator at 230°C through 250 mm diameter schedule 20 pipe.

There are 46 25-MWe modular units in which the HTSE process takes place. Each HTSE block requires tee fittings to divert steam as well as return condensate to the main supply and return lines. Each HTSE block also includes flow control valves that are also used for isolation. This gives a total of 46 tees and ball valves. Included in the design are 4 elbows and 4 expansion joints as well as 4 reducers. A pump circulates water through the IPF heat exchanger, the HTSE steam generators as well as the steam delivery pipes and condensate return. After treatment, feed water is used in the SOEC stack operation. Once the feed water stream is preheated and vaporized, it is combined with the recycle stream of the hydrogen/water process gas exiting the SOEC stack. The concentrations are 50 mol% hydrogen and 50 mol% steam exiting the stack. This is fed into the SOEC module inlet stream. This steam/hydrogen feed stream is heated to the SOEC required stack inlet temperature using high temperature recuperators and electrical topping heaters. The HTSE heat recuperation is as follows [2]:

1. The hydrogen/steam product gas mixture exiting the cathode is used to heat the hydrogen/steam reactant gas mixture entering the cathode in the heat exchanger (HX-133) upstream of the electrical resistance topping heaters

2. The oxygen-rich gas mixture exiting the anode is used to heat the sweep gas (air) entering the anode in the heat exchanger (HX-146) upstream of the electrical resistance topping heaters

3. The oxygen-rich gas mixture exiting the anode is used to heat the hydrogen/steam gas mixture entering the cathode in the heat exchanger (HX-136) upstream of the H2/H2O recuperator

This process achieves SOEC stack inlet conditions of 735°C; 5.2 bar; 50 mol% steam, 50 mol% hydrogen as the mixture enters the cathode side. Oxygen ions are conducted through the electrolyte-anode interface and the steam and hydrogen mixture exit the SOEC stacks with a composition of 80 mol% H_2 and 20 mol% H_2O. This hydrogen/steam mixture is then split into two streams. One stream is combined with steam exiting the nuclear heat-driven generator before flowing into the HTSE module denoted as the H2/H2O Recycle Loop. The other stream is sent to a hydrogen product recovery sub-process where the gas is purified prior to storage and transportation denoted as H2/H2O for Purification. The purification is done by condensing the water from the hydrogen/steam mixture to create a high purity hydrogen product.

2. HTEF COMPONENT LIST

To develop the bottom-up leak frequencies for the HTEF, the components in the system needed to be documented. This list was used in conjunction with the component specific leak frequencies developed in Section 4 to develop system level leak frequencies. The analysis herein focuses on the HTEF and not the heat extraction system connected to the plant. Note that since the detailed design of the HTEF was not available, engineering judgement was used to develop assumptions on the pipe lengths and sizes. The component list was developed with the P&IDs given in Appendix J of [2] as well as the components cost analysis provided in Appendix I of [2] and the heat exchanger specification sheets provided in Appendix N of [2]. Since the inlet and outlet pipe sizes are specified in Appendix N of [2] for Heat Exchanger 1, Heat Exchanger 3, and Heat Exchanger 17, they were used as the starting points to map out the piping system sizes. Assumptions were also made regarding the other heat exchangers, the separators and the tee fittings based on the three prescribed components. Many of the pipe runs contain a control valve inline to help increase or decrease the flow and pressure through certain components based on the plants operation, number of SOEC stacks in use at the time, and to further control the system. Since details on these are not provided in the P&ID [2], the locations of these control valves were assumed.

Pipe lengths in the HTEF were not specified in the P&IDs [4] [2]. Since the HTEF design lacked this detail, the total pipe lengths were estimated through alternate methods. A liquid natural gas processing plant (Jordan Cove Energy Project) was used as a surrogate to define the total length of pipe in the plant [5]. Since most of the pipe diameters have a much larger range than the assumed pipe sizes for this HTEF, only select systems from the liquid natural gas processing plant were used to estimate the pipe length of the HTEF. The report gives two systems that are used: liquid natural gas (LNG) Cold Box with a 254 mm diameter pipe and 46 m of piping as well as the Refrigerant Pumps Discharge which uses 356 mm diameter pipe with a total of 114 m of piping, which result in ~160 m of process piping. This total length of piping was assumed to evenly distributed across the entire HTEF system for simplicity. Since there are 33 distinct pipes in the HTEF, it was assumed that each pipe is 4.8 m in length.

Additional assumptions are needed to define the system pressures. The steam temperatures are ~700-800°C for the HTSE process. The inlet side of the SOEC stack requires a hydrogen/steam vapor phase mixture entering at 735°C and 5.2 bar [2]. This pressure was assumed to be maintained until reaching the separator vessel. Table 2-1 gives details on the temperature and pressure of the mixture.

Table 2-1. Separator Vessel Operating Conditions (as defined in [2])

Separator Vessel	Temperature (°C)	Pressure (bar)	Vapor Flow Rate (m^3/hr)
KO-1	75.0	4.8	1205
KO-1	75.0	10.1	532.5
KO-3	25.0	22.3	393.3

Based on the description from Frick et al. [2], there are 46 different systems and it was assumed they are all fed from a common header and feed into a common header. The system is defined between those two sets of common headers. The components are defined from the P&ID provided in Appendix B in Frick et al. [2]. The complete HTEF component list, along with the general description, sizes, assumptions and references is in Appendix A of this document. A summary of the components and their respective quantity is shown in Table 2-2. As seen, some of the components were grouped together into bins to conform to the leak frequency bins (see Section 4).

Table 2-2. HTEF Component Quantity Summary

Component	Quantity
Compressor	92
Cylinder (Vessel, intercooler, Separator, Heat Exchanger)	874
Joint (Tee, Elbow, Reducer, Expander)	150
Pipe	7,360 m
Pump/Blower	276
Valve	966

3. HTEF HAZOP

A hazard and operability study risk analysis and potential operational disturbances that lead a system to deviate from expected behaviors. In this study, a HAZOP was used to identify what sort of leak scenarios might be significant in an HTEF, so that consequences could be evaluated for those specific scenarios. Generally, a HAZOP is a qualitative, inductive process which examines each system component and identifies scenarios, conditions, or failure modes that could lead to a hazardous condition (i.e., hydrogen release). HAZOPs are useful in refining large sets of possible accident scenarios when evaluation resources are limited. Through a qualitative risk assessment, the most important scenarios can be identified and evaluated in a quantitative manner. However, because the evaluation resources utilized herein are not limited, the HAZOP performed in this evaluation is focused on identifying the components that may fail along with the variables relevant to the consequent analysis. This is appropriate for this analysis because each of the different combinations of relevant variables will be quantitatively evaluated in terms of overpressure consequence. This evaluation methodology will feed into the deterministic evaluation of separation distance (see Section 6.5).

3.1. Failure in an HTEF

In this study, failure was defined as an unexpected or uncontrolled release of gaseous hydrogen. Although other failure events may occur, such as the delamination of electrodes from the bond layer in the cell [6], these types of failures effect the efficiency of the system rather than the overall safety of operation. Therefore, these types of failure are not evaluated herein.

3.2. Guide Words

To provide structure and analytical completeness to this HAZOP, guide words were used to define the leakage event that may occur for a given HTEF component. Each guide word was used in the context of the potential hazard or operational disturbance to determine if the affected process deviates from its intended design. For example, the component "control valve" could be combined with the "no or not" guide word to describe a spontaneous leak (i.e., the valve did not perform the intended function of containing hydrogen). The guide words and their associated meanings are shown in Table 3-1.

Table 3-1: HAZOP Guide Words

Guide Word	Meaning
No or not	Complete negation of design intentions
More	Quantitative increase
Less	Quantitative decrease
As well as	Qualitative increase (some additional activity)
Part of	Qualitative decrease (some intentions achieved, some are not)
Reverse	Logical opposite of intention
Other than	Complete substitution

3.3. HTEF Components

The list of components in the HTEF was evaluated in Section 2 and shown in detail in Appendix A. Table 3-2 shows a list of different components that can fail in the HTEF from different sections of the system. The list is based on information from Frick et al. [2] (see Appendix A).

Table 3-2: Components in Each System Section

System Section	Component
Mix-100 thru HX-K01	Check Valves
	Control Valves
	Heat Exchangers
	Pipes
	Pumps
	SOEC Stacks
	Tees
HX-K01 thru HX-K02	Compressors
	Control Valves
	Heat Exchangers
	Pipes
	Pumps
	Separators
HX-K02 thru HX-K03	Compressors
	Control Valves
	Heat Exchangers
	Pipes
	Pumps
	Separators
HX-K03 thru K-301	Condensers
	Control Valves
	Heat Exchangers
	Pipes
	Separators
K-301 thru System Output	Check Valves
	Control Valves
	Heat Exchangers
	Pipes
	Pressure Relief Valves
	Pumps

3.4. HTEF Operational State

The operational states of the facility are evaluated in the HAZOP as part of the scenario identification process. The operation of an HTEF is primarily automated. Control systems in the system monitor and maintain the temperatures, pressures, and flow rates of different components in the system at the desired levels. The components in the HTEF operate at different temperatures, flow rates, and pressures, which need to be monitored and controlled to maintain the proper operating conditions. The control system is meant to either automatically take action if abnormal operating conditions are detected or alert operators through audible and visual alarms [7]. Manual actions are necessary for start-up activities, production adjustment based on the power supplied from the NPP, maintenance activities, and response to alarms that signal abnormal operating conditions. However, these activities are not specific to a single component, since all of the equipment may be affected through these activities. Also, since the risk is not being qualitatively evaluated in this HAZOP to narrow down the scenarios to quantitatively analyze, the identification of the different operational states is not critical. Therefore, the HTEF is treated as having a single general operational state for the purpose of this analysis.

3.5. Accident Impact Scenarios

The process of analyzing each component within the general operational state, and the HAZOP guide words lead to unique scenarios. Generally, since the components are mostly operating in a steady state, a spontaneous leak would be the main cause of concern in terms of hydrogen release. Also, manual activities such as component maintenance can lead to a release scenario. However, in terms of this analysis, the cause of the hydrogen release scenario is less important than the variations of system conditions that contribute to the consequence of a hydrogen release. Therefore, the different combinations of system variables in each system section were identified to determine the scenarios to be evaluated in this analysis.

Table 3-3 gives details on the hydrogen/steam mixture and the properties at various points along the HTSE process. Each is based on information from Frick et al. [2] (See Appendix A). Table 3-3 also gives the different pipe sizes for each pressure and temperature combination. Each of these scenarios represent a unique evaluation case that will determine the worst-case full rupture break in each system.

Table 3-3. System Scenario Breakdown (as defined in [2])

Scenario	System Section	Temperature (°C)	Pressure (MPa)	Line Sizes (mm)
1	Mix-100 thru HX-KO1	735	0.52	203.2
2				254.0
3				300.0
4	HX-KO1 thru HX-KO2	75	0.48	152.4
5				203.2
6				254.0
7				300.0
8	HX-KO2 thru HX-KO3	75	1.01	88.9
9				101.6
10				200.0
11				254.0
12	HX-KO3 thru K-301	25	2.23	88.9
13				200.0
14				254.0
15	K-301 thru System Output	50	7.00	200.0

4. LEAK FREQUENCY

To quantify the risk of an accident in an HTEF, it is necessary to establish the types of accidents that can occur. To do this, component leakage frequencies representative of hydrogen components must be documented as a function of the normalized leak size. Subsequently, the system characteristics (e.g., system pressure) will be used to calculate the consequence of the accident.

4.1. Bayesian Statistical Method

Industry data on component leakage events can be used to establish the leak frequencies. Unfortunately, there is little available data on hydrogen-specific component leakage events. Although major events are recorded in databases such as the DOE Hydrogen Incident Reporting database for lessons learned [8], the failure to record all events (e.g., small leakage events) and the number of operating hours represented in the database makes utilization of the data for analysis difficult. Previous risk evaluations have utilized published data on leakage events from non-hydrogen sources that are representative of hydrogen components [9].

Rather than selecting one value from generic sources, data from the different sources were collected and combined using a Bayesian statistical method. This approach has several major advantages for cases in which large amounts of data are not available. First, it allows for the generation of leakage rates for different amounts of leakage. Second, it generates uncertainty distributions for the leakage rates that can be propagated through the risk assessment models to establish the uncertainty in the risk results. Finally, it provides a means for incorporating limited hydrogen-specific leakage data with leakage frequencies from other sources to establish estimates for leakage rates for hydrogen components. Bayesian analysis utilizes Bayes' theorem, shown below [9]:

$$P(\theta = \theta_i \mid \epsilon) = \frac{P(\epsilon|\theta = \theta_i)P(\theta = \theta_i)}{P(\epsilon)} = \frac{P(\epsilon \mid \theta = \theta_i)P(\theta = \theta_i)}{\sum_i P(\epsilon \mid \theta = \theta_i)P(\theta = \theta_i)}$$

Where:

- $P(\epsilon|\theta = \theta_i)$ – The conditional probability that the value ϵ will be observed for the random variable X in a given trial, assuming the value θ_i for the parameter θ.
- $P(\theta = \theta_i)$ – The prior distribution – prior to observing the value ϵ for X; can also be stated as "prior to obtaining the evidence" – probability that the value of θ is equal to θ_i.
- $P(\epsilon)$ – The total probability that the value ϵ will be observed for the random variable X, summed over all possible values θ_i for the parameter θ.
- $P(\theta = \theta_i \mid \epsilon)$ - The posterior distribution – after observation of the value ϵ for X – probability that the value of θ is equal to θ_i

Another benefit of using the Bayesian technique is the ability to consistently modify a given analysis any time new evidence is gathered through Bayesian updating. Every time new data is obtained, it may be used to update the existing distribution without changing any of the previous data or the system model. The new information is simply added as extra data points and the distributions are updated through Bayes' theorem. Through this process, what was previously defined as the posterior now becomes the prior and the updated distribution becomes the posterior. The generated component leakage frequencies are used to generate estimates for the total leakage frequency for an HTEF [9].

4.2. Data Sources

Because data on hydrogen systems is extremely limited, sources from commercial operations may be used as a baseline for the Bayesian statistical analysis. Component leakage frequencies have been historically gathered by the chemical processing, compressed gas, nuclear power plant, and offshore petroleum industries; however, there has been little consistency across the disciplines and studies performed. Variances in leakage definitions, component classification, and data reliability make it difficult to directly apply the information to hydrogen specific processes. Unique physical challenges, such as hydrogen embrittlement, provide additional uncertainty when applying statistically determined leakage frequencies to risk assessments. Nevertheless, the identification of the component failure rates and severity of ensuing leaks by performing an extensive review of industrial sources is an appropriate initial phase to the Bayesian process [9].

Sources used in the leakage event data analysis were obtained from a narrow range of available data and studies. They varied in nomenclature, component specifics, and data determination. It was important to consider the origin of the data and determine whether the information was derived from actual component failures or based on expert judgment. The following sources were used to develop the component leakage frequencies [9]:

- CPR 18E ed. 1, "Guidelines for Quantitative Risk Assessment: The Purple Book," Committee for the Prevention of Disasters, The Hague, The Netherlands, 1999.
- Center for Chemical Process Safety of the American Institute of Chemical Engineers, "Guidelines for Process Equipment Reliability Data with Data Tables," 1989.
- S.A. Eide, S.T. Khericha, M.B. Calley, D.A. Johnson, M.L. Marteeny, "Component External Leakage and Rupture Frequency Estimates," EGG-SSRE- 9639, Nov 1991.
- NUREG/CR-6928, "Industry-Average Performance for Components and Initiating Events at U.S. Commercial Nuclear Power Plants," February 2007.
- NUREG-75/014, "Reactor Safety Study: An Assessment of Accident Risks in U.S. Commercial Nuclear Power Plants," WASH-1400, Oct 1975.
- Rijnmond, O.L.; "Risk Analysis of Six Potentially Hazardous Industrial Objects in the Rijnmond Area, A Pilot Study," COVO, 1982.
- Savannah River Site, "Generic Data Base Development," WSRC-TR-93-263, June 1993.
- Canadian Hydrogen Safety Program, "Quantitative Risk Comparison of Hydrogen and CNG Refueling Options," Presentation, IEA Task 19 Meeting, 2006.
- A.J.C.M. Matthijsen, E.S. Kooi, "Safety Distances for Hydrogen Filling Stations," Journal of Loss Prevention in the Process Industries 19, pp. 719 - 723, 2006.
- R. E. Melchers, W. R Feutrill, "Risk Assessment of LPG Automotive Refueling Facilities," Reliability Engineering and System Safety, 74, 2001.
- Rosyid, O.A., "System-Analytic Safety Evaluation of the Hydrogen Cycle for Energetic Utilization," Dissertation, 2006.

These multiple sources provided the raw generic data for the various components used in the hydrogen fueling process. The data is provided in Appendix B. A large variation in the leakage frequencies may be observed from this collection of data. Although many data sources provide leak rates as a function of leak size, very few provide leak rates as a function of pressure. Thus, the analysis performed in this study does not differentiate leak rates for systems operating at different pressures [9].

Limited hydrogen-specific leakage data was obtained through the efforts of members of NFPA 2 TG6 from the Compressed Gas Association. Due to the proprietary nature of the data, it is not presented in this report. The results of traditional statistical analysis of that data are shown in Table 4-1 from LaChance et al. [9]. For many components the fact that there are no reported failures prohibits estimating the maximum likelihood estimate (MLE) or the lower confidence bound (5th percentile). However, an upper confidence bound (95th percentile) can still be estimated but is not useful for evaluating realistic risk values. As shown in Table 4-1, the available hydrogen data is not sufficient for the application of traditional statistical analysis, thus the Bayesian model was used to combine this limited data with generic estimates of component leakage rates [9].

Table 4-1. Traditional Statistical Analysis of Hydrogen Data [9]

Component	Statistic	Break size				
		Very Small	Minor	Medium	Major	Rupture
Compressor	MLE	8.70E-02	1.90E-02	1.90E-02	0.00E+00	0.00E+00
	5%	4.50E-02	3.40E-03	3.40E-03	0.00E+00	0.00E+00
	95%	1.50E-01	6.10E-02	6.10E-02	2.90E-02	2.90E-02
Cylinder	MLE	0.00E+00	0.00E+00	0.00E+00	0.00E+00	0.00E+00
	5%	0.00E+00	0.00E+00	0.00E+00	0.00E+00	0.00E+00
	95%	1.80E-06	1.80E-06	1.80E-06	1.80E-06	1.80E-06
Hoses	MLE	5.90E-04	0.00E+00	0.00E+00	0.00E+00	0.00E+00
	5%	2.60E-04	0.00E+00	0.00E+00	0.00E+00	0.00E+00
	95%	1.20E-03	3.00E-04	3.00E-04	3.00E-04	3.00E-04
Joints	MLE	3.50E-05	0.00E+00	4.10E-06	2.10E-06	2.10E-06
	5%	2.30E-05	0.00E+00	7.30E-07	1.10E-07	1.10E-07
	95%	5.10E-05	6.10E-06	1.30E-05	9.70E-06	9.70E-06
Pipes	MLE	0.00E+00	0.00E+00	0.00E+00	0.00E+00	0.00E+00
	5%	0.00E+00	0.00E+00	0.00E+00	0.00E+00	0.00E+00
	95%	1.90E-05	1.90E-05	1.90E-05	1.90E-05	1.90E-05
Valves	MLE	2.90E-03	5.80E-04	0.00E+00	0.00E+00	0.00E+00
	5%	1.80E-03	1.60E-04	0.00E+00	0.00E+00	0.00E+00
	95%	4.40E-03	1.50E-03	5.80E-04	5.80E-04	5.80E-04

4.3. Hydrogen Leak Frequency Model

A Bayesian model was developed to predict the probability of a leak in various components used in an HTEF. The model was selected based on analysis of actual leakage data from the offshore oil industry. The offshore industry data indicates that the leakage frequencies for components on offshore oil and gas facilities are a power function of the leak diameter with lower frequencies occurring for larger diameter leaks [10]. Additionally, leak frequencies provided in many sources indicated a similar relationship. Specifically, the method suggested by Cox, Lees, and Ang [11] for analyzing liquid natural gas hazards uses leak frequencies that are a power function of the leak area. Based on these sources, the component leak frequencies were modeled as a power function of the leak area. Figure 4-1 shows the power function of leak diameter and probability from the offshore industry data [9].

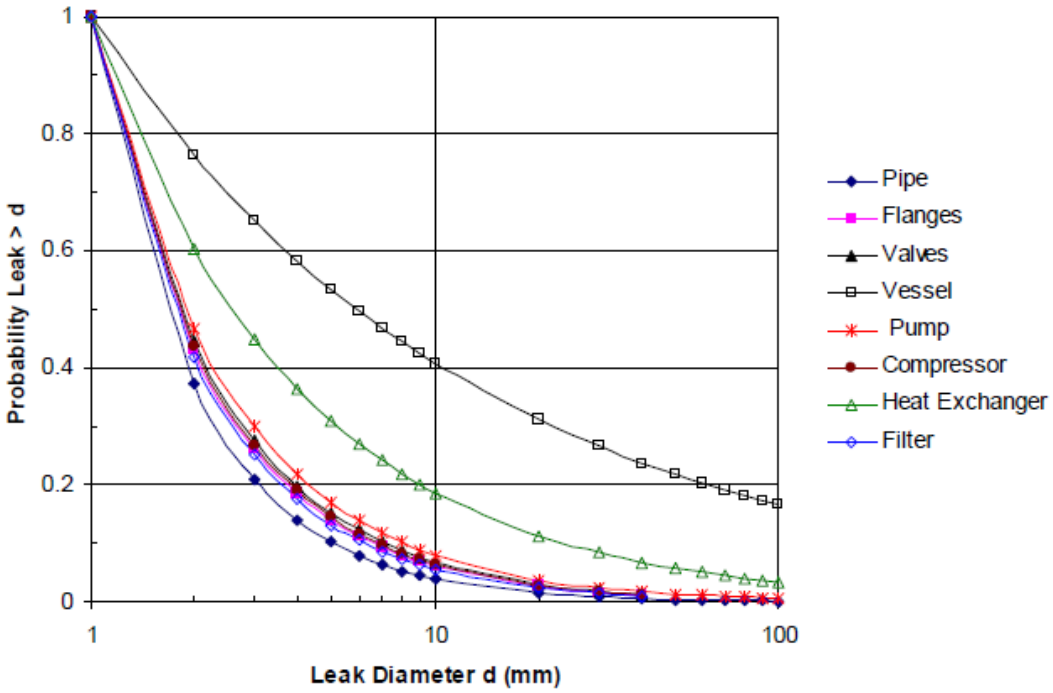

Figure 4-1. Correlation of Offshore Oil and Gas Leakage Data

The model assumes that the mean leak frequency of any component is linearly related to the logarithm of the fractional flow area of the leak. The fractional flow area is the ratio of the leak area to the total flow area of the pipe. The coefficients of the linear relationship – (α_1 and α_2) – are assumed to be normally distributed. The initial from of the model is described below [9]:

$$\log\left(\mu_{LF,j}\right) = \alpha_2 \log_e\left(FLA_j\right) + \alpha_1$$
$$\alpha_1 \sim N(\alpha_{11}, \alpha_{12})$$
$$\alpha_2 \sim N(\alpha_{21}, \alpha_{22})$$
$$\ln\left(LF_j\right) \sim N(\mu_{LF,j}, \tau_j)$$
$$\tau_j \sim Gamma\left(s_j, r_j\right)$$

The variables in the model have the following descriptions:

- μ_{LF} – Mean of the recorded leak frequency

- FLA – Fractional leak area. This is the ratio of the leak area to the total cross-sectional flow area of the pipe.
- LF – The recorded leak frequency
- α_2 – Parameter relating mean leak frequency to FLA.
- α_1 – Scaling parameter for the exponential function relating μ_{LF} and FLA.
- τ_j – Precision of the distribution describing the recorded leak frequency. The precision of a normal random variable is defined as the multiplicative inverse of the variance.
- j – Subscript used to enumerate the different leak sizes.
- α_{11}, α_{12}, α_{21}, α_{22}, s_j, and r_j are the values determined using Bayesian updating to define the model. They are assigned initial (prior) values before the update, and their values after the update define the posteriors.
    - α_{11} and α_{21} are the means of the α_1 and α_2 distributions respectively, assigned an initial value of 0. α_{12} and α_{22} are the precisions of the α_1 and α_2 distributions respectively, assigned an initial value of 10^{-3}.
    - s_j and r_j are the scale and rate, respectively, of the τ_j distribution. The initial value assumed for both s_j and r_j was 1.

For this analysis, the leaks were divided into the following five sizes based on the data categories defined in generic data sources:

- Very Small – Leak area is 0.01% of the total flow area
- Minor – Leak area is 0.1% of the total flow area
- Medium – Leak area is 1% of the total flow area
- Major – Leak area is 10% of the total flow area
- Rupture – Leak area is 100% of the total flow area

The first phase of the Bayesian process uses the data for generic leak frequencies to update the model above. If the hydrogen data was also in the form of annual frequency for leak sizes, the model could be updated a second time with hydrogen data as is. However, the hydrogen data is in the form of number of leaks (per leak area) over component years. In order to use this data, and in particular the data that includes 0 leaks, the model must be modified. The model form used for the second update is:

$$\log\left(\mu_{LF,j}\right) = \alpha_2 \log_e\left(FLA_j\right) + \alpha_1$$
$$\lambda_j = \mu_{LF,j} \times Time_j$$
$$\alpha_1 \sim N(a_{11}', a_{12}')$$
$$\alpha_2 \sim N(a_{21}', a_{22}')$$
$$\ln\left(LF_j\right) \sim N(\mu_{LF,j}, \tau_j)$$
$$\tau_j \sim Gamma\left(s_j', r_j'\right)$$
$$LN_j \sim Poisson(\lambda_j)$$

The variables μ_{LF}, FLA_j, LF, α_1, α_2, τ_j, and j, are defined as before. The values α_{11}', α_{12}', α_{21}', α_{22}', s_j', and r_j' are the posterior values of α_{11}, α_{12}, α_{21}, α_{22}, s_j, and r_j respectively from the first model update. LN_j is the number of leaks over $Time_j$ component years. The hyper-parameter λ_j relates leak count to the frequency in the Poisson distribution.

Both updates were performed using JAGS called from R with the rjags package. No initial values were provided, five chains were used for sampling, the sample size used for model generation was 5×10^6, the sample size used for model updates were 5×10^6, and the sample size used to define the posterior distributions was 5×10^5.

4.3.1. Model Update 1

For the first model update, the initial priors chosen were as follows:

$\alpha_1 \sim N(0, 10^{-3})$
$\alpha_2 \sim N(0, 10^{-3})$
$\tau_j \sim Gamma\ (1,1)$

However, the model failed to converge with these prior distributions; the mean frequency estimated by the model increased without bound. To resolve this, the scale parameter was increased incrementally while the rate parameter was left constant. This shifts the prior distribution to the left, which represents an increased state of knowledge over the initial prior but keeps the spread of the distribution from increasing substantially away from zero (away from low precision). The model converged when the scale parameter was increased to 4, so the priors used for the first updated were:

$\alpha_1 \sim N(0, 10^{-3})$
$\alpha_2 \sim N(0, 10^{-3})$
$\tau_j \sim Gamma\ (4, 1)$

This model was updated with the generic data, resulting in estimates for the α_1, α_2, and τ_j distributions that are characterized empirically by 5×10^5 samples. Typically, the model would be updated with the hydrogen data as well without having to specify the new prior distributions using these samples. Because the model has to be modified to use the hydrogen data in the second update, however, the posterior distributions for α_1, α_2, and τ_j have to be estimated so they can be specified using standard distributions (normal, gamma) rather than samples. Empirical distributions were developed with the leak frequency data points and fitted with standard distributions. An example of these fitted distributions is shown in Figure 4-2. The fitted distributions do not appear to be significantly different from the empirical distributions. The fitted distributions are provided as prior distributions for the second update of the model. Note that some of the gamma distributions for the τ_j did not change – this is because there were no compressor data points for those leak sizes.

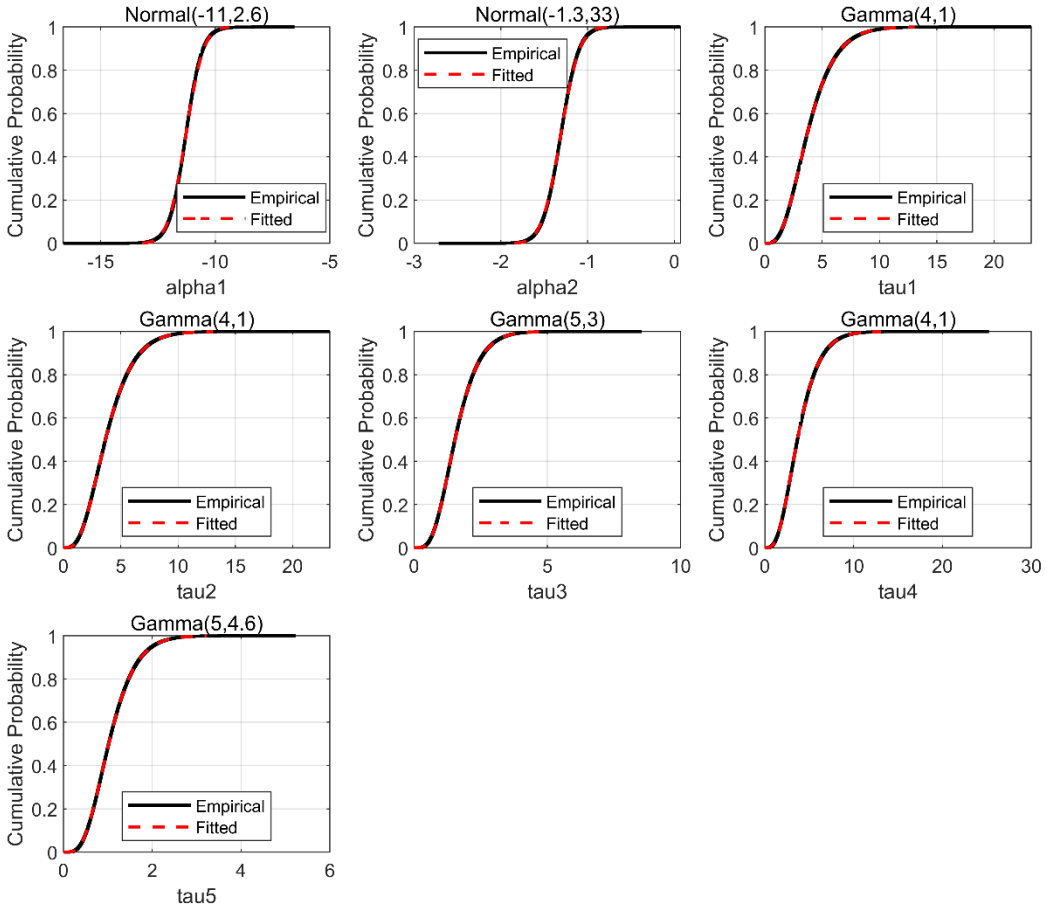

Figure 4-2. Posterior (empirical) distributions from the first update for compressors with their fitted forms used as priors in the second update.

4.3.2. Model Update 2

Hydrogen data was only available for compressors, cylinders, hoses, joints, pipes, and valves, so the second model update was only performed for these components. The prior distributions obtained during the first update for each component are listed in Table 4-2. These distributions are the priors in the model to which the hydrogen-specific leak frequency data is applied to produce the hydrogen leak frequencies (see Section 4.4).

Table 4-2. Posterior distributions from the first update used as priors for the second update.

Component	Distribution	Component	Distribution
Compressor	$\alpha_1 \sim N(-11, 2.6)$	Joint	$\alpha_1 \sim N(-7.3, 7.6)$
	$\alpha_2 \sim N(-1.3, 33)$		$\alpha_2 \sim N(-0.73, 44)$
	$\tau_1 \sim gamma(4, 1)$		$\tau_1 \sim gamma(4, 1)$
	$\tau_2 \sim gamma(4, 1)$		$\tau_2 \sim gamma(4, 1)$
	$\tau_3 \sim gamma(5, 3)$		$\tau_3 \sim gamma(4.3, 2.3)$
	$\tau_4 \sim gamma(4, 1)$		$\tau_4 \sim gamma(4.8, 1)$
	$\tau_5 \sim gamma(5, 4.6)$		$\tau_5 \sim gamma(4.3, 0.98)$
Cylinder	$\alpha_1 \sim N(-6.3, 3.1)$	Pipe	$\alpha_1 \sim N(-15, 5.8)$
	$\alpha_2 \sim N(-0.95, 36)$		$\alpha_2 \sim N(-0.76, 67)$
	$\tau_1 \sim gamma(4, 1)$		$\tau_1 \sim gamma(4, 1)$
	$\tau_2 \sim gamma(4, 1)$		$\tau_2 \sim gamma(4, 1)$
	$\tau_3 \sim gamma(4.4, 1.4)$		$\tau_3 \sim gamma(12, 28)$
	$\tau_4 \sim gamma(4.1, 1.1)$		$\tau_4 \sim gamma(9.1, 13)$
	$\tau_5 \sim gamma(5.4, 7.1)$		$\tau_5 \sim gamma(12, 51)$
Hose	$\alpha_1 \sim N(-6.3, 3.1)$	Valve	$\alpha_1 \sim N(-12, 7.7)$
	$\alpha_2 \sim N(-0.95, 36)$		$\alpha_2 \sim N(-0.78, 73)$
	$\tau_1 \sim gamma(4, 1)$		$\tau_1 \sim gamma(4, 1)$
	$\tau_2 \sim gamma(4, 1)$		$\tau_2 \sim gamma(4, 1)$
	$\tau_3 \sim gamma(4.4, 1.4)$		$\tau_3 \sim gamma(11, 22)$
	$\tau_4 \sim gamma(4.1, 1.1)$		$\tau_4 \sim gamma(4.2, 1.1)$
	$\tau_5 \sim gamma(5.4, 7.1)$		$\tau_5 \sim gamma(10, 18)$

4.4. Leak Frequency Results

Table 4-3 shows the updated component leak frequency values for the different normalized leak sizes. As shown, no hydrogen specific data is available for the filters, flanges, and pumps. Therefore, these components do not have hydrogen specific leak frequency values and the generic leak frequencies are used in this analysis. The associated distributions for each of these values are contained in Appendix C.

Table 4-3. Updated Component Leak Frequencies (yr^{-1})

Component	Leak Size	Generic Leak Frequencies				Hydrogen Leak Frequencies			
		Mean	5th	Median	95th	Mean	5th	Median	95th
Compressor	0.0001	6.0E+00	2.5E-01	2.2E+00	1.9E+01	1.0E-01	5.9E-02	1.0E-01	1.6E-01
	0.001	1.8E-01	2.1E-02	1.1E-01	5.4E-01	1.9E-02	6.8E-03	1.7E-02	3.8E-02
	0.01	9.2E-03	1.0E-03	5.2E-03	2.7E-02	6.3E-03	1.2E-03	4.6E-03	1.7E-02
	0.1	3.4E-04	8.2E-05	2.6E-04	8.0E-04	2.0E-04	4.6E-05	1.5E-04	4.9E-04
	1	3.3E-05	1.7E-06	1.2E-05	9.3E-05	3.2E-05	2.0E-06	1.5E-05	1.0E-04
Cylinder	0.0001	1.5E+00	6.6E-02	6.6E-01	5.3E+00	1.6E-06	3.5E-07	1.4E-06	3.4E-06
	0.001	3.4E-02	3.4E-03	2.0E-02	1.0E-01	1.3E-06	3.7E-07	1.2E-06	2.8E-06
	0.01	8.4E-04	1.6E-04	6.4E-04	2.1E-03	9.0E-07	2.6E-07	7.9E-07	1.9E-06
	0.1	2.5E-05	6.6E-06	1.9E-05	5.9E-05	5.2E-07	1.6E-07	4.5E-07	1.1E-06
	1	7.6E-07	1.9E-07	6.1E-07	1.8E-06	2.7E-07	8.1E-08	2.3E-07	6.0E-07
Filter	0.0001	6.9E-02	3.4E-04	5.3E-03	8.4E-02	NA	NA	NA	NA
	0.001	1.4E-02	6.2E-04	5.1E-03	4.1E-02	NA	NA	NA	NA
	0.01	1.6E-02	6.0E-04	4.8E-03	3.9E-02	NA	NA	NA	NA
	0.1	6.1E-03	1.4E-03	4.6E-03	1.5E-02	NA	NA	NA	NA
	1	6.4E-03	1.2E-03	4.4E-03	1.6E-02	NA	NA	NA	NA
Flange	0.0001	6.5E-02	1.7E-03	2.0E-02	2.3E-01	NA	NA	NA	NA
	0.001	4.3E-03	3.4E-04	2.2E-03	1.4E-02	NA	NA	NA	NA
	0.01	3.5E-03	8.4E-06	2.4E-04	7.0E-03	NA	NA	NA	NA
	0.1	3.5E-05	8.3E-06	2.7E-05	8.6E-05	NA	NA	NA	NA
	1	1.9E-05	1.9E-07	2.9E-06	4.6E-05	NA	NA	NA	NA
Hose	0.0001	2.8E+01	1.6E+00	1.3E+01	9.4E+01	6.1E-04	2.9E-04	5.8E-04	1.0E-03
	0.001	2.2E+00	2.9E-01	1.4E+00	6.4E+00	2.2E-04	6.6E-05	2.0E-04	4.5E-04
	0.01	2.1E-01	4.3E-02	1.6E-01	5.2E-01	1.8E-04	5.3E-05	1.6E-04	3.8E-04
	0.1	2.2E-02	6.0E-03	1.7E-02	5.3E-02	1.7E-04	5.1E-05	1.5E-04	3.4E-04

Component	Leak	Generic Leak Frequencies				Hydrogen Leak Frequencies			
	1	5.6E-03	1.9E-04	2.0E-03	1.8E-02	8.2E-05	9.6E-06	6.2E-05	2.2E-04
Joint	0.0001	1.3E+00	7.0E-02	5.3E-01	4.6E+00	3.6E-05	2.3E-05	3.5E-05	5.1E-05
	0.001	1.7E-01	2.1E-02	1.0E-01	5.2E-01	5.4E-06	8.4E-07	4.7E-06	1.2E-05
	0.01	3.3E-02	4.2E-03	1.8E-02	9.3E-02	8.5E-06	2.9E-06	7.9E-06	1.6E-05
	0.1	4.1E-03	1.3E-03	3.5E-03	8.6E-03	8.3E-06	2.4E-06	7.5E-06	1.7E-05
	1	8.2E-04	2.3E-04	6.3E-04	1.9E-03	7.2E-06	1.8E-06	6.4E-06	1.5E-05
Pipe	0.0001	5.9E-04	7.1E-05	3.6E-04	1.8E-03	9.5E-06	2.1E-06	8.0E-06	2.2E-05
	0.001	8.6E-05	1.7E-05	6.2E-05	2.2E-04	4.5E-06	1.1E-06	3.7E-06	1.1E-05
	0.01	3.5E-05	9.1E-07	1.1E-05	1.3E-04	1.7E-06	9.9E-08	9.6E-07	5.9E-06
	0.1	4.7E-06	2.3E-07	1.9E-06	1.6E-05	8.4E-07	5.8E-08	4.6E-07	2.9E-06
	1	3.7E-06	1.0E-08	3.2E-07	1.0E-05	5.3E-07	5.5E-09	1.5E-07	2.3E-06
Pump	0.0001	3.9E-02	2.4E-03	1.8E-02	1.3E-01	NA	NA	NA	NA
	0.001	6.5E-03	8.5E-04	4.2E-03	1.9E-02	NA	NA	NA	NA
	0.01	2.5E-03	9.9E-05	9.5E-04	8.3E-03	NA	NA	NA	NA
	0.1	2.8E-04	7.2E-05	2.1E-04	6.7E-04	NA	NA	NA	NA
	1	1.2E-04	5.4E-06	4.9E-05	4.1E-04	NA	NA	NA	NA
Valve	0.0001	2.0E-02	2.2E-03	1.2E-02	6.4E-02	2.9E-03	1.9E-03	2.9E-03	4.2E-03
	0.001	2.8E-03	5.0E-04	1.9E-03	7.5E-03	6.3E-04	2.7E-04	5.9E-04	1.1E-03
	0.01	1.2E-03	2.6E-05	3.1E-04	4.0E-03	8.5E-05	6.6E-06	5.4E-05	2.7E-04
	0.1	6.4E-05	1.8E-05	5.3E-05	1.5E-04	3.0E-05	8.7E-06	2.5E-05	6.7E-05
	1	2.6E-05	8.3E-07	8.5E-06	9.1E-05	1.1E-05	4.7E-07	4.8E-06	4.2E-05

The HTEF system frequency can be calculated by summing each of the individual component frequencies for the entire facility. Table 2-2 defines the total number of components in the HTEF, which corresponds directly to the leak frequencies listed in Table 4-3. The quantity of components was multiplied by its associated leak frequency and was summed to calculate the system frequency. Table 4-4 shows the total HTEF system frequency as a function of break size. Note, that the median leak frequency indicates that a very small leak size (normalized leak area of 0.0001) is fairly common (~ 17 expected occurrences/yr). However, a full rupture (normalized leak area of 1) is expected to occur ~2 times every 100 years.

Table 4-4. HTEF System Frequency (yr^{-1})

Leak Size	HTEF System Frequency

Leak Size	HTEF System Frequency			
	Mean	5th	Median	95th
0.0001	2.28E+01	7.95E+00	1.70E+01	5.48E+01
0.001	4.19E+00	1.13E+00	3.32E+00	9.89E+00
0.01	1.37E+00	1.45E-01	7.47E-01	4.16E+00
0.1	1.33E-01	3.34E-02	1.01E-01	3.20E-01
1	5.19E-02	2.51E-03	2.18E-02	1.83E-01

5. TARGET FRAGILITY EVALUATION

NPPs must show that the operation of an HTEF is safe and does not pose a significant threat to the high consequence NPP facilities and structures. Table 5-1 shows the critical external structures of an NPP that have been identified.

Table 5-1. Critical Structures Identified for Pressurized Boiling Water Reactors in High Wind Fragility Assessment

Name of Structure	Abbreviation
Refueling Water Storage Tank	RWST
Condensate Tank	CST
Auxiliary/Emergency Feedwater Tank	AFWT or EFWT
Service Water Intakes	N/A
Switchyard	N/A

External water tanks are located close to the reactor building for use in providing condensate storage and coolant for routine and emergency operations. In some cases, there are concrete walls placed around the external tanks for protection, but some NPPs choose not to include external protection other than the tank's own construction. These tanks built to extreme standards, which according to the Individual Plant Examination of External Events (IPEEE) of the Duane Arnold NPP and others, is equivalent in structural integrity to wind pressure as a Category I Structure. This means that the tanks are as durable as the reactor building itself when it comes to handling pressure. The condensate storage tank (CST) is assumed to be a Category II structure, which is susceptible to wind missiles. The probability of failure per instance of wind speed for CSTs and Category I Structures is listed in Table 5-2. Note that these are based on 6 second gusts and the wind speeds follow the Fujita tornadic wind scale of 234mph = F4, 290mph = F5, and 318mph = F6. Service water intakes are solid structures; however, the pump house is not typically built to withstand tornadic or hurricane winds. Loss of service water is in itself an initiator which challenges the NPP to shut down safely. The probability of failure per instance of wind speed for a typical pump house is listed in Table 5-2.

Table 5-2. Wind pressure and wind missile fragilities from excerpt of Duane Arnold IPEEE

Component Structure	Windspeed (mph)	Fragility Due to Wind Pressure		Fragility due to Tornado Generated Missiles	Total Fragility
		Straight Wind	Tornado Wind		
All Category I Structures	75	ϵ	N/A	N/A	ϵ
	105	ϵ	N/A	N/A	ϵ
	125	ϵ	N/A	N/A	ϵ
	182	N/A	ϵ	ϵ	ϵ
	234	N/A	4.0E-04	ϵ	4.0E-04
	290	N/A	4.6E-03	ϵ	6.4E-03
	349	N/A	4.0E-02	ϵ	4.0E-02
CST A/CST B	75	ϵ	N/A	N/A	ϵ
	105	ϵ	N/A	N/A	ϵ
	125	ϵ	N/A	N/A	ϵ
	182	N/A	ϵ	2.1E-03	2.1E-03
	234	N/A	4.0E-04	2.4E-03	2.8E-03
	290	N/A	6.4E-03	9.2E-03	1.6E-02
	349	N/A	4.0E-02	1.4E-02	5.4E-02
Circulating Water/ Service Water pump Area in Pump House	75	8.5E-04	N/A	N/A	8.0E-04
	105	5.3E-04	N/A	N/A	5.3E-02
	125	1.5E-01	N/A	N/A	1.5E-01
	182	N/A	7.2E-01	2.5E-03	5.2E-01
	234	N/A	9.4E-01	2.8E-03	9.4E-01
	290	N/A	9.9E-01	1.1E-02	1.0E+00
	349	N/A	1.0E+00	1.7E-02	1.0E+00

Loss of switchyard components means a loss of offsite power (LOOP) event which challenges the NPP to shut down safely. Switchyard components are fragile to wind pressure, and therefore are also fragile to an over-pressure event. A high wind fragility analysis of the Vogtle NPP determined the mean fragilities listed in Table 5-3 for components commonly found in the switchyard. The tornadic wind speeds in Table 5-3 were based on the Enhanced Fujita tornadic wind scale.

Table 5-3. Windspeed fragilities of Switchyard Components

SSC	Windspeed (mph)	Tornadic Wind Pressure	Wind Generated Missiles
Switchyard, General	135	3.10E-01	6.83E-02
	165	8.49E-01	1.25E-01
	200	9.95E-01	1.65E-01
Transmission Tower	135	9.18E-01	N/A
	165	1.00E+00	N/A
	200	1.00E+00	N/A
Standby Auxiliary Transformer	135	N/A	1.99E-01
	165	N/A	2.68E-01
	200	N/A	3.11E-01

In addition to critical structures, some other structures that affect operations, but not typically the ability to safely shut down the reactor, are located in the plant yard as well: circulating water and standby service water pump houses, demineralized water storage tank(s), cooling towers, well water pump houses, liquid nitrogen tank, and nitrogen gas cylinders which present stored energy in the form of chilled and pressurized gas. Further, the day to day operations of the NPP would be affected by damage to the turbine building, administrative building, and maintenance support buildings located throughout the site.

Table 5-2 and Table 5-3 give wind fragility information for nuclear power plant structures and switchyard components. Table 5-4 shows the effective overpressure at that windspeed. This is done by determining the total dynamic energy that transforms into pressure across the component surface as shown below [12]:

$$\frac{F_W}{A} = p_d = \frac{1}{2}\rho v^2 \qquad \text{Equation 4-1}$$

Where F_W is the total force in Newtons, A is the effective area in m^2, p_d is pressure in lb_f/in^2, ρ is the air density assumed to be 1.225 kg/m^3 for ambient air conditions, and v is the velocity in m/s.

Table 5-4. Windspeed and Effective Pressure Fragilities for Safety Critical Structures and Systems

Structure/ Component	Wind speed (mph)	Effective Pressure (psi)	Fragility due to Wind Pressure		Fragility due to Tornado Generated Missiles	Total Fragility
			Wind	Tornado		
Infrastructure						
All Category I	75	0.10	ϵ	N/A	N/A	ϵ
	105	0.20	ϵ	N/A	N/A	ϵ
	125	0.28	ϵ	N/A	N/A	ϵ
	182	0.59	N/A	ϵ	ϵ	ϵ
	234	0.97	N/A	4.00E-4	ϵ	4.00E-4
	290	1.49	N/A	4.60E-3	ϵ	4.60E-3
	349	2.16	N/A	4.00E-2	ϵ	4.00E-2
CST A & B	75	0.10	ϵ	N/A	N/A	ϵ
	105	0.20	ϵ	N/A	N/A	ϵ
	125	0.28	ϵ	N/A	N/A	ϵ
	182	0.59	N/A	ϵ	2.10E-3	2.10E-3
	234	0.97	N/A	4.00E-4	2.40E-3	2.80E-3
	290	1.49	N/A	6.40E-3	9.20E-3	1.60E-3
	349	2.16	N/A	4.00E-2	1.40E-2	5.40E-2
Circulating Water/Service Water Pump Area in Pump House	75	0.10	8.00E-4	N/A	N/A	8.00E-4
	105	0.20	5.30E-4	N/A	N/A	5.80E-2
	125	0.28	1.50E-1	N/A	N/A	1.50E-1
	182	0.59	N/A	7.2E-1	2.5E-3	5.20E-1
	234	0.97	N/A	9.4E-1	2.8E-3	9.40E-1
	290	1.49	N/A	9.9E-1	1.1E-2	1.0
	349	2.16	N/A	1.0	1.7E-2	1.0
Systems, structures and components						

Structure/	Wind	Effective Pressure	Fragility due to Wind Pressure		Fragility due to	
Switchyard, General	135	0.32	N/A	3.10E-1	6.83E-2	3.78E-1
	165	0.48	N/A	8.49E-1	1.25E-1	9.74E-1
	200	0.71	N/A	9.95E-1	1.65E-1	1.16E+0
Transmission Tower	135	0.32	N/A	9.18E-1	N/A	9.18E-1
	165	0.48	N/A	1.00E+0	N/A	1.00E+0
	200	0.71	N/A	1.00E+0	N/A	1.00E+0
Standby Auxiliary Transformer	135	0.32	N/A	N/A	1.99E-1	1.99E-1
	165	0.48	N/A	N/A	2.68E-1	2.68E-1
	200	0.71	N/A	N/A	3.11E-1	3.11E-1

While the effective pressure due to windspeed does give an idea of the overall fragility of the structures and components, it would be conservative to use this as the fragility criteria. For example, the standard containment building wall of an LWR has a static pressure capacity of 1.5 psi [4], which would correspond to a 290 mph wind speed effective pressure. An appropriate and conservative fragility criterion on which to evaluate the consequence of an explosive overpressure on NPP structures, systems and components is defined in Regulatory Guide 1.91 [13]. The incident overpressure below which critical targets of an NPP are expected to experience no significant damage is conservatively 1 psi [13]. Therefore, this criterion will be used to determine whether failure is expected to occur after exposure to overpressure from detonation of hydrogen leaked from the HTEF system.

6. CONSEQUENCE OF DETONATION

The consequence of an accident in the HTEF system is an important parameter in the overall risk assessment. A leak in the system could release an unconfined high-pressure hydrogen jet with the potential to damage surrounding structures. The flammable jet released from the leak could result in a detonation, which would expose nearby targets to damaging overpressure. However, due to the strong concentration gradients in the hydrogen jet, the detonable region of the cloud is reduced when compared to the total amount of fuel within the flammability range. Detonations are inherently unstable and depend on critical dimensions and the concentration gradient of the hydrogen jet, which determine if a propagating detonation wave can be supported. The limits of the hydrogen concentration in the jet to support detonation reduce the portion of the flammable cloud that is available as fuel. The overpressure released through detonation of the large cloud can be calculated from the detonable region, which is compared to the target fragility criteria to determine if critical damage occurs [14]. Note that this analysis does not account for possible natural and man-made barriers between the detonation area and the targets (i.e., the HTEF facility walls were not credited to reduce the overpressure at the critical NPP targets).

6.1. Hydrogen Concentration in High-Pressure Jet

Initially, the concentration of hydrogen in the high-pressure jet must be calculated. To do this, the HyRAM software toolkit was used [15]. HyRAM provides a basis for conducting quantitative risk assessment and consequence modeling for hydrogen infrastructure and transportation systems. HyRAM has been designed to facilitate the use of state-of-the-art science and engineering models to conduct robust, repeatable assessments of hydrogen safety, hazards, and risk. With regard to calculation of the concentration of the high-pressure hydrogen jet, HyRAM incorporates computationally and experimentally validated models of various aspects of hydrogen release and flame physics.

The thermodynamic properties of hydrogen gas and hydrogen release are needed to calculate different aspects of hydrogen dispersion. The Abel-Noble equation of state is used in HyRAM for gaseous hydrogen properties (e.g., pressure, density, temperature):

$$P = \frac{\left(\frac{R}{M}\right)\rho T}{1 - b\rho}$$ Equation 5-1

Where:

- P is the pressure
- R is the ideal gas constant (8.3145 J/mol/K)
- M is the molecular weight (2.016E-03 m^3/kg for H_2)
- ρ is the density
- T is the temperature
- B is the co-volume constant (7.691E-03 m^3/kg for H_2 that accounts for intermolecular gas interactions)

Using this relationship, and the Maxwell relationships, the density after an isentropic expansion can be calculated as follows:

$$\frac{\rho_0}{1-b\rho_0} = \frac{\rho}{1-b\rho}\left(1+\frac{\gamma-1}{2(1-b\rho)^2}Ma^2\right)^{\frac{1}{\gamma-1}} \quad \text{Equation 5-2}$$

Where:

- The subscript 0 indicates the stagnant condition before expansion
- *Ma* is the Mach number (velocity/speed of sound)
- γ is the ratio of heat capacities (1.4 for hydrogen)

Once the density after expansion is known, the temperature can be calculated through one of several equivalent relationships (depending on the known quantities):

$$T = T_0\left(\frac{1-b\rho_0}{\rho_0}\frac{\rho}{1-b\rho}\right)^{\gamma-1} \quad \text{Equation 5-3}$$

$$T = \frac{T_0}{1+\left(\frac{\gamma-1}{2(1-b\rho)^2}\right)Ma^2} \quad \text{Equation 5-4}$$

$$T = T_0 + \frac{b(P_0-P)+\frac{v_0^2-v^2}{2}}{c_p} \quad \text{Equation 5-5}$$

Where:

- c_p is the heat capacity at constant pressure

The relationship of the speed of sound is also needed:

$$a = \frac{1}{1-b\rho}\left(\frac{\gamma RT}{M}\right)^{0.5} \quad \text{Equation 5-6}$$

When the pressure ratio across the leak orifice is above the critical ratio (≈ 1.9 for hydrogen), the flow chokes, meaning that it is sonic, or flowing at the speed of sound through the throat, but remains at a higher pressure than the outlet pressure. These relationships for isentropic expansion are used to calculate the flow rate of the released hydrogen through the leak orifice and the thermodynamic state in the throat. Orifices in HyRAM are assumed to be circular, characterized by their diameter, d, and a coefficient of discharge, C_d. The choked flow through any orifice can then be calculated as follows:

$$\dot{m} = \frac{\pi}{4d^2 \rho v C_d}$$ Equation 5-7

Notional nozzles are used to calculate the effective diameter, velocity, and thermodynamic state after the complex shock structure of an under-expanded jet. The Yüceil and Ötügen methodology was used [15], which conserves mass, momentum, and energy. The velocity after the shock is determined by the simultaneous solution to the conservation of mass and momentum equations, with temperature determined through isentropic expansion. The effective area is calculated as follows:

$$A_{eff} = \frac{\rho_{throat} v_{throat}^2 A_{throat} C_D^2}{\rho_{eff}\left(P_{throat} - P_{ambient} + \rho_{throat} v_{throat}^2 C_D^2\right)}$$ Equation 5-8

Where:

- ρ is the density
- v is the velocity
- A is the cross-sectional area
- C_D is the discharge coefficient
- P is the pressure

To calculate the hydrogen plume from the leak orifice, HyRAM follows the one-dimensional model described by Houf and Schefer [15]. The model evaluates the plume along the streamline, and the plume can curve due to buoyancy effects. Figure 6-1 shows a sketch of the plume model coordinates.

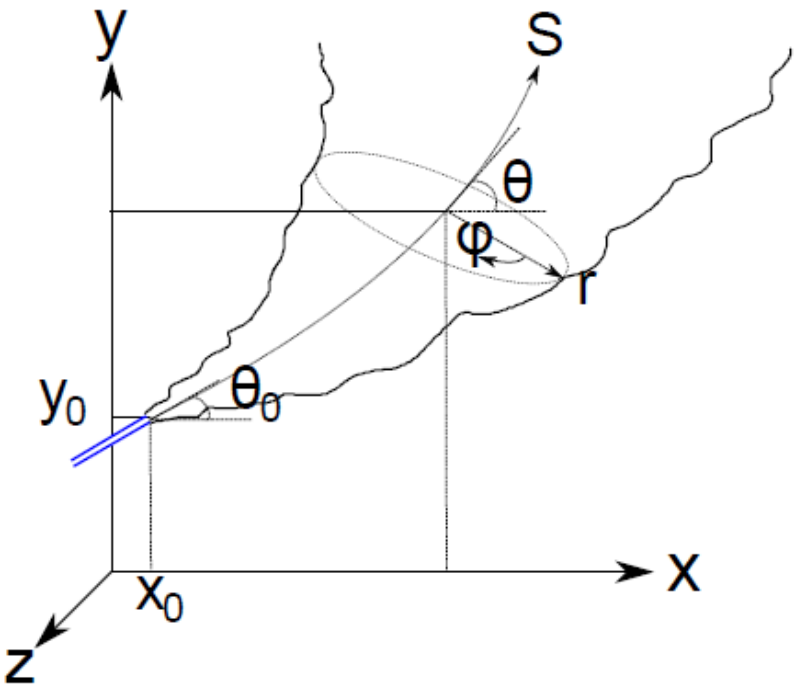

Figure 6-1. Plume Model Coordinates [15]

The reduction in dimension comes from the assumption that the mean profile of the velocity (v), density (ϱ), and product of density and mass fraction (Y) of hydrogen are Gaussian, as shown below:

$$v = v_{cl}\exp\left(-\frac{r^2}{B^2}\right)$$ Equation 5-9

$$\rho = (\rho_{cl} - \rho_{amb})\exp\left(-\frac{r^2}{\gamma^2 B^2}\right) + \rho_{amb}$$ Equation 5-10

$$\rho Y = \rho_{cl} Y_{cl}\exp\left(-\frac{r^2}{\gamma^2 B^2}\right)$$ Equation 5-11

Where:

- B is the characteristic half-width
- γ is the ratio of density spreading relative to velocity
- r is the perpendicular to the stream-wise direction

The subscript "cl" denotes the centerline and the subscript "amb" denotes ambient. Gravity acts in the negative y-direction, and the plume angle, θ, is relative to the x-axis. The derivatives of the spatial dimensions are therefore:

$$\frac{dx}{dS} = cos\theta$$ Equation 5-12

$$\frac{dy}{dS} = sin\theta$$ Equation 5-13

The Gaussian profiles, in addition to the conservation equations of continuity, x-momentum, y-momentum, and species (hydrogen) continuity, are used to derive a system of first order differential equations where the independent variable is S (streamline) and the dependent variables are v_{cl}, B, ϱ_{cl}, Y_{cl}, x, and y. These variables are then integrated from the starting point to the distance desired.

The entrainment model also follows Houf and Schefer [15], where there is a combination of momentum and buoyancy driven entrainment:

$$E = E_{mom} + E_{buoy}$$ Equation 5-14

$$E_{mom} = 0.282\left(\frac{\pi D^2 \rho_{exit} v_{exit}^2}{4 \quad \rho_\infty}\right)^{0.5}$$ Equation 5-15

$$E_{buoy} = \frac{a}{Fr_l}(2\pi v_{cl} B)sin$$ Equation 5-16

$$Fr_l = \frac{v_{cl}^2}{\frac{gD(\rho_\infty - \rho_{cl})}{\rho_{exit}}}$$ Equation 5-17

In these equations, a was empirically determined [15]:

$$a = \begin{cases} 17.313 - 0.116665 Fr_{den} + 2.0771E - 4 * Fr_{den}^2, Fr_{den} < 268 \\ 0.97, Fr_{den} \geq 268 \end{cases}$$ Equation 5-18

As the jet/plume becomes very buoyant (as opposed to momentum-dominated), the non-dimensional number

$$\alpha = \frac{E}{2\pi B v_{cl}}$$ Equation 5-19

Will increase. When α reaches a limiting value of 0.082, it is held constant and the entrainment value becomes:

$$E = 2\pi\alpha B v_{cl} = 0.164\pi B v_{cl}$$ Equation 5-20

6.2. Detonable Region

If the hydrogen jet were to ignite, the flammable mixture would be consumed through deflagration or detonation. Deflagration occurs when the jet is ignited by a weak ignition source and the wave would be characterized by laminar burning velocity, which is controlled by diffusion. Detonation occurs through ignition by a strong ignition source, and the wave is characterized by adiabatic ignition of the unburned fuel-air mixture. The propagation velocity of the detonation is supersonic, and the unburned fuel-air mixture is compressed and heated by the leading shock wave. Fuel is consumed at a high rate during detonation and results in detonation velocities of approximately 2,000 m/s for some stoichiometric fuel-air mixtures.

The detonation cell size, λ, which is a measure of the scale of the instability of detonation, is used to characterize the detonation sensitivity of a given mixture [14]. The detonation cell size of a material depends on the mixture composition. The cell size defines the spacing between the transverse waves (the secondary waves that propagate perpendicular to the direction of detonation propagation) and

is integral in determining whether a detonation will propagate or not. Detonations are more likely to initiate and propagate when the mixture has a small cell size (i.e., there is a tighter spacing of transverse waves). Smaller cell sizes are a result of faster chemical reactions and typically require less energy to begin the detonation or transition from deflagration to detonation [14].

However, in application, a high-pressure hydrogen release will result in a plume with non-uniform fuel distribution. The gradient of the detonation cell size also limits the ability of a detonation to propagate through a mixture. Work in this area has shown that detonation waves will fail to propagate if the cell size increases by more than ~10% across a single cell length [14]. Therefore, in this application, detonation propagation is only considered in regions for which $d\lambda/dx < 0.1$. To determine whether the cell size is small enough to support detonation, the thickness of the flammable mixture for the region in which $d\lambda/dx < 0.1$ is evaluated to see how many detonation cells can fit within the layer. According to the critical layer height criterion, a threshold of at least 5 cells within the layer is used to define the detonable region of the hydrogen mixture [14].

For this analysis, experimental values of detonation cell size for a range of hydrogen-air mixture compositions were taken from the CALTECH Detonation Database [16]. Figure 6-2 shows the detonation cell size as a function of equivalence ratio, which is the ratio of the actual hydrogen/air ratio to the stoichiometric hydrogen/air ratio. To ensure a continuous transition of the computed cell size gradients, the outliers were removed from the dataset through visual inspection and the values were linearly interpolated to obtain an acceptable variation when calculating the cell size gradients.

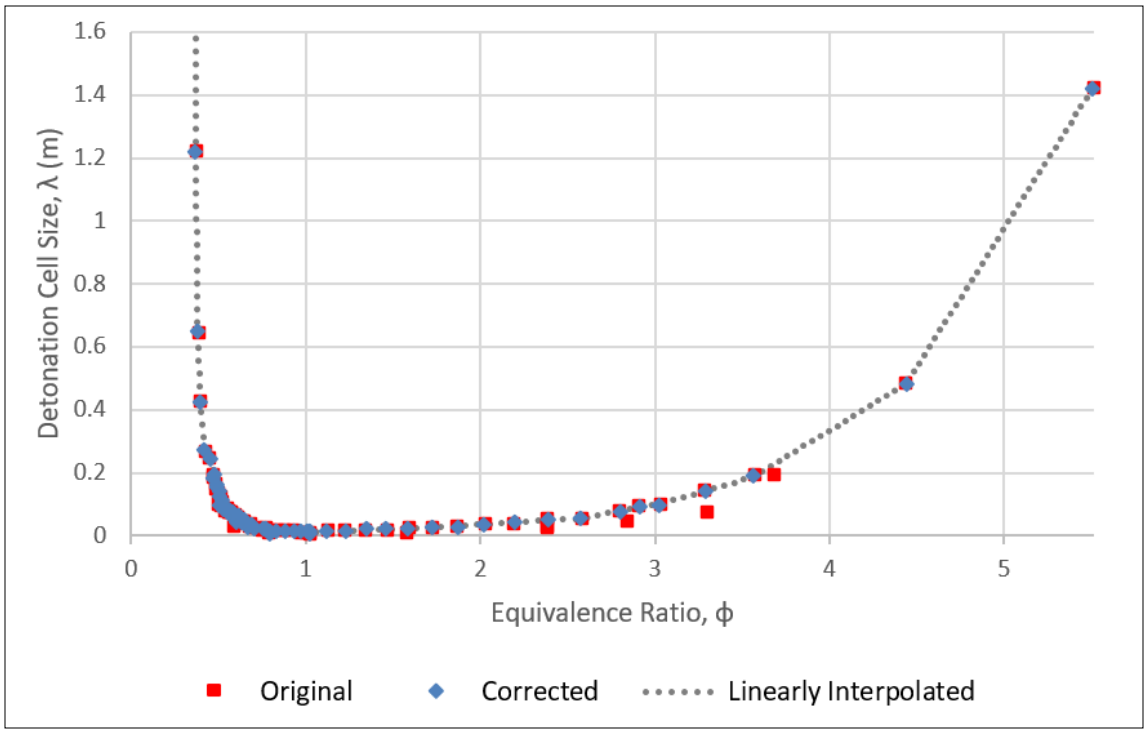

Figure 6-2. Detonation Cell Size for Hydrogen-Air Mixtures

6.3. Overpressure

Detonation of the hydrogen jet release can result in significant overpressures [14]. The overpressure can be estimated with a model informed by experimental studies of large-scale hydrogen jet releases that were ignited. The dimensionless pressure generated by the detonation of the limited detonable region in the hydrogen-air mixture is calculated as follows:

$$P^* = \frac{0.34}{(R^*)^{\frac{4}{3}}} + \frac{0.062}{(R^*)^2} + \frac{0.0033}{(R^*)^3}$$ Equation 5-21

Where:

- P^* is the peak pressure normalized by the ambient pressure, (P_{peak}/P_0)

R^* is a dimensionless standoff distance and is calculated as follows:

$$R^* = \frac{R_D P_0^{\frac{1}{3}}}{E_n^{\frac{1}{3}}}$$ Equation 5-22

Where:

- R_D is the dimensional distance from the center of the detonable region
- E_n is the total energy released from the mass of hydrogen contained in the detonable region, calculated as the mass of fuel multiplied by the heat of combustion (119 MJ/kg for hydrogen)

6.4. Overpressure Results at 1 km away from NPP

The overpressure from ignition of a hydrogen leak in the HTEF was evaluated for a location 1 km away from the NPP. Calculations were performed for two ignition scenarios: ignition of the high-pressure jet and ignition of an accumulated cloud of hydrogen. Note that both of these scenarios were evaluated deterministically using full break diameters of the piping (i.e., no partial breaks were considered). Therefore, the frequency associated with these breaks equate to the 1.0 normalized leak size from Table 4-4 .

6.4.1. High Pressure Jet

Each of the scenarios in Table 3-3 have been evaluated using the methodology outlined in Sections 6.1 through 6.3. A Python script was written to perform all of the necessary calculations and determine the overpressure at 1 km away from the accident. Additional results, including the plume concentration, cell size, cell size gradient, detonable region, and overpressure as a function of distance for each scenario are documented in Appendix D. Table 6-1 shows the summary overpressure results at 1 km away from the accident location. As shown in the table, the largest impulse overpressure at a distance of 1 km away is ~400 Pa (0.06 psi), which is well below the 1 psi fragility failure criterion. Even when compared to the constant 75 mph effective wind pressure (0.1 psi), there is margin in the target fragility. Note that it is conservative to compare the impulse overpressure caused by the detonation of the hydrogen jet to the constant wind pressure fragility criteria. However, there is a ~66% margin of safety in this conservative comparison. Therefore, the fragility of the critical targets at an NPP would not be compromised at a distance of 1 km away from the break scenario.

Table 6-1. Overpressure Results for Worst-case Scenarios

Scenario	Overpressure at 1 km	
	(MPa)	(psi)
1	3.03E-05	0.00440
2	4.37E-05	0.00633
3	5.69E-05	0.00826
4	2.90E-05	0.00420
5	4.68E-05	0.00679
6	6.70E-05	0.00972
7	8.76E-05	0.0127
8	2.16E-05	0.00313
9	2.70E-05	0.00392
10	8.13E-05	0.0118
11	11.9E-05	0.0173
12	4.52E-05	0.00656
13	16.4E-05	0.0238
14	24.0E-05	0.0349
15	38.4E-05	0.0557

6.4.2. Hydrogen Accumulation Scenario

An alternate consequence of a hydrogen leak in the HTEF system is ignition of an accumulated cloud of a hydrogen/air mixture. If ignition of the high-pressure hydrogen jet does not occur immediately after the hydrogen release, the hydrogen can accumulate and mix with ambient air before being ignited. The total quantity of hydrogen released in this case would contribute to the overpressure experienced by the critical NPP structures. The amount of hydrogen released is a function of the system flowrate at the leak location as well as the time to leak isolation. Table 6-2 shows the two largest flowrates in the HTEF system [17], along with assumed leak times and the total hydrogen quantity that would be released. Note, that the isolation times were assumed to range between 5 minutes and 120 minutes, which span the assumed range of operator response times to isolate the hydrogen leak. As shown, due to the low flowrates, the total mass of hydrogen released is fairly limited. Also, 100% of the released quantity is treated as hydrogen, even though the actual concentration of hydrogen is less than 100%. Similar to the high-pressure jet release detonation calculations, the hydrogen is assumed to be well mixed in air and the heat of combustion value of 119 MJ/kg is used to calculate the overall energy. A 100% yield (i.e., the fraction of available combustion energy participating in blast wave generation) was assumed for the overall energy calculation as well.

Table 6-2. Total Quantity of Hydrogen Released for Varying Flowrates and Isolation Time

System	Flowrate (nlpm)	Isolation Time (min)	Total Hydrogen Quantity (kg)
Hydrogen Product, 93% H_2	750	5	0.3
		10	0.7
		20	1.3
		30	2.0
		60	4.0
		120	8.1
Hydrogen Product Manifold to Condenser, 62% H2	1,223	5	0.5
		10	1.1
		20	2.2
		30	3.3
		60	6.6
		120	13.2

Due to this variability, a range of released quantities will be evaluated. The overpressure can be calculated as a function of distance from the accident location with the same methodology as for the plume hydrogen release cases (see Section 6.3). However, in this case, the entire quantity of released hydrogen will be considered as the detonable region. The energy from the released hydrogen is calculated and input into the overpressure calculation. Figure 6-3 shows the total energy and overpressure at a distance of 1 km from the accident as a function of total amount of leaked hydrogen. As shown, the overpressure experienced at 1 km is ~ 0.7 psi for the case that estimates 50 kg of hydrogen released. When compared to the fragility criterion of 1 psi for the static pressure capacity, there is more than a 40% margin. Also, note that even for a maximum credible accident (MCA) postulated isolation time of 120 minutes, the maximum quantity of hydrogen released is ~13 kg (~0.4 psi overpressure). Therefore, the overpressure generated by the release of 50 kg of hydrogen is a conservative comparison case. Similar to the comparison made in the overpressure from detonation of a high-pressure hydrogen jet, the critical targets would not be compromised at a distance of 1 km.

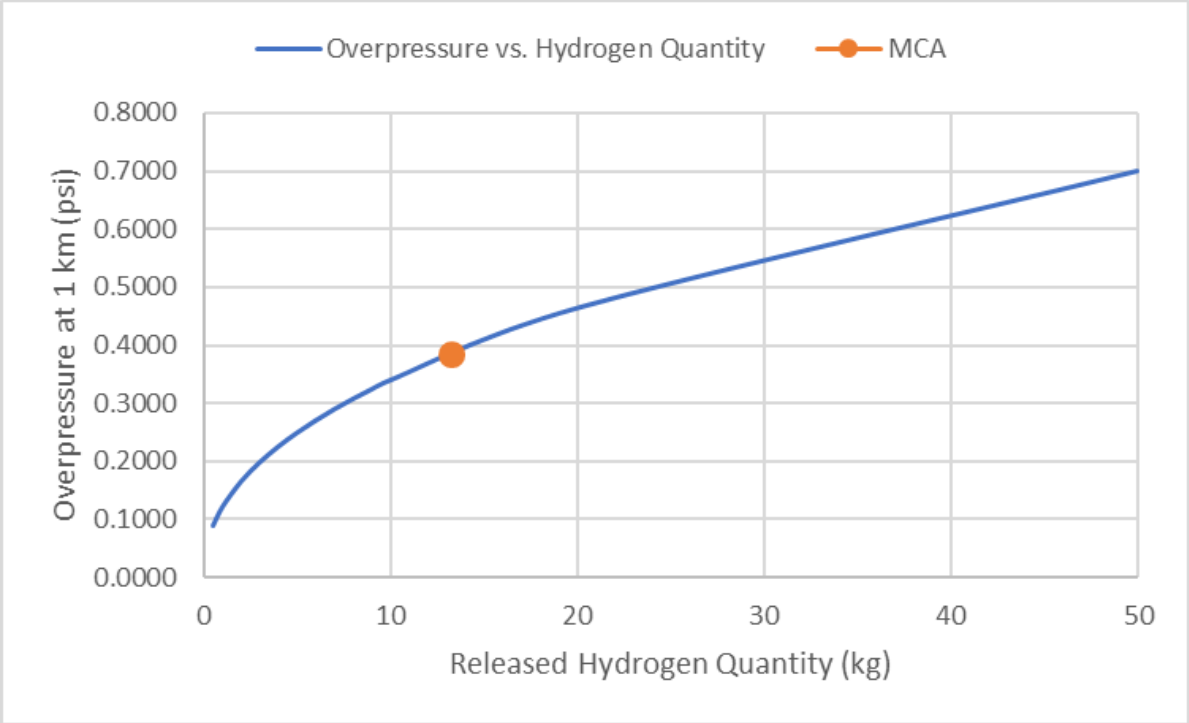

Figure 6-3. Overpressure as a Function of Hydrogen Quantity in Cloud

6.5. Minimum Separation Distance

The minimum separation distance at which the overpressure from ignition of a hydrogen leak in the HTEF reached the 1 psi fragility criteria was evaluated herein. Similar to the 1 km distance evaluation, calculations were performed for two ignition scenarios: ignition of the high-pressure jet and ignition of an accumulated cloud of hydrogen.

6.5.1. High Pressure Jet

Each of the scenarios in Table 3-3 have been evaluated using the methodology outlined in Sections 6.1 through 6.3. A Python script was written to perform all of the necessary calculations and determine the minimum separation distance at which the overpressure value reached 1 psi. The overpressure as a function of distance for each scenario is documented in Appendix E. Table 6-3 shows the separation distance for each of the different scenarios. As shown in the table, the largest separation distance is ~120 meters away from the NPP. Note, that this is in comparison to the 1 psi fragility failure criterion, which was deemed to be conservative. Therefore, a factor of safety was not addressed in these calculations.

Table 6-3. Minimum Separation Distance for High-Pressure Jet Cases

Scenario	Separation Distance (m)
1	18.0
2	23.7
3	28.9
4	17.4
5	24.9
6	32.6
7	39.8
8	14.0
9	16.5
10	37.7
11	50.1
12	24.3
13	63.6
14	84.5
15	119.8

6.5.2. *Hydrogen Accumulation Scenario*

Each of the scenarios in Table 6-2 have been evaluated using the methodology outlined in Sections 6.1 through 6.3. The overpressure as a function of distance for each scenario is documented in Appendix F. Table 6-4 shows the separation distance for each of the different scenarios. As shown in the table, the largest separation distance is ~492.1 meters away from the NPP. Note, that this is in comparison to the 1 psi fragility failure criterion, which was deemed to be conservative. Also note that it was assumed that the escaped gas was 100% hydrogen, which effects the total energy and resulting overpressure of the blast.

Table 6-4: Separation Distance for Hydrogen Accumulation Scenarios

System	Flowrate (nlpm)	Isolation Time (min)	Total Hydrogen Quantity (kg)	Separation Distance (m)
Hydrogen Product, 93% H_2	750	5	0.3	139.4
		10	0.7	184.9
		20	1.3	227.2
		30	2.0	262.3
		60	4.0	330.5
		120	8.1	418.2
Hydrogen Product Manifold to Condenser, 62% H2	1,223	5	0.5	165.2
		10	1.1	214.9
		20	2.2	270.8
		30	3.3	310.0
		60	6.6	390.6
		120	13.2	492.1

6.6. Effect of Obstructions on Target Overpressure

The calculations herein did not account for possible natural and man-made barriers between the detonation area and the targets (i.e., the HTEF facility walls were not credited to reduce the overpressure at the critical NPP targets). To evaluate the effect that obstructions may have on the overpressure experienced by NPP targets, a literature survey was performed of relevant modeling efforts and experiments.

6.6.1. Xiao et al.

Xiao et al. investigated the effectiveness of different configurations of blast walls in reducing downstream overpressure from air blasts [18]. This paper performed experiments and developed numerical models to measure the blast loads behind the obstructions. Three full-scale experiments were carried out that evaluated different blast wall constructions. Figure 6-4 shows the experimental setup. The base obstruction structure (M2) was a vertical wall comprised of broken stones with dimensions of 2 m x 2 m x 1 m (length x height x width). This base structure was modified with a metal canopy with dimensions 2 m x 0.75 m with a thickness of 8 mm. Test structure M1 had a canopy inclined opposite to the charge at an angle of 45° with respect to the horizontal, while M3 had a canopy inclined towards the charge at an angle of 45° with respect to the horizontal. A spherical bare charge of PETN (5 kg TNT equivalent) was detonated in the center at a distance of 5 m in front of the blast wall, with various gauge points located between the charge and a wall representing the target.

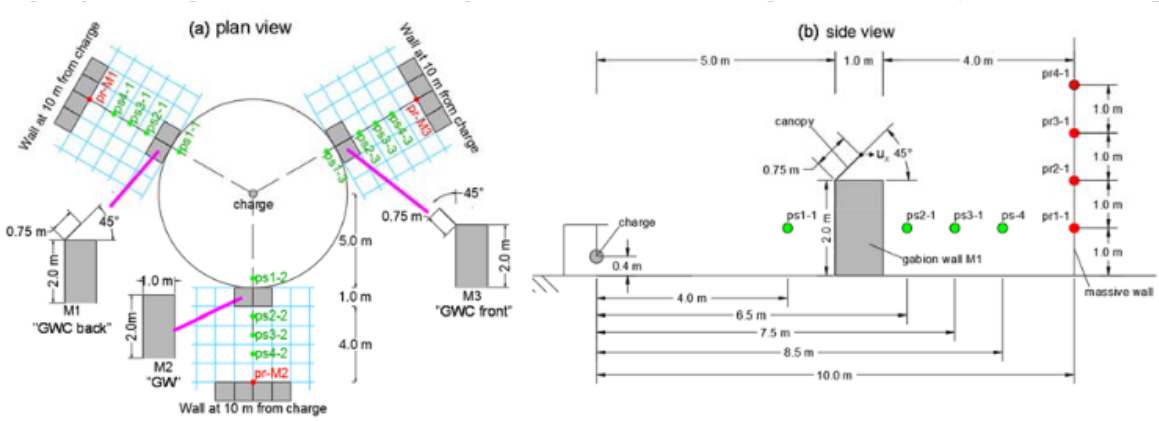

Figure 6-4: Xiao et al. Experimental Setup [18]

Figure 6-5 shows the overpressure and impulse results as a function of distance from the charge for the different wall configurations, as well as a free field configuration with no blast wall. A reduction in overpressure was seen for each of the blast wall configurations; however, it was shown that the geometry of the wall had an impact on the overall reduction in overpressure. Also, the reduction in overpressure decreases as the distance from the charge to the gauge point increases.

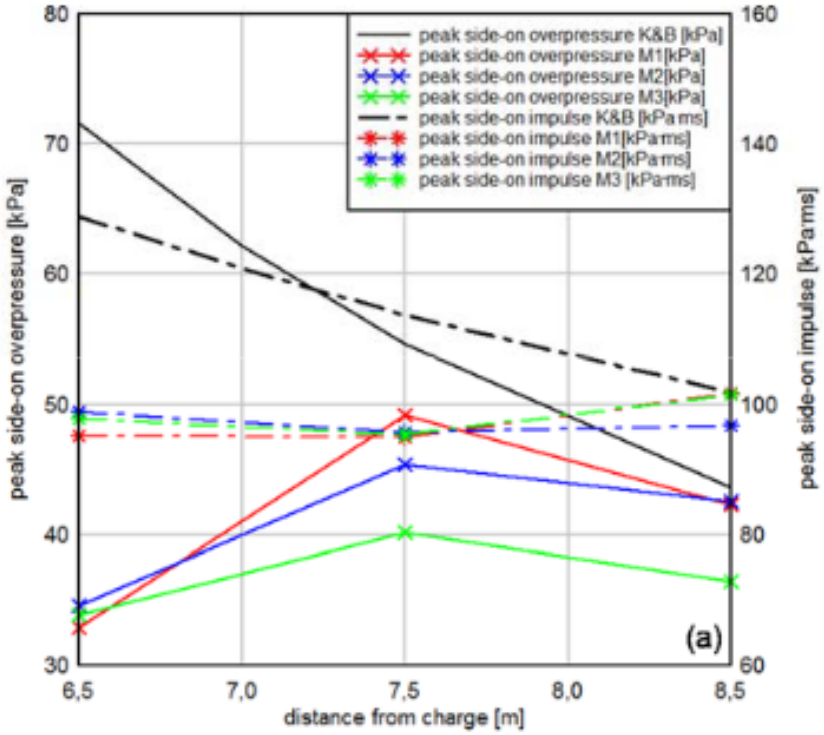

Figure 6-5: Xiao et al. Overpressure vs. Distance [18]

Numerical simulations were also performed that evaluated the different geometries. These simulations evaluated the experimental blast wall dimensions against a full perimeter wall, modeled as an infinite width in the two-dimensional case. Figure 6-6 shows the overpressure measured at 10 m from the charge at different elevations. As shown, the infinite wall was more effective at reducing overpressure, since the shock wave from the blast can only travel over the top of the wall. Also, the reduction in overpressure varies with elevation of the gauge points.

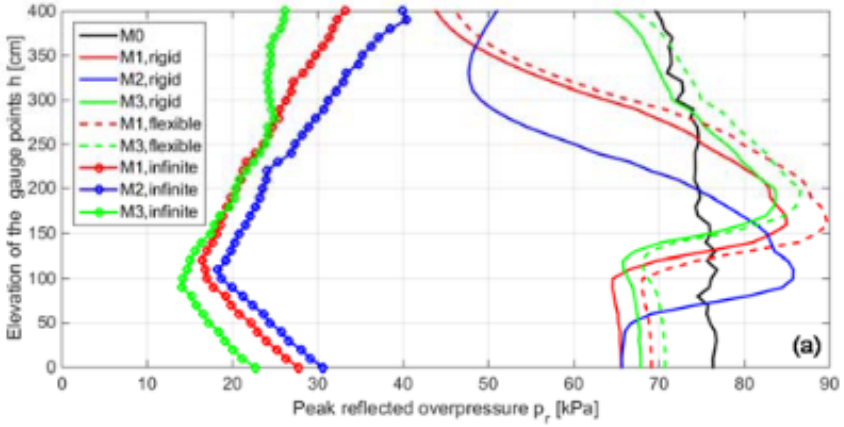

Figure 6-6: Xiao et al. Distribution of Peak Overpressures vs. Elevation [18]

6.6.2. *Vyazmina et al.*

Vyazmina et al. developed a CFD-based method to evaluate protective walls against the effects of hydrogen fast deflagration [19]. Figure 6-7 shows the reservoir burst problem that was modeled with a protective barrier. The wall was placed 9.2 m downstream from the burst location, with an incoming overpressure of 150 mbarg. The wall is 2.5 m x 0.5 m (height x thickness) and considered to have infinite length. Also, the monitoring pints are located upstream and downstream to study the mitigation effects of the wall.

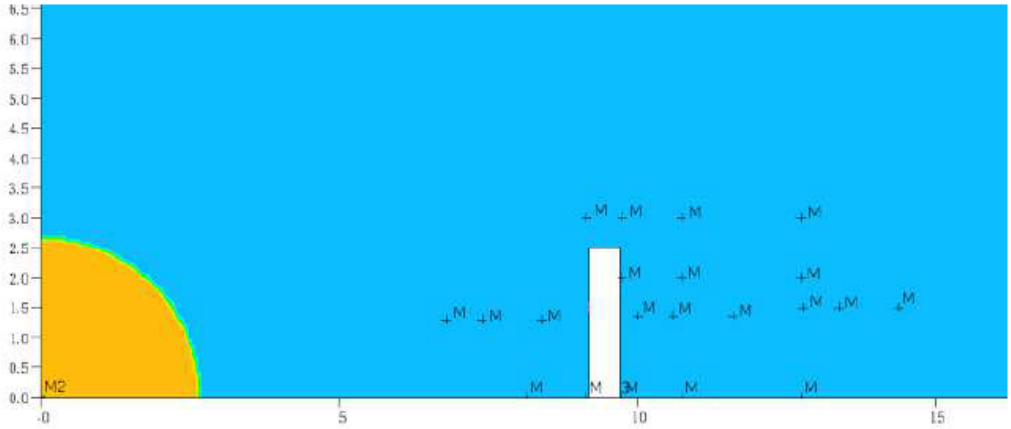

Figure 6-7: Vyazmina et al. Reservoir Burst Problem with Wall, Monitoring Positions [19]

Figure 6-8 shows the effect the wall has on the overpressure downstream of the wall in comparison to the free field configuration. As shown, the overpressure downstream of the wall is reduced. However, the reduction in overpressure decreases as distance from the burst location increases.

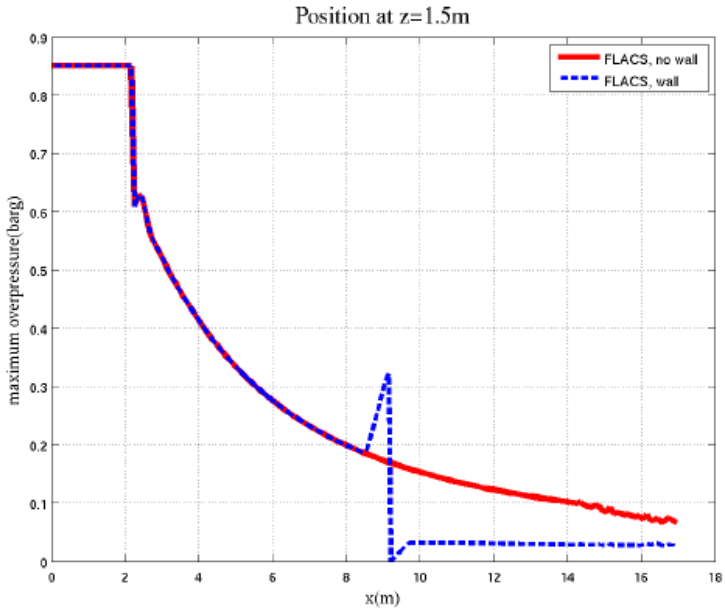

Figure 6-8: Vyazmina, et al., Overpressure vs. Distance [19]

Additionally, a mitigation factor was calculated for the overpressure ($P_{mas\ free\ field}/P_{max\ wall}$) that demonstrates the efficiency of the protective barrier. Figure 6-9 shows the mitigation factor as a

function of distance from the wall. As shown, the mitigation factor decreases as distance from the wall increases. At long distances, the mitigation factor decreases to 1, which means that the pressure downstream of the wall approaches the pressure seen in the free field.

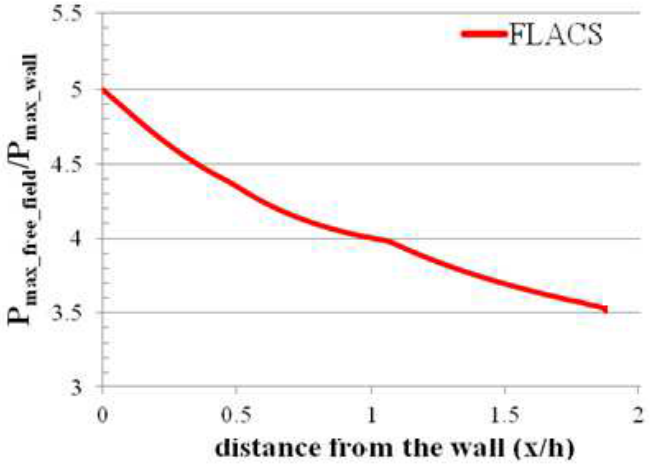

Figure 6-9: Vyazmina et al. Mitigation Factor vs. Distance [19]

6.6.3. Conclusions

There have been many studies conducted on the effectiveness of obstructions in reducing downstream overpressure in addition to those outlined in this section. The general conclusion in these papers is similar in that although there is definitive reduction in overpressure, the magnitude is variable. The reduction in overpressure downstream of an obstruction varies as a function of the design and arrangement of the blast wall as well as the distance from the blast wall. The experiments/models show that the reduction decreases as the distance from the wall increases. Because of these variables, it would be difficult to credit the decrease in overpressure in the calculations performed herein. Although it is reasonable to assume that the overpressure would likely be reduced based on obstructions between the HTEF and NPP, it is difficult to quantify. This may be pursued in future work when the geometry and location of the obstructions are known.

7. CONCLUSION

The risk of an HTEF located near an NPP has been evaluated herein, including the likelihood of an accident and the consequence. The frequency was developed with a bottom-up approach by documenting the components in an HTEF and calculating the cumulative frequency contribution from each component. The frequency of a leak in the evaluated HTEF system is fairly high (~17 expected occurrences/year for a very small leak and ~2 expected occurrences every 100 years for a full rupture). This is because there are 46 modular units that increase the number of components, which increases the likelihood of a leak. Although the frequency of a leak in an HTEF is not negligible, the consequence of a detonation does not detrimentally affect critical targets at the NPP at a distance of 1 km. A full rupture leak was evaluated at different locations in the HTEF system with varying line sizes and system pressures. Also, the consequence of detonation of the high-pressure jet release of hydrogen and the detonation of accumulated hydrogen were evaluated as worst-case scenarios. The largest overpressure seen at a distance of 1 km away from the accident location was ~0.06 psi for detonation of the high-pressure hydrogen jet and ~0.4 psi for detonation of the MCA accumulated hydrogen cloud. This does not challenge the fragility criteria of the critical targets. Note, that consequences for leak sizes smaller than full rupture were not evaluated because the full rupture consequences (worst-case) did not challenge the fragility criteria. Therefore, failure due to a smaller leak size would not be expected to occur. The minimum separation distance was calculated for all of the worst-case scenarios as well. The largest minimum separation distance was 120 m for the high-pressure hydrogen jet and 492 m for the MCA accumulated hydrogen cloud. Both of these separation distances show the opportunity to safely decrease the 1 km assumed distance from the NPP.

REFERENCES

[1] J.-P. Py and A. Capitaine, "Hydrogen Production by High Temperature Electrolysis," Areva/EDF.

[2] I.-1.-X.-. DRAFT, "Techno-economic Analysis of Hydrogen Generation for the "REDACTED" Generating Station," Idaho National Laboratories, Idaho Falls, 2019.

[3] Y. Naimi and A. Antar, "Hydrogen Generation by Water Electrolysis," 22 08 2018. [Online]. Available: https://www.intechopen.com/books/advances-in-hydrogen-generation-technologies/hydrogen-generation-by-water-electrolysis. [Accessed 13 02 2020].

[4] K. Vedros and C. Otani, "Preliminary Probabilistic Risk Assessment of a Light Water Reactor Supplying Process Heat to a Hydrogen Production Plant," Idaho National Laboratories INL/EXT-19-55884, Idaho Falls, 2019.

[5] J1-000-HES-LST-KBJ-50001-00, "Summary of Hazardous Releases," Jordan Cove LNG, August 2017.

[6] INL/EXT-09-16140, "High Temperature Electrolysis for Hydrogen Production from Nuclear Energy - Technology Summary," February 2010.

[7] INL/EXT-06-11232, "Balance of Plant Requirements for a Nuclear Hydrogen Plant," April 2006.

[8] "DOE Hydrogen Incident Reporting Database," [Online]. Available: http://www.h2incidents.org/.

[9] J. LaChance, W. Houf, B. Middleton and L. Fluer, "Analyses to Support Development of Risk-Informed Separation Distances for Hydrogen Codes and Standards," Sandia National Laboratories, SAND2009-0874, March 2009.

[10] J. Spouge, "New Generic Leak Frequencies for Process Equipment," *Process Safety Progress,* vol. 24, no. 4, December 2005.

[11] A. Cox, F. Lees and M. Ang, "Classification of Hazardous Locations," *Institution of Chemical Engineers,* May 2003.

[12] NASA, "Dynamic Pressure," [Online]. Available: https://www.grc.nasa.gov/www/k-12/airplane/dynpress.html. [Accessed 24 2 2020].

[13] U. N. R. Commission, "Regulatory Guide 1.91: Evaluations of Explosions Postulated to Occur at Nearby Facilities and on Transportation Routes near Nuclear Power Plants," April 2013.

[14] C. Bauwens and S. Dorofeev, "Quantifying the Potential Consequences of a Detonation in a Hydrogen Jet Release".

[15] K. Groth, E. Hecht, J. Reynolds, M. Blaylock and E. Carrier, "Methodology for Assessing the Safety of Hydrogen Systems: HyRAM 1.1 Technical Reference Manual," Sandia National Laboratories, SAND2017-2998, March 2017.

[16] M. Kaneshige and J. Shepherd, "Detonation Database," GALCIT Technical Report FM97, [Online]. Available: http://shepherd.caltech.edu/detn_db/html/db.html. [Accessed February 2020].

[17] INL, "System Design Description: 150 kW SOEC System," September 30, 2019.

[18] W. Xiao, M. Andrae, L. Ruediger and N. Gebbeken, "Numerical Prediction of Blast Wall Effectiveness for Structural Protection," *X International Conference on Structural Dynamics, Procedia Engineering,* vol. 199, pp. 2519-2524, 2017.

[19] E. Vyazmina, S. Jallais, A. Beccantini and S. Trelat, "CFD Design of Protective Walls Against

the Effects of Vapor Cloud Fast Deflagration of Hydrogen," in *International Conference on Hydrogen Safety, At Japan*, January 2015.

APPENDIX A. HTEF COMPONENT LIST

Table A-1 shows each component in the HTEF, the general description, as well as the sizes, assumptions, and references. Based on the description from Frick et al. [2], there are 46 different systems and it was assumed they are all fed from a common header and feed into a common header. The system is defined between those two sets of common headers. The components are defined from the P&ID provided in Appendix B by Frick et al. [2].

Table A-1. HTSE System Component Breakdown

Component Name	Description	Size/Specs	Assumptions	Reference
General HTSE Component				
HTSE modular units		46 Modules. Each module with a tee and ball valve type control valve.		Appendix I [2]
HTSE Module Tee		46 Module Tees		Appendix B [2]
HTSE Module Control Valve		46 Module Ball Control Valve		Appendix B [2]
HTSE Module Elbows		4 Elbows		Appendix B [2]
HTSE Module Reducer		4 Reducers		Appendix B [2]
HTSE Module Expander		4 Expanders		Appendix B [2]
Steam/Hydrogen System- 46 Total				
H2/H2O Recycle Loop	Pipe Tee: Mixes with Process Feedwater	254 mm diameter with Control Valve	Control Valve assumed to control quantity of mixture sent through process. Assume 254 mm based on Pipe 301 Size from Tee 4	Appendix J [2]
Check Valve in line with H2/H2O Recycle Loop	Check Valve		Not directly called out in P&ID, but necessary to control flow	
Control Valve in line with H2/H2O Recycle Loop	Control Valve		Not directly called out in P&ID, but necessary to control flow	

Component Name	Description	Size/Specs	Assumptions	Reference
Mix-100	Pipe Tee: Mixes process feed water with recycled H2/H2O mixture	254 mm diameter inlets and 300 mm diameter outlet	Assume Tee 4 match with Mix-100 sizes	Appendix J [2]
Pipe 141	Pipe	300 mm diameter	Assumed size increased from inlets on Mix-100	Appendix J [2]
Control Valve in line with Pipe 141	Control Valve		Not directly called out in P&ID, but necessary to control flow	
Pump/BlowerK103	Blower: Hydrogen recycle blower	9200 m^3/hr	From [2] Spec Sheet in Appendix H	Appendix J & I [2]
Pipe 142	Pipe	300 mm diameter	Same size as 141	Appendix J [2]
RCY-1			Function Unknown	Appendix J [2]
Pipe 143	Pipe	300 mm diameter	Same size as 141	Appendix J [2]
HX-136 (tube side)	Heat Exchanger	19.5 m^2 Connections: Tube Side: 300 mm diameter Inlet and 300 mm diameter Outlet	Assume matches with HX-1 but with 300 mm inlet and outlet on Tube Side	Appendix J [2]
Pipe 144	Pipe	300 mm diameter	Same size as 141	Appendix J [2]

Component Name	Description	Size/Specs	Assumptions	Reference
HX-133 (tube side)	Heat Exchanger	19.5 m^2 Connections: Shell Side: 254 mm Inlet and 203.2 mm Outlet Tube Side: 300 mm Inlet and 300 mm Outlet	Assume matches with HX-1 but with 300 mm inlet and outlet on Tube Side	Appendix J [2]
Pipe 145	Pipe	300 mm diameter	Same size as 141	Appendix J [2]
HX-30	Heat Exchanger	19.5 m^2 Connections: Shell Side: 254 mm Inlet and 203.2 mm Outlet Tube Side: 300 mm Inlet and 300 mm Outlet	Assume matches with HX-1 but with 300 mm inlet and outlet on Tube Side	Appendix J [2]
Inlet to SOEC Stack	Pipe	300 mm diameter	Same size as 141	Appendix J [2]
Control Valve in line with Inlet to SOEC Stack	Control Valve		Not directly called out in P&ID, but necessary to control flow	
SOEC Stacks	40 Stacks per Module.	800 total stacks (20 modules)		Appendix B [2] Fig. 11 + 12
Outlet from SOEC Stack	Pipe	254 mm diameter	Same size as 141	Appendix J [2]
Control Valve in line with Outlet from SOEC Stack	Control Valve		Not directly called out in P&ID, but necessary to control flow	

Component Name	Description	Size/Specs	Assumptions	Reference
HX-133 (shell side)	Heat Exchanger	19.5 m^2 Connections: Shell Side: 254 mm diameter Inlet and 300 mm diameter Outlet	Assume matches with HX-1 but with 254 mm inlet and 300 mm outlet on Shell side	Appendix J [2]
H2/H2O Product Mix	Pipe	300 mm diameter with Control Valve		Appendix J [2]
Control Valve in line with H2/H2O Product Mix	Control Valve: Regulates bypass back through SOEC stack loop		Not directly called out in P&ID, but necessary to control flow	
Tee-4	Pipe Tee: Diverts H2/H2O mixture	254 mm diameter outlets and 300 mm diameter inlet		Appendix J [2]
Pipe 301	Pipe: Feeds HX-1	254 mm diameter with Control Valve	Based on inlet side of the shell on HX-1	Appendix J [2]
Check Valve in line with Pipe 301	Check Valve: Regulates flow through H2 recovery loop		Not directly called out in P&ID, but necessary to control flow	
Control Valve in line with Pipe 301	Control Valve: Regulates flow through H2 recovery loop		Not directly called out in P&ID, but necessary to control flow	
HX-1	Heat Exchanger: Condenser & water preheater	19.5 m^2 Connections: Shell Side: 254 mm diameter Inlet and 203.2 mm diameter Outlet Tube Side: 76.2 mm diameter Inlet and 152.4 mm diameter Outlet	From [2] Spec Sheet	Appendix J [2]
Pipe 302 to H2/H2O	Pipe	203.2 mm diameter	Based on outlet side of shell on HX-1	Appendix J [2]

Component Name	Description	Size/Specs	Assumptions	Reference
Purification				
Hydrogen Purification System- 46 Total				
HX-KO1	Heat Exchanger: Separation Vessel #1 precooler	9 m^2 Connections: Tube Side: 203.2 mm diameter Inlet and 300 mm diameter Outlet	Based on Pipe 302 for inlet and assumed outlet size	Appendix J [2]
Pipe 303	Pipe	300 mm diameter	Based on outlet from HX-KO1	Appendix J [2]
KO-1 Separator	H2 Separation Vessel #1	0.6 m^3 with 300 mm diameter inlet and 254 mm diameter outlets	Assumed outlet size	Appendix J [2]
Pipe 310	Pipe	254 mm diameter with Control Valve	Based on outlet from KO-1	Appendix J [2]
K101	Pump/Blower	9200 m^3/hr	Flow Rate matches Pump/Blower K103	Appendix J [2]
Pipe 311	Pipe	254 mm diameter with Control Valve		Appendix J [2]
HX-K101	Heat Exchanger	9 m^2 Connections: Tube Side: 254 mm diameter Inlet and 203.2 mm diameter Outlet	Assume same as HX-KO1 but with different tube side connection sizes	Appendix J [2]
Pipe 312	Pipe	203.2 mm diameter with Control Valve		Appendix J [2]
Control Valve in line with Pipe 312	Control Valve		Not directly called out in P&ID, but necessary to control flow	
K102 Purification Compressor	Compressor	9200 m^3/hr 152.4 mm diameter outlet		Appendix J [2]
Pipe 313	Pipe	152.4 mm diameter with Control Valve		Appendix J

Component Name	Description	Size/Specs	Assumptions	Reference
				[2]
Control Valve in line with Pipe 313	Control Valve		Not directly called out in P&ID, but necessary to control flow	
HX-3	Heat Exchanger: Feedwater heater #1	41 m^2 Connections: Shell Side: 152.4 mm diameter Inlet and 152.4 mm diameter Outlet	From [2] Spec Sheet	Appendix J [2]
Pipe 314	Pipe	152.4 mm diameter with Control Valve		Appendix J [2]
Control Valve in line with Pipe 314	Control Valve		Not directly called out in P&ID, but necessary to control flow	
HX-KO2	Heat Exchanger: Vessel #2 precooler	0.5 m^2 Connections: Tube Side: 152.4 mm diameter Inlet and 254 mm diameter Outlet		Appendix J [2]
Pipe 315	Pipe	254 mm diameter		
KO-2 Separator	H2 Separation Vessel #2	0.6 m^3 254 mm diameter inlet and 200 mm diameter outlets		Appendix J [2]
Pipe 320	Pipe	200 mm diameter with Control Valve		Appendix J [2]
Control Valve in line with Pipe 320	Control Valve		Not directly called out in P&ID, but necessary to control flow	
K201	Pump/Blower	9200 m^3/hr	Flow Rate matches Pump/Blower K103	Appendix J [2]
Pipe 321	Pipe	200 mm diameter		Appendix J [2]
HX-K201	Heat Exchanger	0.5 m^2		Appendix J

Component Name	Description	Size/Specs	Assumptions	Reference
		Connections: Tube Side: 200 mm diameter Inlet and 101.6 mm diameter Outlet		[2]
Pipe 322	Pipe	101.6 mm diameter with Control Valve		Appendix J [2]
Control Valve in line with Pipe 322	Control Valve		Not directly called out in P&ID, but necessary to control flow	
K202 Purification Compressor	Compressor	9200 m^3/hr	Flow Rate matches Pump/Blower K103	Appendix J [2]
Pipe 323	Pipe	101.6 mm diameter with Control Valve		Appendix J [2]
Control Valve in line with Pipe 322	Control Valve		Not directly called out in P&ID, but necessary to control flow	
HX-17	Heat Exchanger: Feedwater Heater #2	61.5 m^2 Connections: Shell Side: 101.6 mm diameter Inlet and 88.9 mm diameter Outlet Tube Side: 31.75 mm diameter Inlet and 31.75 mm diameter Outlet	From [2] Spec Sheet	Appendix J [2]
Pipe 324	Pipe	88.9 mm with control valve		Appendix J [2]
Control Valve in line with Pipe 324	Control Valve		Not directly called out in P&ID, but necessary to control flow	
HX-KO3	Heat Exchanger: Separation Vessel #3 precooler	36 m^2 Connections: Tube Side: 88.9 mm diameter Inlet and 254 mm diameter Outlet		Appendix J [2]

Component Name	Description	Size/Specs	Assumptions	Reference
Pipe 325	Pipe	254 mm diameter with Control Valve		Appendix J [2]
Control Valve in line with Pipe 325	Control Valve		Not directly called out in P&ID, but necessary to control flow	
KO-3 Separator	H2 Separation Vessel #3	0.6 m^3 254 mm diameter inlet and 200 mm diameter outlets		Appendix J [2]
Pipe 330	Pipe	200 mm diameter with Control Valve		Appendix J [2]
Control Valve in line with Pipe 330	Control Valve		Not directly called out in P&ID, but necessary to control flow	
X-100	Condenser	200 mm diameter Inlet and Outlet		Appendix J [2]
Hydrogen Product Sent to Storage/Usage Header- 46 Total				
H2 Product		Approx. 9200 m^3/hr leads to storage vessels		Appendix J [2]
Pipe 440	Pipe	200 mm diameter		Appendix J [2]
K-301	Pump/Blower	9200 m^3/hr	Flow Rate matches Pump/Blower K103	Appendix J [2]
Pipe 441	Pipe	200 mm diameter		Appendix J [2]
K301 Intercooler	Heat Exchanger	200 mm diameter inlet and outlet		Appendix J [2]
Pipe 442	Pipe	200 mm diameter		Appendix J [2]
K-302	Pump/Blower	9200 m^3/hr	Flow Rate matches Pump/Blower K103	Appendix J [2]

Component Name	Description	Size/Specs	Assumptions	Reference
Pipe 451	Pipe	200 mm diameter		Appendix J [2]
K302 Intercooler	Heat Exchanger	200 mm diameter inlet and outlet		Appendix J [2]
Pipe 452	Pipe	200 mm diameter		Appendix J [2]
K-303	Pump/Blower	9200 m^3/hr	Flow Rate matches Pump/Blower K103	Appendix J [2]
Pipe 453	Pipe	200 mm diameter		Appendix J [2]
K303 Intercooler	Heat Exchanger	200 mm diameter inlet and outlet		Appendix J [2]
Pipe 454 to Common Header	Pipe	200 mm diameter with check valve and control/isolation valve	Feeds to common header	Appendix J [2]
Check Valve in line with Pipe 454	Check Valve		Not directly called out in P&ID, but necessary to control flow	
Control Valve in line with Pipe 454	Control Valve		Not directly called out in P&ID, but necessary to control flow	
Pressure Relief Valve in line with Pipe 454	Pressure Relief Valve	Route to relief vent	Not directly called out in P&ID, but necessary for safety	

APPENDIX B. GENERIC COMPONENT LEAKAGE FREQUENCIES

The identification of component failure rates from other industries is an appropriate initial phase to the Bayesian process. Component leakage frequencies have been identified from sources related to the chemical processing, compressed gas, nuclear power, and offshore petroleum industries. Sources used in the data analysis were obtained from a narrow range of available studies listed below. They varied in nomenclature, component specifics, component classification, and data reliability. The identified component leakage frequencies are provided in Table B-1. Because of the scarcity of component leakage data, the data for specific component types were binned together into one component category. For example, leakage data for both reciprocating and centrifugal compressors were combined in the Bayesian analysis to generate generic compressor leakage rates.

Most of the identified data sources provided leakage frequencies as a coarse function of leak size. In general, the leakage frequencies were binned into one of the following leak sizes:

- Small Leak
- Large Leak
- Rupture

The definition of each of these leak sizes varied between sources. Thus, based on the leakage size description presented in the available data sources, some judgment was needed to bin the available data consistently into one of these three groups. Furthermore, these definitions are different than the definitions used in this study. The relationship between the generic leak size definitions and the definitions used in this study are shown below. Note that no leakage frequencies were identified in the literature for "very small" and "minor" leaks that are less than 0.1% of the total flow area.

- Very Small- Leak area is 0.01 % of total flow area (no generic data was available for this size leak)
- Minor – Leak area is 0.1% of total flow area (no generic data was available for this size leak)
- Small Leak = Medium – Leak area is 1% of total flow area
- Large Leak = Major – Leak area is 10% of total flow area
- Rupture – Leak area is 100% of total flow area (the same definition is used in the referenced sources and this study)

Table B-1. Generic Component Leak Frequencies

Component	Specific Component Type	Severity	Frequency	Units	Leak Size Description	Source Type	Source
Compressor							
Compressor	Centrifugal	Small Leak	2.00E-03	Per Year	>1 mm	Hydrocarbon Process	Spouge, John, "New Generic Leak Frequencies for Process Equipment, “Process Safety Progress, Vol. 24, No. 4, 2005
Compressor	Motor Driven	Small Leak	2.63E-03	Per Year	No definition of leak size was provided	Compressed Gas	Savannah River Site, "Generic Data Base Development," WSRC-TR-93-263, June 1993.
Compressor	Reciprocating	Small Leak	2.70E-02	Per Year	>1 mm	Hydrocarbon Process	Spouge, John, "New Generic Leak Frequencies for Process Equipment, “Process Safety Progress, Vol. 24, No. 4, 2005
Compressor	Centrifugal	Rupture	2.00E-06	Per Year	> 50 mm	Hydrocarbon Process	Spouge, John, "New Generic Leak Frequencies for Process Equipment, “Process Safety Progress, Vol. 24, No. 4, 2005
Compressor	Reciprocating	Rupture	1.10E-05	Per Year	> 50 mm	Hydrocarbon Process	Spouge, John, "New Generic Leak Frequencies for Process Equipment, “Process Safety Progress, Vol. 24, No. 4, 2005
Compressor	Motor Driven	Rupture	8.76E-05	Per Year	No definition of leak size was provided	Compressed Gas	Savannah River Site, "Generic Data Base Development," WSRC-TR-93-263, June 1993.
Cylinder							
Cylinder	Pressure	Small Leak	8.76E-04	Per Year	No definition of leak size was provided	Compressed Gas	Savannah River Site, "Generic Data Base Development," WSRC-TR-93-263, June 1993.
Vessel	Pressure	Large Leak	1.00E-05	Per Year	10 mm diameter	General	Guidelines for quantitative risk assessment. "Purple Book" CPR 18E, ed. 1, 1999

Component	Specific Component	Severity	Frequency	Units	Leak Size	Source Type	Source
Tube Trailer	Transportation	Rupture	5.00E-07	Per Year	Instantaneous release	General	Guidelines for quantitative risk assessment. "Purple Book" CPR 18E, ed. 1, 1999
Cylinder	Gas	Rupture	1.00E-06	Per Year	Instantaneous Release	General	Guidelines for quantitative risk assessment. "Purple Book" CPR 18E, ed. 1, 1999
Filter							
Filter	No Additional Information	Small Leak	8.90E-04	Per Year	>1 mm	Hydrocarbon Process	Spouge, John, "New Generic Leak Frequencies for Process Equipment, “Process Safety Progress, Vol. 24, No. 4, 2005
Filter	No Additional Information	Small Leak	2.63E-02	Per Year	No definition of leak size was provided	Compressed Gas	Savannah River Site, "Generic Data Base Development," WSRC-TR-93-263, June 1993.
Filter	No Additional Information	Rupture	4.38E-03	Per Year	No definition of leak size was provided	Compressed Gas	Savannah River Site, "Generic Data Base Development," WSRC-TR-93-263, June 1993.
Flange							
Flange	No Additional Information	Small Leak	4.70E-06	Per Year	Hole diameter from original source was not stated; EIGA assumed 2% flow area	Compressed Gas	EIGA, "Determination of Safety Distances," IGC Doc 75/01/E/rev, 2001

Component	Specific Component	Severity	Frequency	Units	Leak Size	Source Type	Source
Flanged Joints	Flanged, 2 inch diameter	Small Leak	3.20E-05	Per Year	> 1 mm	Hydrocarbon Process	Spouge, John, "New Generic Leak Frequencies for Process Equipment, “Process Safety Progress, Vol. 24, No. 4, 2005
Flanged Joints	Flanged, 6 inch diameter	Small Leak	4.30E-05	Per Year	> 1 mm	Hydrocarbon Process	Spouge, John, "New Generic Leak Frequencies for Process Equipment, “Process Safety Progress, Vol. 24, No. 4, 2005
Flange	No Additional Information	Small Leak	8.76E-05	Per Year	50 gpm (water) or less	Nuclear	Eide, S.A, Khericha, S.T., Calley, M.B., Johnson, D.A., Marteeny, M.L., "Component External Leakage and Rupture Frequency Estimates," EGG-SSRE-9639, Nov 1991.
Flanged Joints	Flanged, 18 inch diameter	Small Leak	1.20E-04	Per Year	> 1 mm	Hydrocarbon Process	Spouge, John, "New Generic Leak Frequencies for Process Equipment, “Process Safety Progress, Vol. 24, No. 4, 2005
Flange	No Additional Information	Small Leak	1.70E-04	Per Year	Hole diameter from original source was not stated; EIGA assumed 2% flow area	Chemical Process	EIGA, "Determination of Safety Distances," IGC Doc 75/01/E/rev, 2001
Flange	No Additional Information	Small Leak	8.76E-04	Per Year	No definition of leak size was provided	Compressed Gas	Savannah River Site, "Generic Data Base Development," WSRC-TR-93-263, June 1993.
Flange	All Sizes	Small Leak	1.00E-03	Per Year	10% of flange area	Chemical Process	Cox, A.W., Lees, F.P., Ang, M.L., "Classifications of Hazardous Locations," Institution of Chemical Engineers, 2003
Flange	No Additional Information	Small Leak	2.60E-03	Per Year	Hole diameter from original source was	Hydrogen Fueling Process	EIGA, "Determination of Safety Distances," IGC Doc 75/01/E/rev, 2001

Component	Specific Component	Severity	Frequency	Units	Leak Size	Source Type	Source
					not stated; EIGA assumed 2% flow area		
Flange	Gasket	Small Leak	2.63E-02	Per Year	No definition of leak size was provided	Nuclear	NUREG-75/014, "Reactor Safety Study: An Assessment of Accident Risks in U.S. Commercial Nuclear Power Plants," WASH-1400, Oct 1975
Flanged Joints	Flanged, 6 inch diameter	Rupture	3.60E-07	Per Year	> 50 mm	Hydrocarbon Process	Spouge, John, "New Generic Leak Frequencies for Process Equipment, “Process Safety Progress, Vol. 24, No. 4, 2005
Flanged Joints	Flanged, 18 inch diameter	Rupture	1.10E-06	Per Year	> 50 mm	Hydrocarbon Process	Spouge, John, "New Generic Leak Frequencies for Process Equipment, “Process Safety Progress, Vol. 24, No. 4, 2005

Component	Specific Component	Severity	Frequency	Units	Leak Size	Source Type	Source
Flange	No Additional Information	Rupture	3.50E-07	Per Year	Hole diameter from original source was not stated; EIGA assumed 100% flow area	Compressed Gas	EIGA, "Determination of Safety Distances," IGC Doc 75/01/E/rev, 2001
Flange	No Additional Information	Rupture	8.76E-07	Per Year	>50 gpm (water) or complete failure	Nuclear	Eide, S.A, Khericha, S.T., Calley, M.B., Johnson, D.A., Marteeny, M.L., "Component External Leakage and Rupture Frequency Estimates," EGG-SSRE-9639, Nov 1991.
Flange	No Additional Information	Rupture	8.76E-06	Per Year	No definition of leak size was provided	Compressed Gas	Savannah River Site, "Generic Data Base Development," WSRC-TR-93-263, June 1993.
Flange	No Additional Information	Rupture	1.70E-05	Per Year	Hole diameter from original source was not stated; EIGA assumed 100% flow area	Chemical Process	EIGA, "Determination of Safety Distances," IGC Doc 75/01/E/rev, 2001
Flange	All Sizes	Rupture	1.00E-04	Per Year	100% of flange area	Chemical Process	Cox, A.W., Lees, F.P., Ang, M.L., "Classifications of Hazardous Locations," Institution of Chemical Engineers, 2003

Component	Specific Component	Severity	Frequency	Units	Leak Size	Source Type	Source
Hose							
Hose	No Additional Information	Small Leak	1.00E-01	Per Year	Hole diameter from original source was not stated; EIGA assumed 2% flow area	Hydrogen Fueling Process	EIGA, "Determination of Safety Distances," IGC Doc 75/01/E/rev, 2001
Hose	Transportation, Tube Trailer	Small Leak	3.50E-01	Per Year	10% of hose diameter (1% of area)	General	Guidelines for quantitative risk assessment. "Purple Book" CPR 18E, ed. 1, 1999
Hose	No Additional Information	Large Leak	1.00E-02	Per Year	Hole diameter from original source was not stated; EIGA assumed 20% flow area	Hydrogen Fueling Process	EIGA, "Determination of Safety Distances," IGC Doc 75/01/E/rev, 2001
Hose	No Additional Information	Rupture	3.40E-04	Per Year	Hole diameter from original source was not stated; EIGA assumed 100% flow area	Hydrogen Fueling Process	EIGA, "Determination of Safety Distances," IGC Doc 75/01/E/rev, 2001

Component	Specific Component	Severity	Frequency	Units	Leak Size	Source Type	Source
Hose	No Additional Information	Rupture	1.00E-03	Per Year	Hole diameter from original source was not stated; EIGA assumed 100% flow area	Hydrogen Fueling Process	EIGA, "Determination of Safety Distances," IGC Doc 75/01/E/rev, 2001
Hose	No Additional Information	Rupture	4.99E-03	Per Year	Hole diameter was not stated	Process Equipment Data	Guidelines for Process Equipment Reliability Data with Data Tables, Center for Chemical Process Safety of the American Institute of Chemical Engineers, 1989.
Hose	Transportation, Tube Trailer	Rupture	3.50E-02	Per Year	100% of hose flow area	General	Guidelines for quantitative risk assessment. "Purple Book" CPR 18E, ed. 1, 1999
Instrument							
Instrument	0.5 inch	Small Leak	2.30E-04	Per Year	>1 mm	Hydrocarbon Process	Spouge, John, "New Generic Leak Frequencies for Process Equipment, “Process Safety Progress, Vol. 24, No. 4, 2005
Joints							
Joints	No Additional Information	Small Leak	3.60E-03	Per Year	Hole diameter from original source was not stated; EIGA assumed 2% flow area	Hydrogen Fueling Process	EIGA, "Determination of Safety Distances," IGC Doc 75/01/E/rev, 2001

Component	Specific Component	Severity	Frequency	Units	Leak Size	Source Type	Source
Joints	No Additional Information	Small Leak	3.30E-02	Per Year	Hole diameter from original source was not stated; EIGA assumed 2% flow area	Hydrogen Fueling Process	EIGA, "Determination of Safety Distances," IGC Doc 75/01/E/rev, 2001
Joints	No Additional Information	Large Leak	4.00E-03	Per Year	Hole diameter from original source was not stated; EIGA assumed 20% flow area	Hydrogen Fueling Process	EIGA, "Determination of Safety Distances," IGC Doc 75/01/E/rev, 2001
Joints	No Additional Information	Large Leak	4.99E-03	Per Year	10% cross sectional area or more	Process Equipment Data	Guidelines for Process Equipment Reliability Data with Data Tables, Center for Chemical Process Safety of the American Institute of Chemical Engineers, 1989.

Component	Specific Component	Severity	Frequency	Units	Leak Size	Source Type	Source
Joints	No Additional Information	Large Leak	5.00E-03	Per Year	Hole diameter from original source was not stated; EIGA assumed 20% flow area	Hydrogen Fueling Process	EIGA, "Determination of Safety Distances," IGC Doc 75/01/E/rev, 2001

Joints	No Additional Information	Rupture	5.00E-04	Per Year	Hole diameter from original source was not stated; EIGA assumed 100% flow area	Hydrogen Fueling Process	EIGA, "Determination of Safety Distances," IGC Doc 75/01/E/rev, 2001
Joints	No Additional Information	Rupture	5.00E-04	Per Year	Hole diameter from original source was not stated; EIGA assumed 100% flow area	Hydrogen Fueling Process	EIGA, "Determination of Safety Distances," IGC Doc 75/01/E/rev, 2001
Pipe							
Pipe	Pipe Diameter is Greater than or Equal to 150 mm	Small Leak	5.00E-07	Per Meter Year	10% of pipe diameter (1% of area)	General	Guidelines for quantitative risk assessment. "Purple Book" CPR 18E, ed. 1, 1999
Pipe	Pipe Diameter is between 75 mm to 150 mm	Small Leak	2.00E-06	Per Meter Year	10% of pipe diameter (1% of area)	General	Guidelines for quantitative risk assessment. "Purple Book" CPR 18E, ed. 1, 1999
Pipe	Pipe Diameter Equals 100 mm	Small Leak	2.50E-06	Per Meter Year	Hole diameter from original source was not stated; EIGA assumed 2% flow area	Hydrogen Fueling Process	EIGA, "Determination of Safety Distances," IGC Doc 75/01/E/rev, 2001
Pipe	Pipe Diameter is Greater than	Small Leak	3.00E-06	Per Meter	5% of flow area	Chemical Process	Rjinmond, Openbaar Lichaam; Risk Analysis of Six Potentially Hazardous Industrial

Component	Specific Component	Severity	Frequency	Units	Leak Size	Source Type	Source
	150 mm			Year			Objects in the Rijnmond Area, A Pilot Study; COVO; 1982
Pipe	Pipe Diameter is Less than 75 mm	Small Leak	5.00E-06	Per Meter Year	10% of pipe diameter (1% of area)	General	Guidelines for quantitative risk assessment. "Purple Book" CPR 18E, ed. 1, 1999
Pipe	Pipe Diameter Equals 100 mm	Small Leak	6.00E-06	Per Meter Year	Hole diameter from original source was not stated; EIGA assumed 2% flow area	Hydrogen Fueling Process	EIGA, "Determination of Safety Distances," IGC Doc 75/01/E/rev, 2001
Pipe	Pipe Diameter Equals 100 mm	Small Leak	6.00E-06	Per Meter Year	Hole diameter from original source was not stated; EIGA assumed 2% flow area	Hydrogen Fueling Process	EIGA, "Determination of Safety Distances," IGC Doc 75/01/E/rev, 2001
Pipe	Pipe Diameter is between 50 mm and 150 mm	Small Leak	6.00E-06	Per Meter Year	5% of flow area	Chemical Process	Rjinmond, Openbaar Lichaam; Risk Analysis of Six Potentially Hazardous Industrial Objects in the Rijnmond Area, A Pilot Study; COVO; 1982
Pipe	Pipe Diameter Equals 25 mm	Small Leak	7.50E-06	Per Meter Year	Hole diameter from original source was not stated; EIGA assumed 2%	Hydrogen Fueling Process	EIGA, "Determination of Safety Distances," IGC Doc 75/01/E/rev, 2001

Component	Specific Component	Severity	Frequency	Units	Leak Size	Source Type	Source
					flow area		
Pipe	No Additional Information	Small Leak	8.01E-06	Per Meter Year	50 gpm (water) or less	Nuclear	Eide, S.A, Khericha, S.T., Calley, M.B., Johnson, D.A., Marteeny, M.L., "Component External Leakage and Rupture Frequency Estimates," EGG-SSRE-9639, Nov 1991.
Pipe	No Additional Information	Small Leak	8.01E-06	Per Meter Year	No definition of leak size was provided	Chemical Process	Savannah River Site, "Generic Data Base Development," WSRC-TR-93-263, June 1993.
Pipe	Pipe Diameter Equals 300 mm	Small Leak	1.00E-05	Per Meter Year	1% cross sectional area	Chemical Process	Cox, A.W., Lees, F.P., Ang, M.L., "Classifications of Hazardous Locations," Institution of Chemical Engineers, 2003

Component	Specific Component	Severity	Frequency	Units	Leak Size	Source Type	Source
Pipe	Pipe Diameter is Less than or Equal to 50 mm	Small Leak	1.00E-05	Per Meter Year	5% of flow area	Chemical Process	Rjinmond, Openbaar Lichaam; Risk Analysis of Six Potentially Hazardous Industrial Objects in the Rijnmond Area, A Pilot Study; COVO; 1982
Pipe	Pipe Diameter Equals 450 mm	Small Leak	1.10E-05	Per Meter Year	>1 mm	Hydrocarbon Process	Spouge, John, "New Generic Leak Frequencies for Process Equipment, “Process Safety Progress, Vol. 24, No. 4, 2005
Pipe	Pipe Diameter Equals 150 mm	Small Leak	2.00E-05	Per Meter Year	>1 mm	Hydrocarbon Process	Spouge, John, "New Generic Leak Frequencies for Process Equipment, “Process Safety Progress, Vol. 24, No. 4, 2005
Pipe	Pipe Diameter Equals 100 mm	Small Leak	3.00E-05	Per Meter Year	1% cross sectional area	Chemical Process	Cox, A.W., Lees, F.P., Ang, M.L., "Classifications of Hazardous Locations," Institution of Chemical Engineers, 2003
Pipe	Pipe Diameter Equals 50 mm	Small Leak	5.70E-05	Per Meter Year	>1 mm	Hydrocarbon Process	Spouge, John, "New Generic Leak Frequencies for Process Equipment, “Process Safety Progress, Vol. 24, No. 4, 2005
Pipe	No Additional Information	Small Leak	8.01E-05	Per Meter Year	No definition of leak size was provided	Compressed Gas	Savannah River Site, "Generic Data Base Development," WSRC-TR-93-263, June 1993.
Pipe	Pipe Diameter Equals 25 mm	Small Leak	1.00E-04	Per Meter Year	1% cross sectional area	Chemical Process	Cox, A.W., Lees, F.P., Ang, M.L., "Classifications of Hazardous Locations," Institution of Chemical Engineers, 2003
Pipe	Pipe Diameter Equals 50 mm	Small Leak	1.00E-04	Per Meter Year	1% cross sectional area	Chemical Process	Cox, A.W., Lees, F.P., Ang, M.L., "Classifications of Hazardous Locations," Institution of Chemical Engineers, 2003

Tubing	No Additional Information	Small Leak	8.01E-04	Per Meter Year	No definition of leak size was provided	Compressed Gas	Savannah River Site, "Generic Data Base Development," WSRC-TR-93-263, June 1993.
Pipe	Pipe Diameter is Greater than 150 mm	Large Leak	1.00E-07	Per Meter Year	20% of flow area	Chemical Process	Rjinmond, Openbaar Lichaam; Risk Analysis of Six Potentially Hazardous Industrial Objects in the Rijnmond Area, A Pilot Study; COVO; 1982
Pipe	Pipe Diameter Equals 100 mm	Large Leak	3.00E-07	Per Meter Year	Hole diameter from original source was not stated; EIGA assumed 20% flow area	Hydrogen Fueling Process	EIGA, "Determination of Safety Distances," IGC Doc 75/01/E/rev, 2001
Pipe	Pipe Diameter is between 50 mm and 150 mm	Large Leak	3.00E-07	Per Meter Year	20% of flow area	Chemical Process	Rjinmond, Openbaar Lichaam; Risk Analysis of Six Potentially Hazardous Industrial Objects in the Rijnmond Area, A Pilot Study; COVO; 1982
Pipe	Pipe Diameter Equals 100 mm	Large Leak	6.00E-07	Per Meter Year	Hole diameter from original source was not stated; EIGA assumed 20% flow area	Hydrogen Fueling Process	EIGA, "Determination of Safety Distances," IGC Doc 75/01/E/rev, 2001

Component	Specific Component	Severity	Frequency	Units	Leak Size	Source Type	Source
Pipe	Pipe Diameter Equals 100 mm	Large Leak	7.50E-07	Per Meter Year	Hole diameter from original source was not stated; EIGA assumed 20% flow area	Hydrogen Fueling Process	EIGA, "Determination of Safety Distances," IGC Doc 75/01/E/rev, 2001
Pipe	Pipe Diameter is Less than or Equal to 50 mm	Large Leak	1.00E-06	Per Meter Year	20% of flow area	Chemical Process	Rjinmond, Openbaar Lichaam; Risk Analysis of Six Potentially Hazardous Industrial Objects in the Rijnmond Area, A Pilot Study; COVO; 1982

Component	Specific Component	Severity	Frequency	Units	Leak Size	Source Type	Source
Pipe	Pipe Diameter Equals 25 mm	Large Leak	2.00E-06	Per Meter Year	Hole diameter from original source was not stated; EIGA assumed 20% flow area	Hydrogen Fueling Process	EIGA, "Determination of Safety Distances," IGC Doc 75/01/E/rev, 2001
Pipe	Pipe Diameter Equals 300 mm	Large Leak	3.00E-06	Per Meter Year	10% cross sectional area	Chemical Process	Cox, A.W., Lees, F.P., Ang, M.L., "Classifications of Hazardous Locations," Institution of Chemical Engineers, 2003
Pipe	Pipe Diameter Equals 100 mm	Large Leak	6.00E-06	Per Meter Year	10% cross sectional area	Chemical Process	Cox, A.W., Lees, F.P., Ang, M.L., "Classifications of Hazardous Locations," Institution of Chemical Engineers, 2003
Pipe	Pipe Diameter Equals 25 mm	Large Leak	1.00E-05	Per Meter Year	10% cross sectional area	Chemical Process	Cox, A.W., Lees, F.P., Ang, M.L., "Classifications of Hazardous Locations," Institution of Chemical Engineers, 2003
Pipe	Pipe Diameter Equals 50 mm	Large Leak	1.00E-05	Per Meter Year	10% cross sectional area	Chemical Process	Cox, A.W., Lees, F.P., Ang, M.L., "Classifications of Hazardous Locations," Institution of Chemical Engineers, 2003

Component	Specific Component	Severity	Frequency	Units	Leak Size	Source Type	Source
Pipe	Pipe Diameter Equals 100 mm	Rupture	3.00E-08	Per Meter Year	Hole diameter from original source was not stated; EIGA assumed 100% flow area	Hydrogen Fueling Process	EIGA, "Determination of Safety Distances," IGC Doc 75/01/E/rev, 2001

Pipe	Pipe Diameter Equals 450 mm	Rupture	4.20E-08	Per Meter Year	>50 mm	Hydrocarbon Process	Spouge, John, "New Generic Leak Frequencies for Process Equipment, “Process Safety Progress, Vol. 24, No. 4, 2005
Pipe	Pipe Diameter Equals 100 mm	Rupture	6.00E-08	Per Meter Year	Hole diameter from original source was not stated; EIGA assumed 100% flow area	Hydrogen Fueling Process	EIGA, "Determination of Safety Distances," IGC Doc 75/01/E/rev, 2001
Pipe	Pipe Diameter Equals 150 mm	Rupture	7.70E-08	Per Meter Year	>50 mm	Hydrocarbon Process	Spouge, John, "New Generic Leak Frequencies for Process Equipment, “Process Safety Progress, Vol. 24, No. 4, 2005
Pipe	No Additional Information	Rupture	8.01E-08	Per Meter Year	>50 gpm (water) or complete failure	Nuclear	Eide, S.A, Khericha, S.T., Calley, M.B., Johnson, D.A., Marteeny, M.L., "Component External Leakage and Rupture Frequency Estimates," EGG-SSRE-9639, Nov 1991.

Component	Specific Component	Severity	Frequency	Units	Leak Size	Source Type	Source
Pipe	Pipe Diameter Equals 300 mm	Rupture	1.00E-07	Per Meter Year	100% cross sectional area	Chemical Process	Cox, A.W., Lees, F.P., Ang, M.L., "Classifications of Hazardous Locations," Institution of Chemical Engineers, 2003

Pipe	Pipe Diameter is Greater than or Equal to 150 mm	Rupture	1.00E-07	Per Meter Year	100% of flow area	General	Guidelines for quantitative risk assessment. "Purple Book" CPR 18E, ed. 1, 1999
Pipe	Pipe Diameter Equals 100 mm	Rupture	2.30E-07	Per Meter Year	Hole diameter from original source was not stated; EIGA assumed 100% flow area	Hydrogen Fueling Process	EIGA, "Determination of Safety Distances," IGC Doc 75/01/E/rev, 2001
Pipe	No Additional Information	Rupture	2.67E-07	Per Meter Year	No definition of leak size was provided	Chemical Process	Savannah River Site, "Generic Data Base Development," WSRC-TR-93-263, June 1993.
Pipe	Pipe Diameter Equals 100 mm	Rupture	3.00E-07	Per Meter Year	100% cross sectional area	Chemical Process	Cox, A.W., Lees, F.P., Ang, M.L., "Classifications of Hazardous Locations," Institution of Chemical Engineers, 2003
Pipe	Pipe Diameter is between 75 mm to 150 mm	Rupture	3.00E-07	Per Meter Year	100% of flow area	General	Guidelines for quantitative risk assessment. "Purple Book" CPR 18E, ed. 1, 1999
Pipe	No Additional Information	Rupture	3.20E-07	Per Meter Year	>50 gpm (water) or complete failure	Nuclear	Eide, S.A, Khericha, S.T., Calley, M.B., Johnson, D.A., Marteeny, M.L., "Component External Leakage and Rupture Frequency Estimates," EGG-SSRE-9639, Nov 1991.
Pipe	Pipe Diameter Equals 25 mm	Rupture	4.60E-07	Per Meter Year	Hole diameter from original source was not stated; EIGA assumed 100% flow	Hydrogen Fueling Process	EIGA, "Determination of Safety Distances," IGC Doc 75/01/E/rev, 2001

Component	Specific Component	Severity	Frequency	Units	Leak Size	Source Type	Source
					area		
Pipe	Pipe Diameter Equals 25 mm	Rupture	1.00E-06	Per Meter Year	100% cross sectional area	Chemical Process	Cox, A.W., Lees, F.P., Ang, M.L., "Classifications of Hazardous Locations," Institution of Chemical Engineers, 2003
Pipe	Pipe Diameter Equals 50 mm	Rupture	1.00E-06	Per Meter Year	100% cross sectional area	Chemical Process	Cox, A.W., Lees, F.P., Ang, M.L., "Classifications of Hazardous Locations," Institution of Chemical Engineers, 2003
Pipe	Pipe Diameter is Less than 75 mm	Rupture	1.00E-06	Per Meter Year	100% of flow area	General	Guidelines for quantitative risk assessment. "Purple Book" CPR 18E, ed. 1, 1999
Pipe	No Additional Information	Rupture	2.67E-06	Per Meter Year	No definition of leak size was provided	Compressed Gas	Savannah River Site, "Generic Data Base Development," WSRC-TR-93-263, June 1993.
Tubing	No Additional Information	Rupture	2.67E-05	Per Meter Year	No definition of leak size was provided	Compressed Gas	Savannah River Site, "Generic Data Base Development," WSRC-TR-93-263, June 1993.
Pipe	Small Bore Equals 16 mm	Rupture	5.00E-04	Per Meter Year	100% cross sectional area	Chemical Process	Cox, A.W., Lees, F.P., Ang, M.L., "Classifications of Hazardous Locations," Institution of Chemical Engineers, 2003
Pressure Relief Device							

Component	Specific Component	Severity	Frequency	Units	Leak Size	Source Type	Source
Pressure Relief Device	All types	Inadvertent opening	2.00E-05	Per Year	Maximum release rate	General	Guidelines for quantitative risk assessment. "Purple Book" CPR 18E, ed. 1, 1999
Pressure Relief Device	Safety relief valve	Inadvertent opening	4.45E-03	Per Year	Maximum release rate	Nuclear	NUREG/CR-6928, "Industry-Average Performance for components and Initiating Events at U.S. Commercial Nuclear Power Plants," February 2007
Pressure Relief Device	Pressure relief valve	Inadvertent opening	8.76E-02	Per Year	Maximum release rate	Nuclear	NUREG-75/014, "Reactor Safety Study: An Assessment of Accident Risks in U.S. Commercial Nuclear Power Plants," WASH-1400, Oct 1975

Component	Specific Component	Severity	Frequency	Units	Leak Size	Source Type	Source
Pump							
Pump	Canned Pumps	Small Leak	5.00E-05	Per Year	10% of connecting pipe diameter (1% of area)	General	Guidelines for quantitative risk assessment. "Purple Book" CPR 18E, ed. 1, 1999
Pump	Pumps	Small Leak	5.00E-04	Per Year	10% of connecting pipe diameter (1% of area)	General	Guidelines for quantitative risk assessment. "Purple Book" CPR 18E, ed. 1, 1999
Pump	Motor-driven	Small Leak	1.01E-03	Per Year	1 to 50 gpm (water)	Nuclear	NUREG/CR-6928, "Industry-Average Performance for components and Initiating Events at U.S. Commercial Nuclear Power Plants," February 2007
Pump	Centrifugal	Small Leak	1.80E-03	Per Year	>1 mm	Hydrocarbon Process	Spouge, John, "New Generic Leak Frequencies for Process Equipment, “Process Safety Progress, Vol. 24, No. 4, 2005
Pump	Pumps	Small Leak	3.00E-03	Per Year	1% cross sectional area of connecting pipe	Chemical Process	Cox, A.W., Lees, F.P., Ang, M.L., "Classifications of Hazardous Locations," Institution of Chemical Engineers, 2003
Pump	Reciprocating	Small Leak	3.70E-03	Per Year	>1 mm	Hydrocarbon Process	Spouge, John, "New Generic Leak Frequencies for Process Equipment, “Process Safety Progress, Vol. 24, No. 4, 2005
Pump	Motor-, Turbine-, and Diesel-Driven	Small Leak	8.76E-03	Per Year	No definition of leak size was provided	Chemical Process	Savannah River Site, "Generic Data Base Development," WSRC-TR-93-263, June 1993.

Component	Specific Component	Severity	Frequency	Units	Leak Size	Source Type	Source
Pump	Pumps	Large Leak	1.00E-04	Per Year	10% cross sectional area of connecting pipe	Chemical Process	Cox, A.W., Lees, F.P., Ang, M.L., "Classifications of Hazardous Locations," Institution of Chemical Engineers, 2003
Pump	Canned Pumps	Rupture	1.00E-05	Per Year	100% of connecting pipe diameter (1% of area)	General	Guidelines for quantitative risk assessment. "Purple Book" CPR 18E, ed. 1, 1999
Pump	Pumps	Rupture	1.00E-05	Per Year	100% cross sectional area of connecting pipe	Chemical Process	Cox, A.W., Lees, F.P., Ang, M.L., "Classifications of Hazardous Locations," Institution of Chemical Engineers, 2003
Pump	Centrifugal	Rupture	2.40E-05	Per Year	>50 mm	Hydrocarbon Process	Spouge, John, "New Generic Leak Frequencies for Process Equipment, “Process Safety Progress, Vol. 24, No. 4, 2005
Pump	Motor-driven	Rupture	7.05E-05	Per Year	> 50 gpm (water)	Nuclear	NUREG/CR-6928, "Industry-Average Performance for components and Initiating Events at U.S. Commercial Nuclear Power Plants," February 2007
Pump	Pumps	Rupture	1.00E-04	Per Year	100% of connecting pipe diameter (1% of area)	General	Guidelines for quantitative risk assessment. "Purple Book" CPR 18E, ed. 1, 1999
Pump	Motor-, Turbine-, and Diesel-Driven	Rupture	4.38E-04	Per Year	No definition of leak size was provided	Chemical Process	Savannah River Site, "Generic Data Base Development," WSRC-TR-93-263, June 1993.

Component	Specific Component	Severity	Frequency	Units	Leak Size	Source Type	Source
Pump	Reciprocating	Rupture	5.20E-04	Per Year	>50 mm	Hydrocarbon Process	Spouge, John, "New Generic Leak Frequencies for Process Equipment, “Process Safety Progress, Vol. 24, No. 4, 2005
Valve							
Valve	Manual, 2 inch diameter	Small Leak	1.40E-05	Per Year	>1 mm	Hydrocarbon Process	Spouge, John, "New Generic Leak Frequencies for Process Equipment, “Process Safety Progress, Vol. 24, No. 4, 2005
Valve	Manual, 6 inch diameter	Small Leak	4.80E-05	Per Year	>1 mm	Hydrocarbon Process	Spouge, John, "New Generic Leak Frequencies for Process Equipment, “Process Safety Progress, Vol. 24, No. 4, 2005
Valve	Solenoid Operated	Small Leak	8.17E-05	Per Year	1 to 50 gpm (water)	Nuclear	NUREG/CR-6928, "Industry-Average Performance for components and Initiating Events at U.S. Commercial Nuclear Power Plants," February 2007
Valve	No Additional Information	Small Leak	8.76E-05	Per Year	<50 gpm (water)	Nuclear	Eide, S.A, Khericha, S.T., Calley, M.B., Johnson, D.A., Marteeny, M.L., "Component External Leakage and Rupture Frequency Estimates," EGG-SSRE-9639, Nov 1991.
Valve	Air Operated	Small Leak	1.13E-04	Per Year	1 to 50 gpm (water)	Nuclear	NUREG/CR-6928, "Industry-Average Performance for components and Initiating Events at U.S. Commercial Nuclear Power Plants," February 2007
Valve	Motor Operated	Small Leak	1.24E-04	Per Year	1 to 50 gpm (water)	Nuclear	NUREG/CR-6928, "Industry-Average Performance for components and Initiating Events at U.S. Commercial Nuclear Power Plants," February 2007
Valve	Hydraulic-operated	Small Leak	1.30E-04	Per Year	1 to 50 gpm (water)	Nuclear	NUREG/CR-6928, "Industry-Average Performance for components and Initiating Events at U.S. Commercial Nuclear Power Plants," February 2007

Component	Specific Component	Severity	Frequency	Units	Leak Size	Source Type	Source
Valve	Manual, 18 inch diameter	Small Leak	2.20E-04	Per Year	>1 mm	Hydrocarbon Process	Spouge, John, "New Generic Leak Frequencies for Process Equipment, “Process Safety Progress, Vol. 24, No. 4, 2005
Valve	Check	Small Leak	2.58E-04	Per Year	1 to 50 gpm (water)	Nuclear	NUREG/CR-6928, "Industry-Average Performance for components and Initiating Events at U.S. Commercial Nuclear Power Plants," February 2007
Valve	Actuated, 6 inch diameter, nonpipeline	Small Leak	2.60E-04	Per Year	>1 mm	Hydrocarbon Process	Spouge, John, "New Generic Leak Frequencies for Process Equipment, “Process Safety Progress, Vol. 24, No. 4, 2005
Valve	Manual	Small Leak	3.91E-04	Per Year	1 to 50 gpm (water)	Nuclear	NUREG/CR-6928, "Industry-Average Performance for components and Initiating Events at U.S. Commercial Nuclear Power Plants," February 2007
Valve	All types	Small Leak	8.76E-04	Per Year	No definition of leak size was provided	Compressed Gas	Savannah River Site, "Generic Data Base Development," WSRC-TR-93-263, June 1993.
Valve	All Sizes	Small Leak	1.00E-03	Per Year	1% cross sectional area	Chemical Process	Cox, A.W., Lees, F.P., Ang, M.L., "Classifications of Hazardous Locations," Institution of Chemical Engineers, 2003
Valve	All types	Small Leak	4.38E-03	Per Year	No definition of leak size was provided	Chemical Process	Savannah River Site, "Generic Data Base Development," WSRC-TR-93-263, June 1993.
Valve	No Additional Information	Small Leak	1.30E-02	Per Year	Gland leak	Hydrogen Fueling Process	EIGA, "Determination of Safety Distances," IGC Doc 75/01/E/rev, 2001
Valve	All Sizes	Large Leak	1.00E-04	Per Year	10% cross sectional area	Chemical Process	Cox, A.W., Lees, F.P., Ang, M.L., "Classifications of Hazardous Locations," Institution of Chemical Engineers, 2003

Valve	Manual, 6 inch diameter	Rupture	4.80E-07	Per Year	>50 mm	Hydrocarbon Process	Spouge, John, "New Generic Leak Frequencies for Process Equipment, “Process Safety Progress, Vol. 24, No. 4, 2005
Valve	No Additional Information	Rupture	8.76E-07	Per Year	>50 gpm (water) or complete failure	Nuclear	Eide, S.A, Khericha, S.T., Calley, M.B., Johnson, D.A., Marteeny, M.L., "Component External Leakage and Rupture Frequency Estimates," EGG-SSRE-9639, Nov 1991.
Valve	Actuated, 6 inch diameter, nonpipeline	Rupture	1.90E-06	Per Year	>50 mm	Hydrocarbon Process	Spouge, John, "New Generic Leak Frequencies for Process Equipment, “Process Safety Progress, Vol. 24, No. 4, 2005
Valve	Manual, 18 inch diameter	Rupture	2.30E-06	Per Year	>50 mm	Hydrocarbon Process	Spouge, John, "New Generic Leak Frequencies for Process Equipment, “Process Safety Progress, Vol. 24, No. 4, 2005

Component	Specific Component	Severity	Frequency	Units	Leak Size	Source Type	Source
Valve	No Additional Information	Rupture	3.50E-06	Per Year	>50 gpm (water) or complete failure	Nuclear	Eide, S.A, Khericha, S.T., Calley, M.B., Johnson, D.A., Marteeny, M.L., "Component External Leakage and Rupture Frequency Estimates," EGG-SSRE-9639, Nov 1991.
Valve	Solenoid Operated	Rupture	5.72E-06	Per Year	> 50 gpm (water)	Nuclear	NUREG/CR-6928, "Industry-Average Performance for components and Initiating Events at U.S. Commercial Nuclear Power Plants," February 2007
Valve	Air Operated	Rupture	7.88E-06	Per Year	> 50 gpm (water)	Nuclear	NUREG/CR-6928, "Industry-Average Performance for components and Initiating Events at U.S. Commercial Nuclear Power Plants," February 2007
Valve	Motor Operated	Rupture	8.62E-06	Per Year	> 50 gpm (water)	Nuclear	NUREG/CR-6928, "Industry-Average Performance for components and Initiating Events at U.S. Commercial Nuclear Power Plants," February 2007
Valve	Hydraulic-operated	Rupture	9.02E-06	Per Year	> 50 gpm (water)	Nuclear	NUREG/CR-6928, "Industry-Average Performance for components and Initiating Events at U.S. Commercial Nuclear Power Plants," February 2007
Valve	All Sizes	Rupture	1.00E-05	Per Year	100% cross sectional area	Chemical Process	Cox, A.W., Lees, F.P., Ang, M.L., "Classifications of Hazardous Locations," Institution of Chemical Engineers, 2003
Valve	Check	Rupture	1.80E-05	Per Year	> 50 gpm (water)	Nuclear	NUREG/CR-6928, "Industry-Average Performance for components and Initiating Events at U.S. Commercial Nuclear Power Plants," February 2007

Component	Specific Component	Severity	Frequency	Units	Leak Size	Source Type	Source
Valve	Manual	Rupture	2.73E-05	Per Year	> 50 gpm (water)	Nuclear	NUREG/CR-6928, "Industry-Average Performance for components and Initiating Events at U.S. Commercial Nuclear Power Plants," February 2007
Valve	All types	Rupture	4.38E-05	Per Year	No definition of leak size was provided	Compressed Gas	Savannah River Site, "Generic Data Base Development," WSRC-TR-93-263, June 1993.
Valve	All types	Rupture	2.63E-04	Per Year	No definition of leak size was provided	Chemical Process	Savannah River Site, "Generic Data Base Development," WSRC-TR-93-263, June 1993.

APPENDIX C. LEAK FREQUENCY DISTRIBUTIONS

This appendix contains the leak frequency distributions for each of the different components. The 90% bounds were calculated as the 5th and 95th percentiles of the leak frequency samples that were obtained by sampling from the posterior distributions of the log-linear leak frequency model parameters and propagating the samples through the model. The interpretation is that 90% of the leak frequencies predicted by the model are within the bounds. Furthermore, the bounds are symmetric in the sense that 5% of predicted leak frequencies will be below this interval and 5% of predicted leak frequencies will be above this interval.

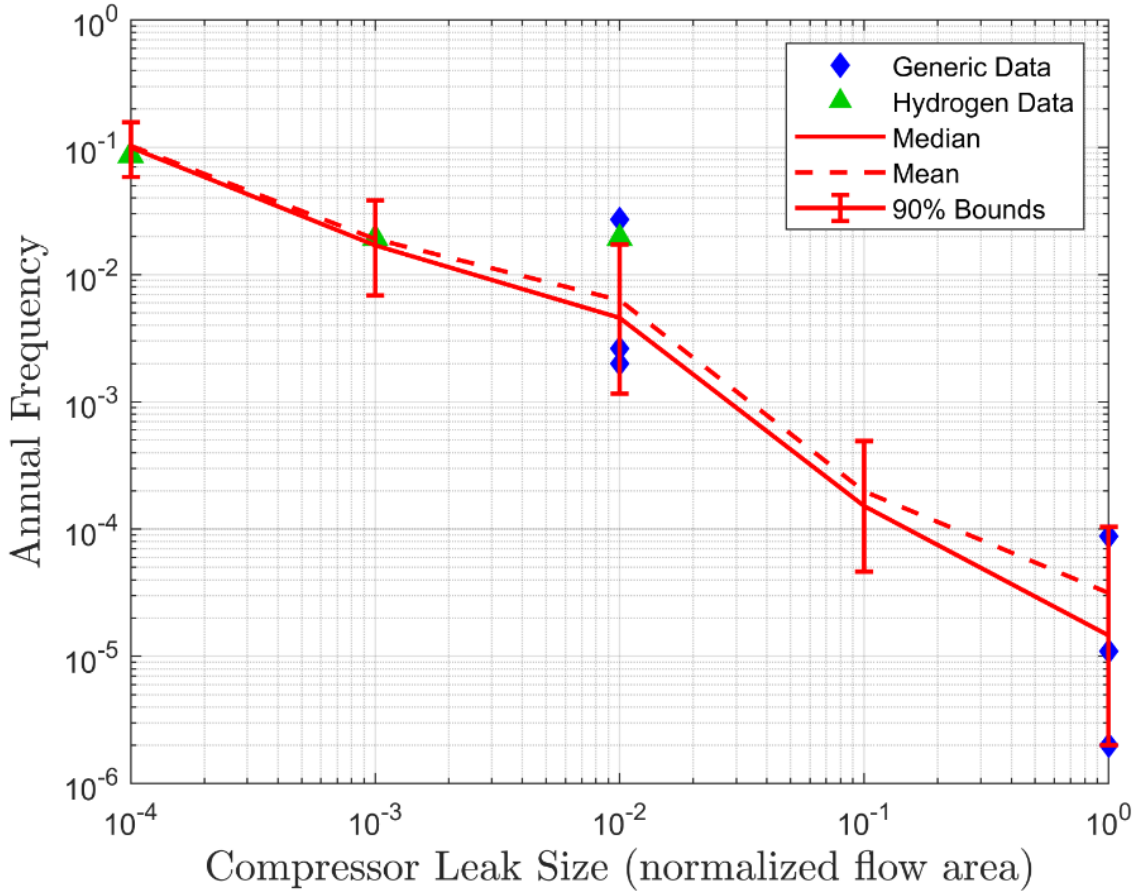

Figure C-1. Leak frequency results for compressors.

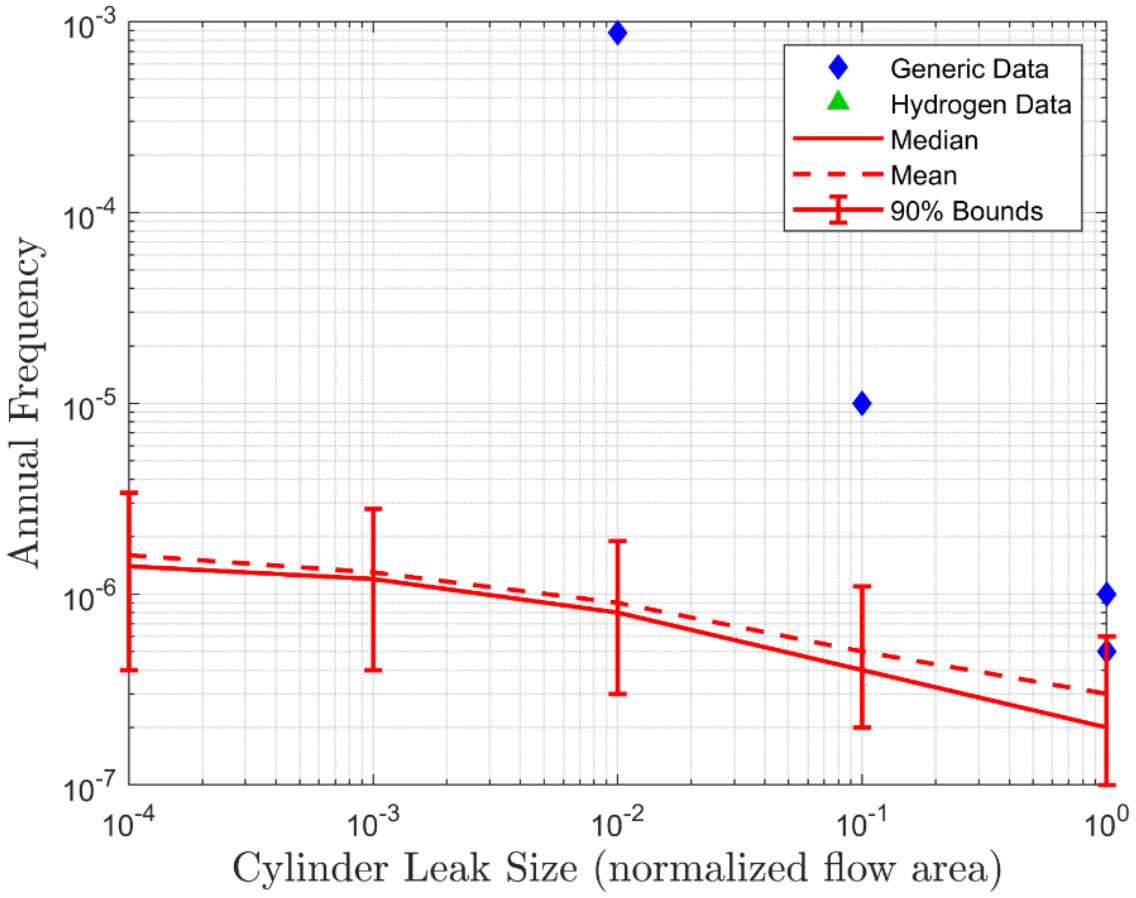

Figure C-2. Leak frequency results for cylinders.

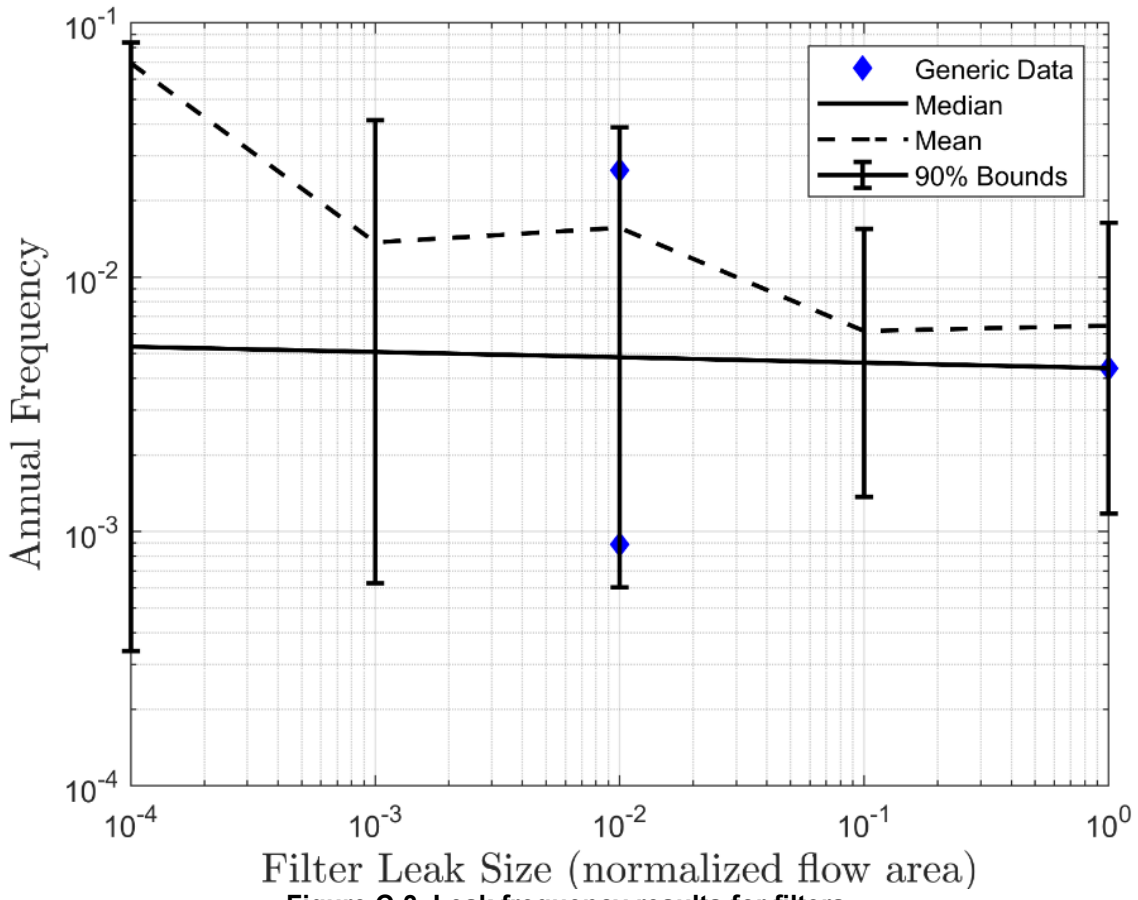

Figure C-3. Leak frequency results for filters.

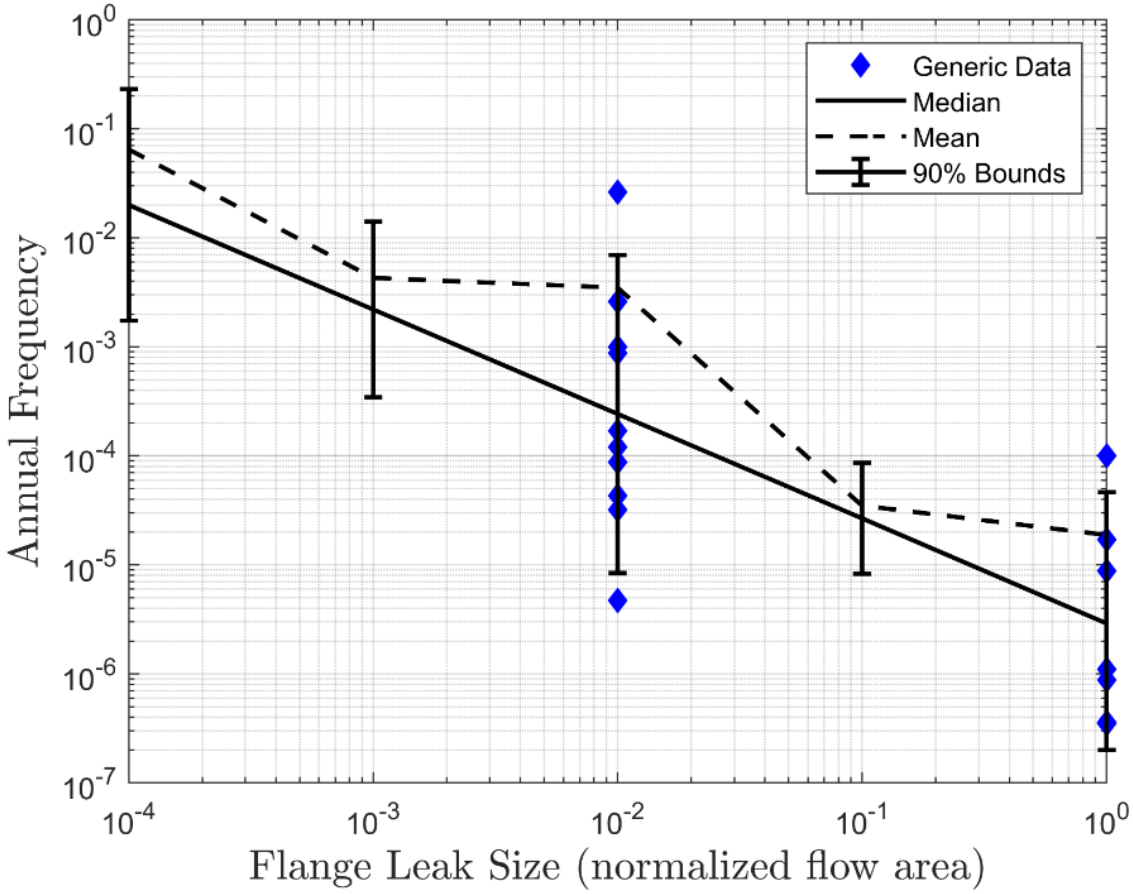

Figure C-4. Leak frequency results for flanges.

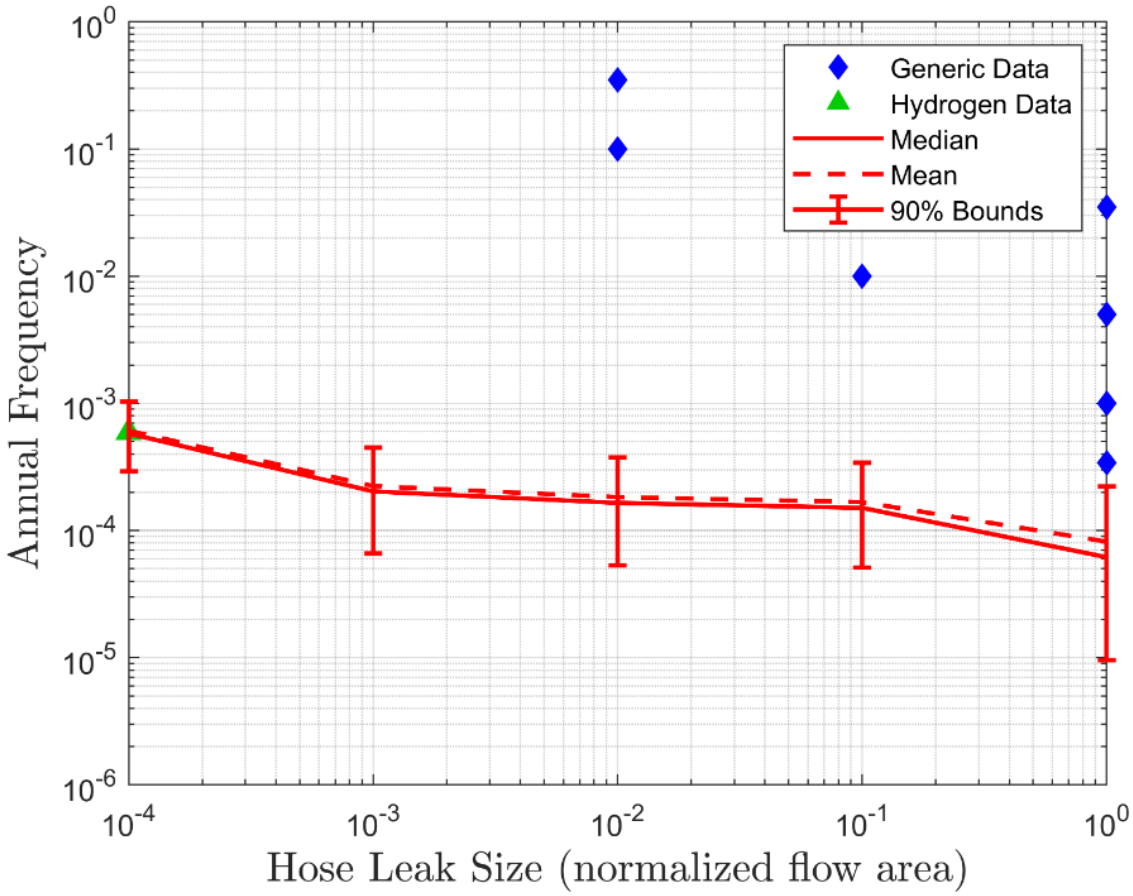

Figure C-5. Leak frequency results for hoses.

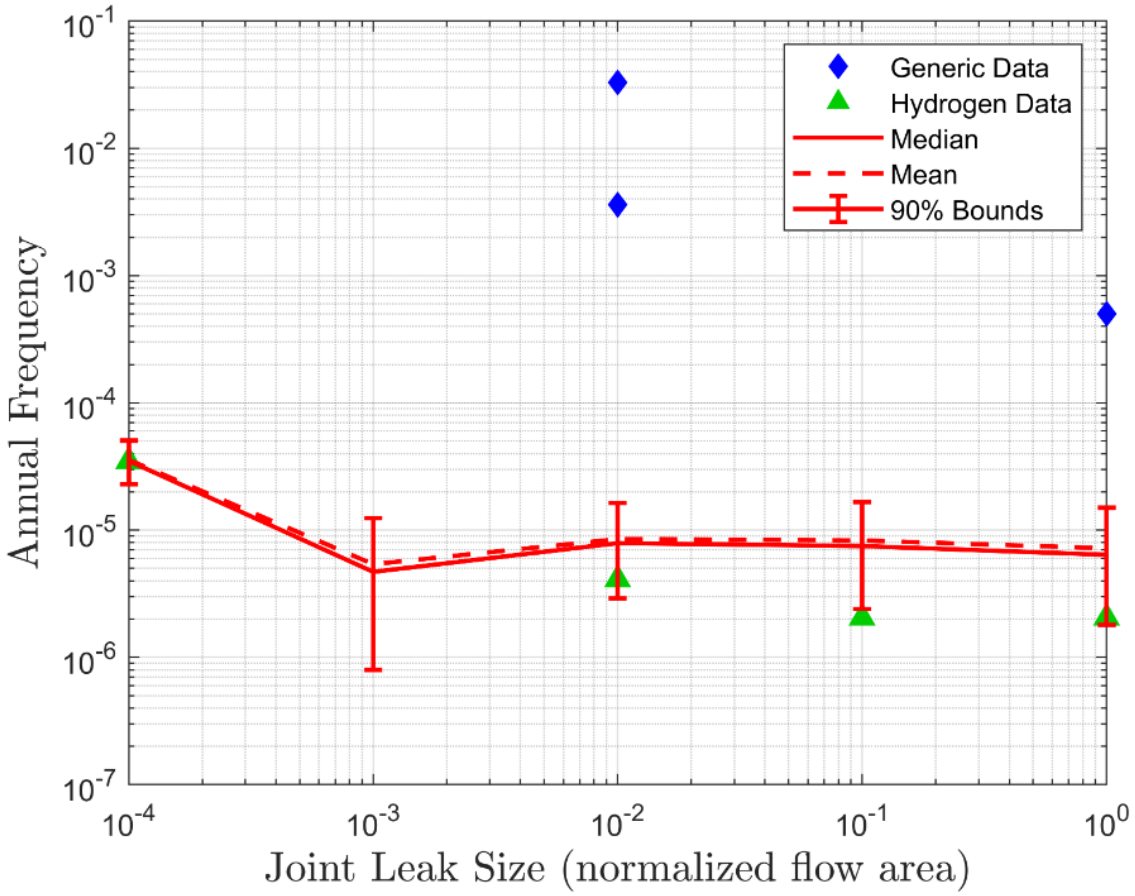

Figure C-6. Leak frequency results for joints.

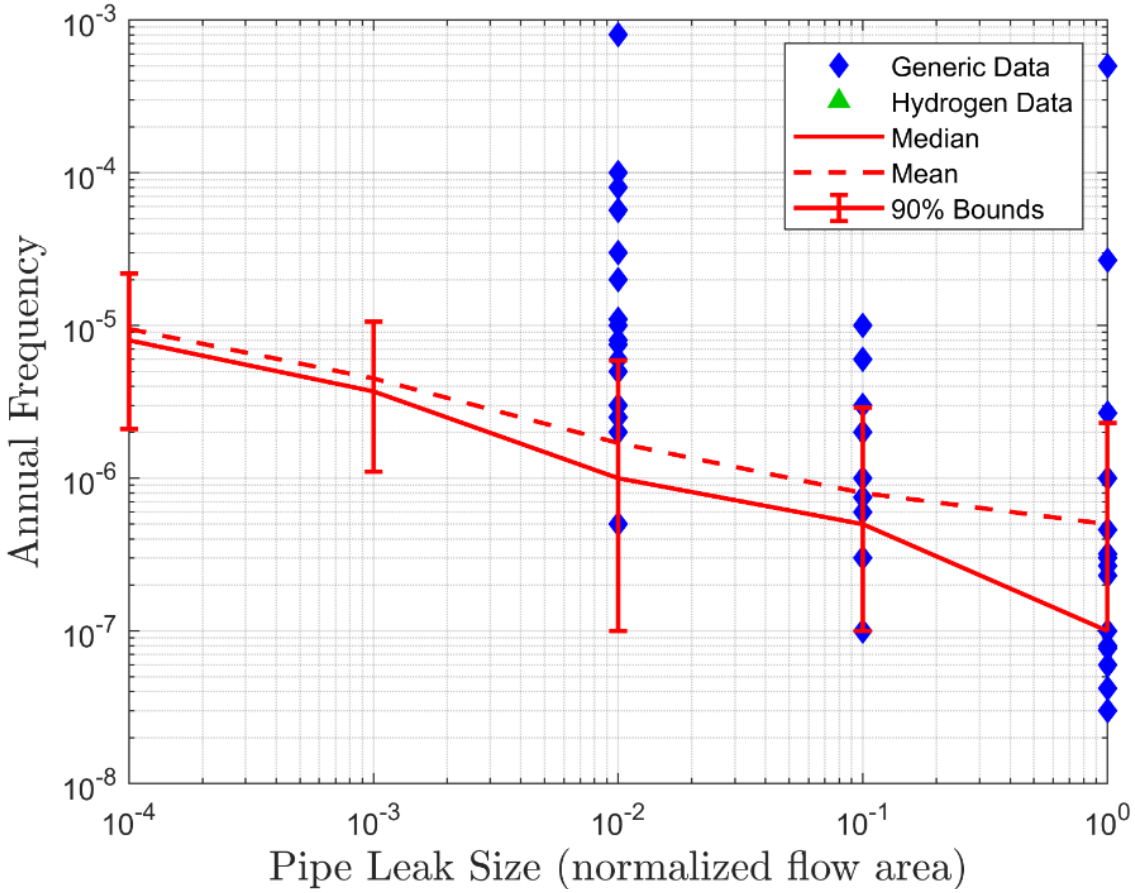

Figure C-7. Leak frequency results for pipes.

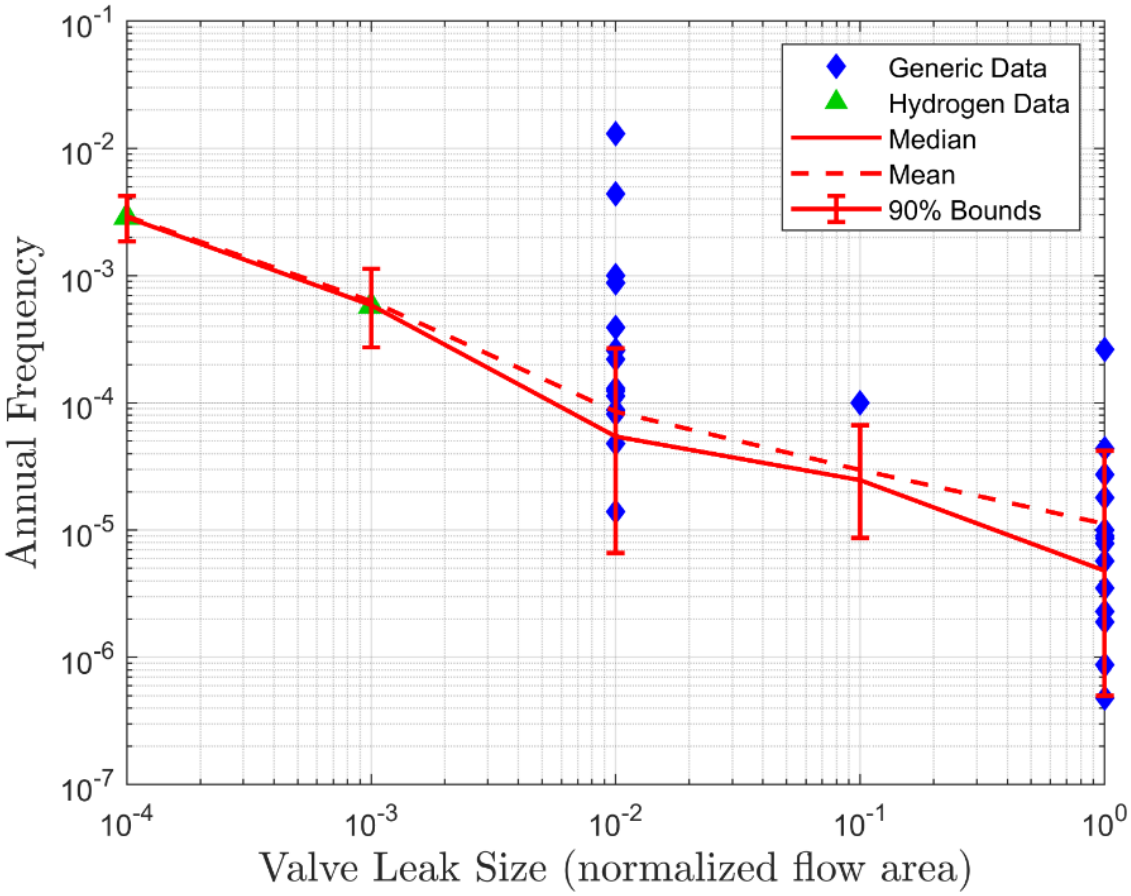

Figure C-8. Leak frequency results for valves.

APPENDIX D. CONSEQUENCE EVALUATION RESULTS AT 1 KM

This appendix contains the detailed consequence evaluation results for each of the scenarios outlined in Table 3-3. Note that cell size units are in meters.

Scenario 1

Scenario 1 is a 203.2 mm break with a temperature of 735°C and pressure of 0.52 MPa.

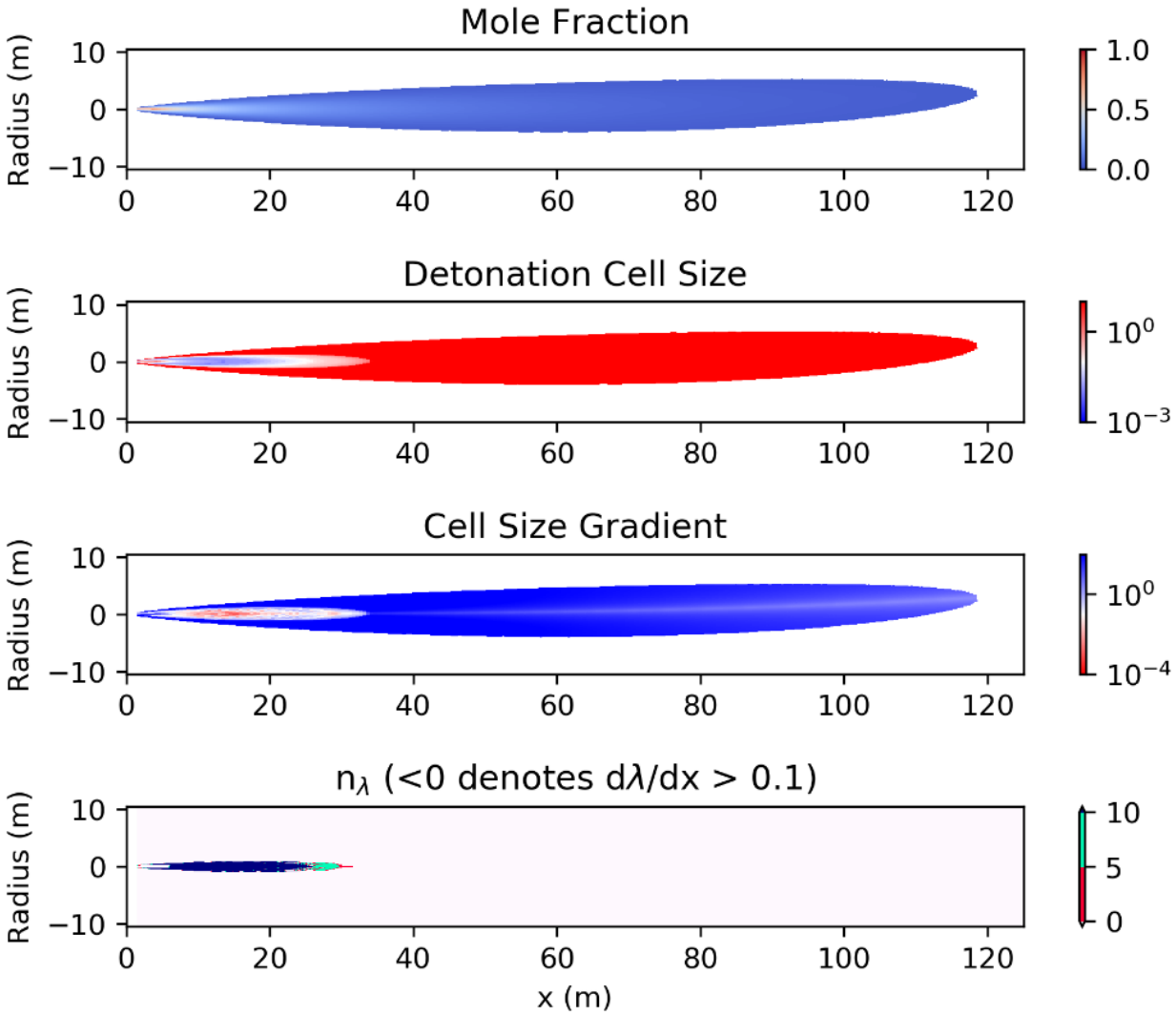

Figure D-1. Scenario 1 Consequence Evaluation Results

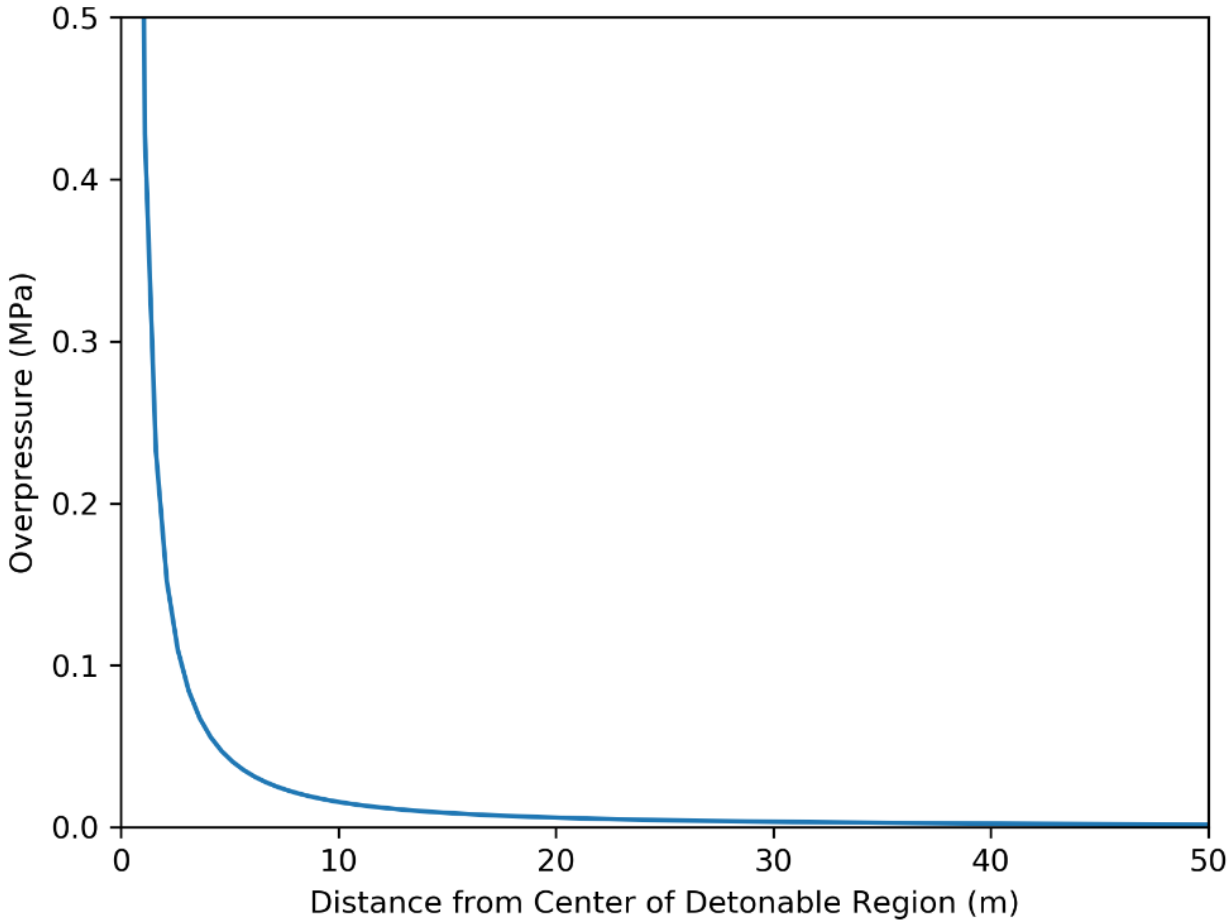

Figure D-2. Scenario 1 Overpressure Evaluation Results

Scenario 2

Scenario 2 is a 254.0 mm break with a temperature of 735°C and pressure of 0.52 MPa.

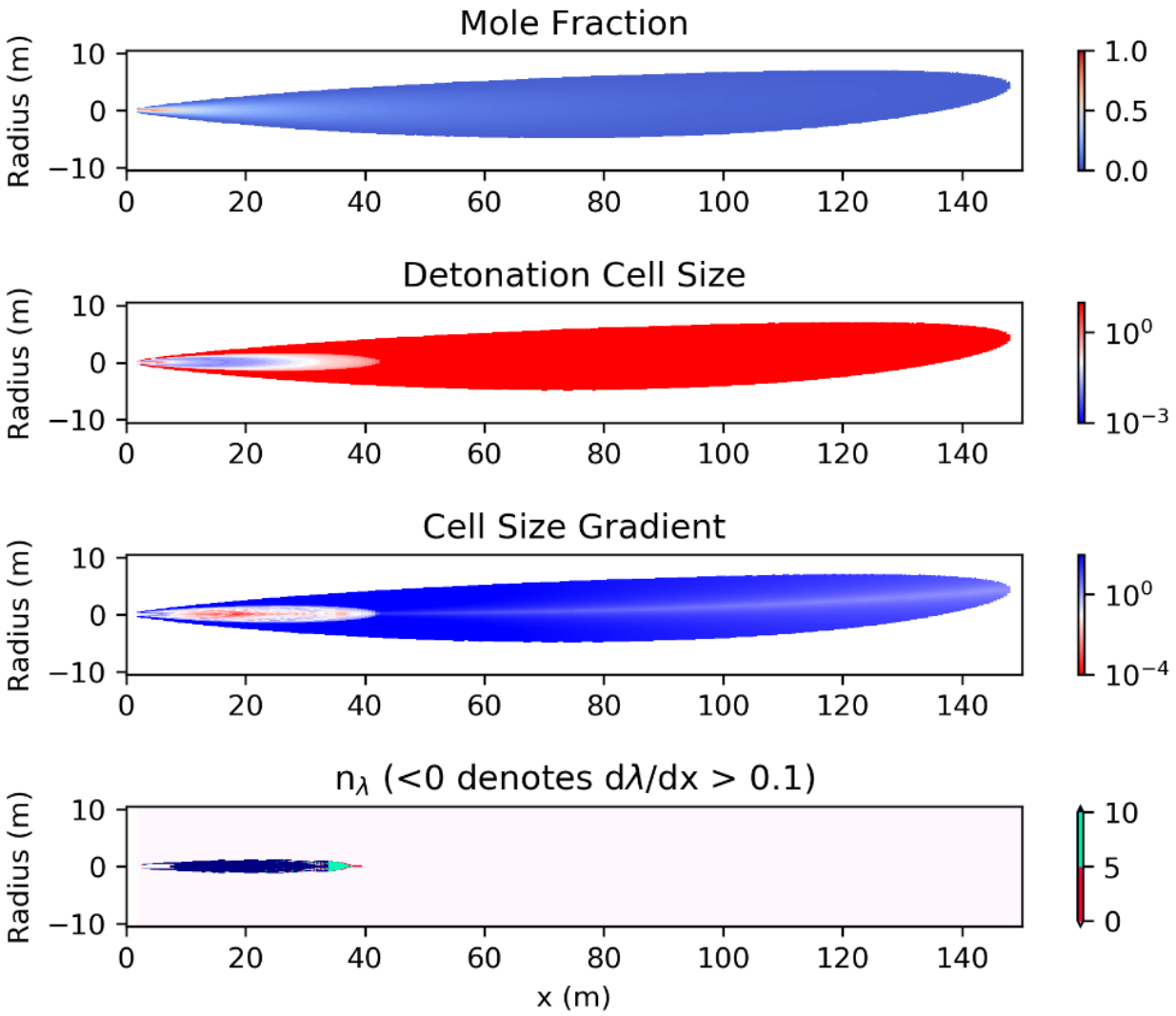

Figure D-3. Scenario 2 Consequence Evaluation Results

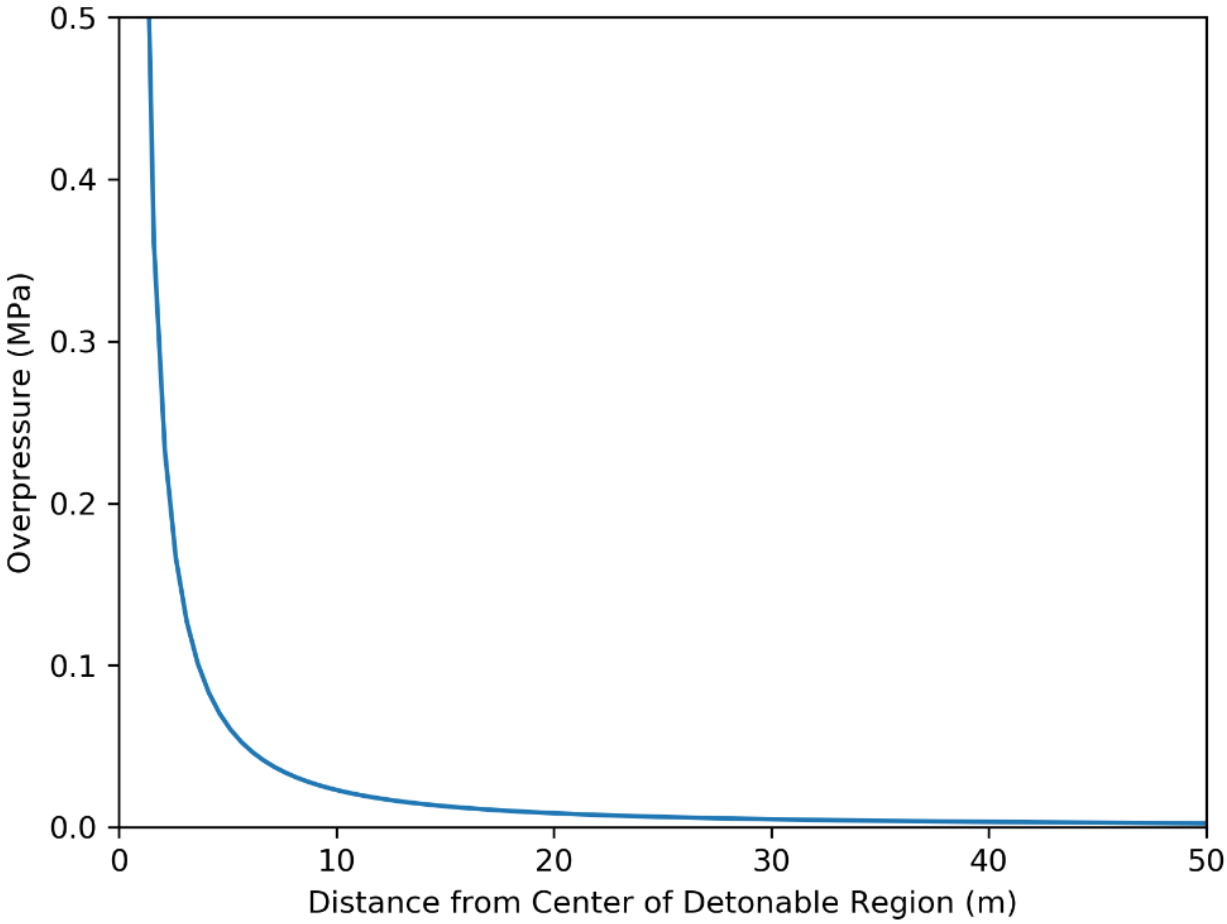

Figure D-4. Scenario 2 Overpressure Evaluation Results

Scenario 3

Scenario 3 is a 300.0 mm break with a temperature of 735°C and pressure of 0.52 MPa.

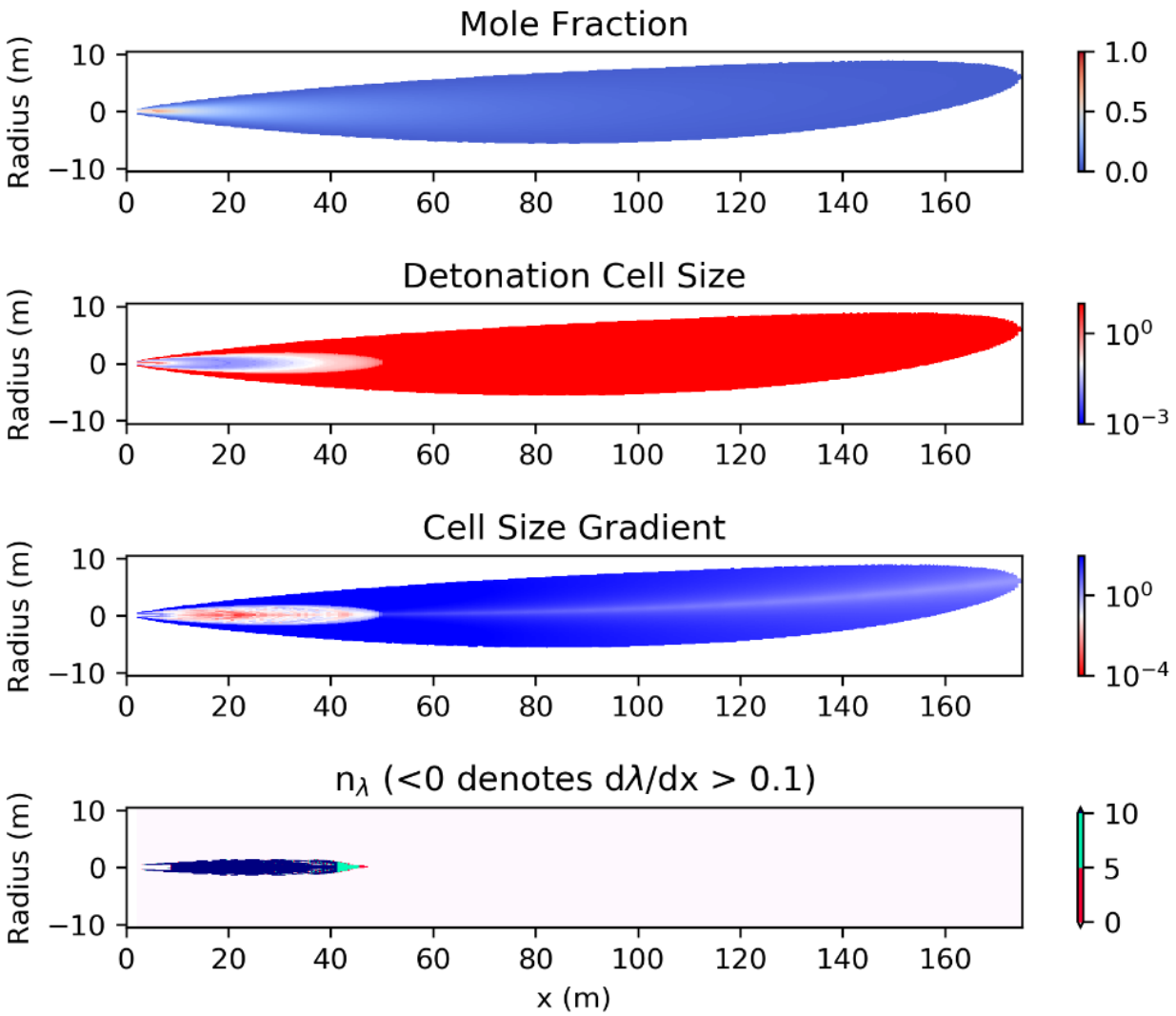

Figure D-5. Scenario 3 Consequence Evaluation Results

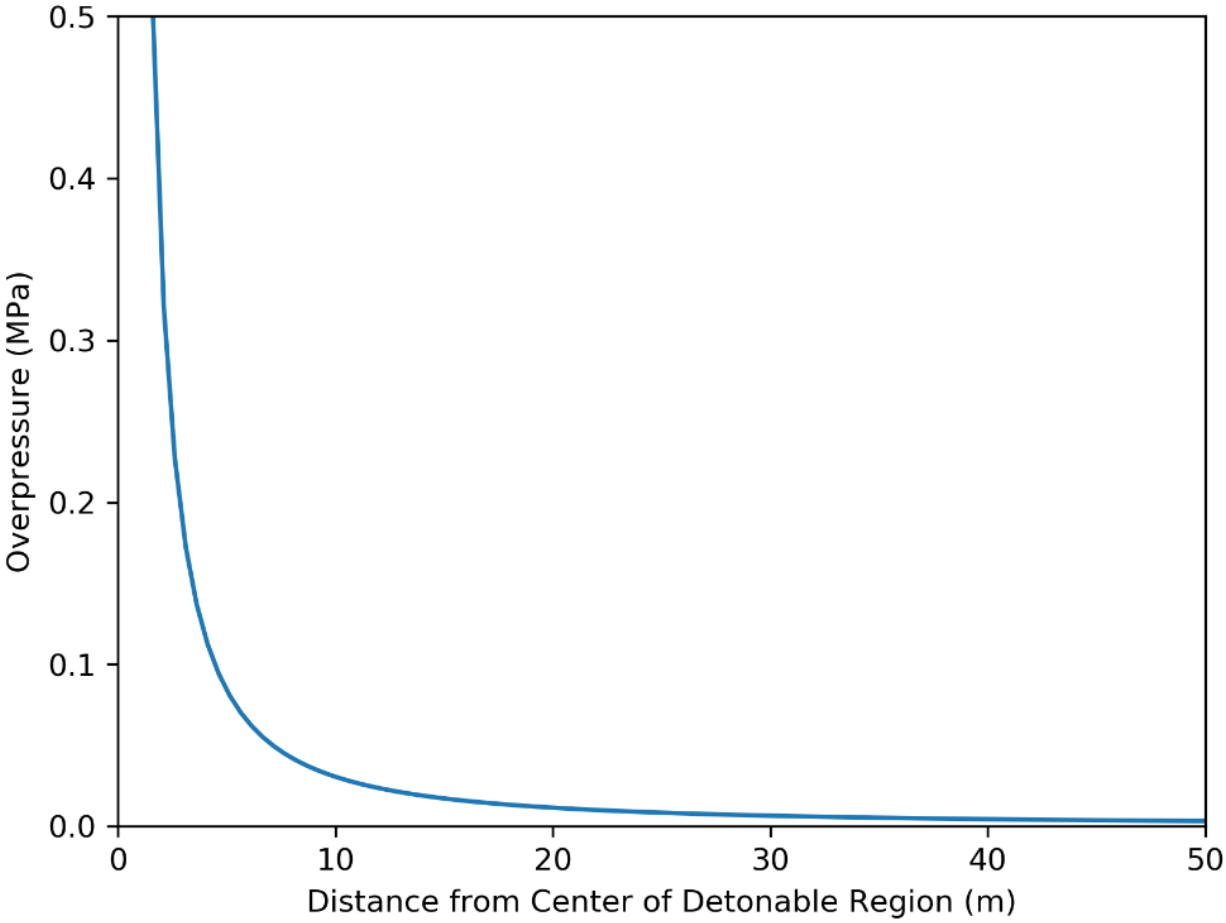

Figure D-6. Scenario 3 Overpressure Evaluation Results

Scenario 4

Scenario 4 is a 152.4 mm break with a temperature of 75°C and pressure of 0.48 MPa.

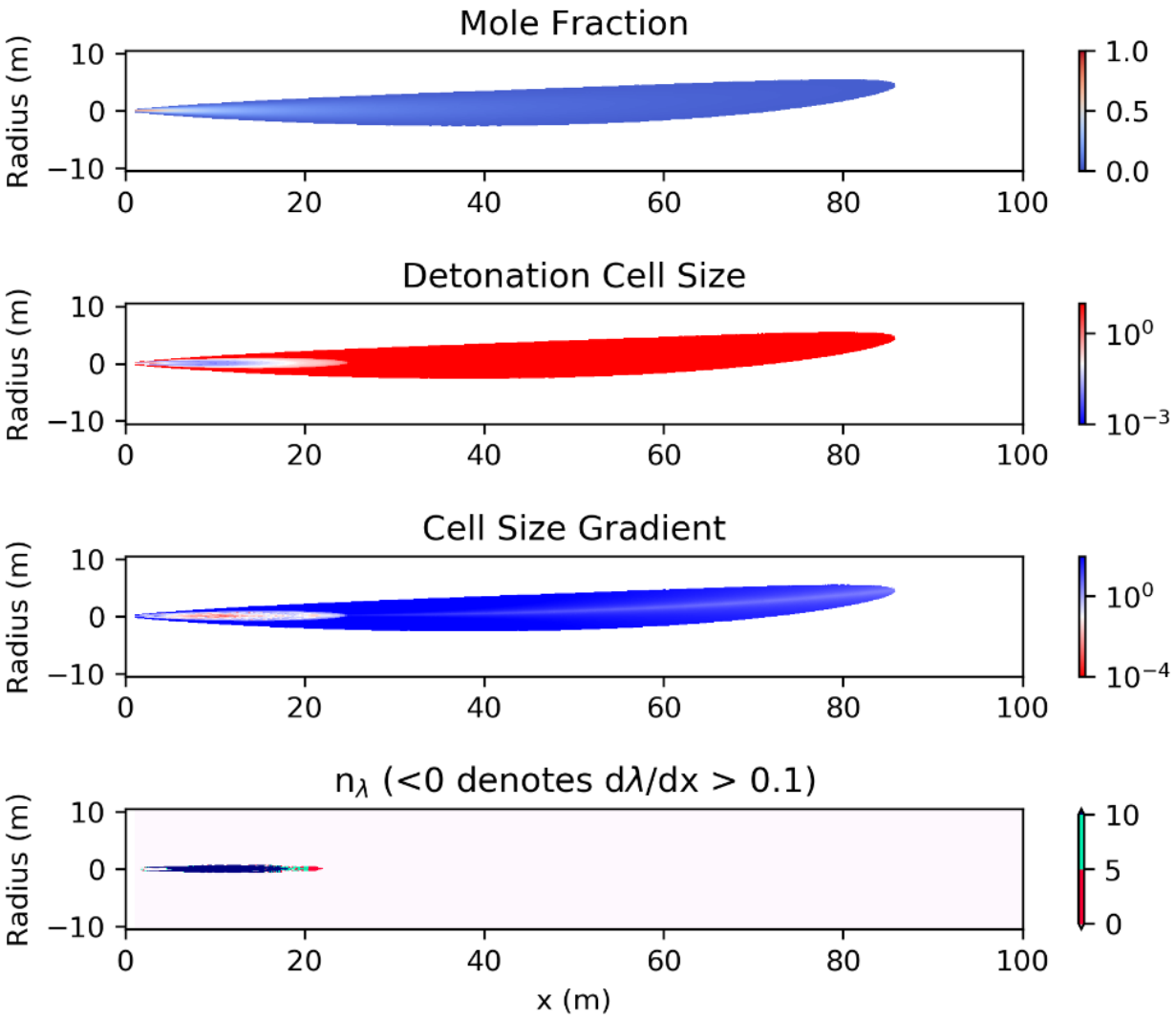

Figure D-7. Scenario 4 Consequence Evaluation Results

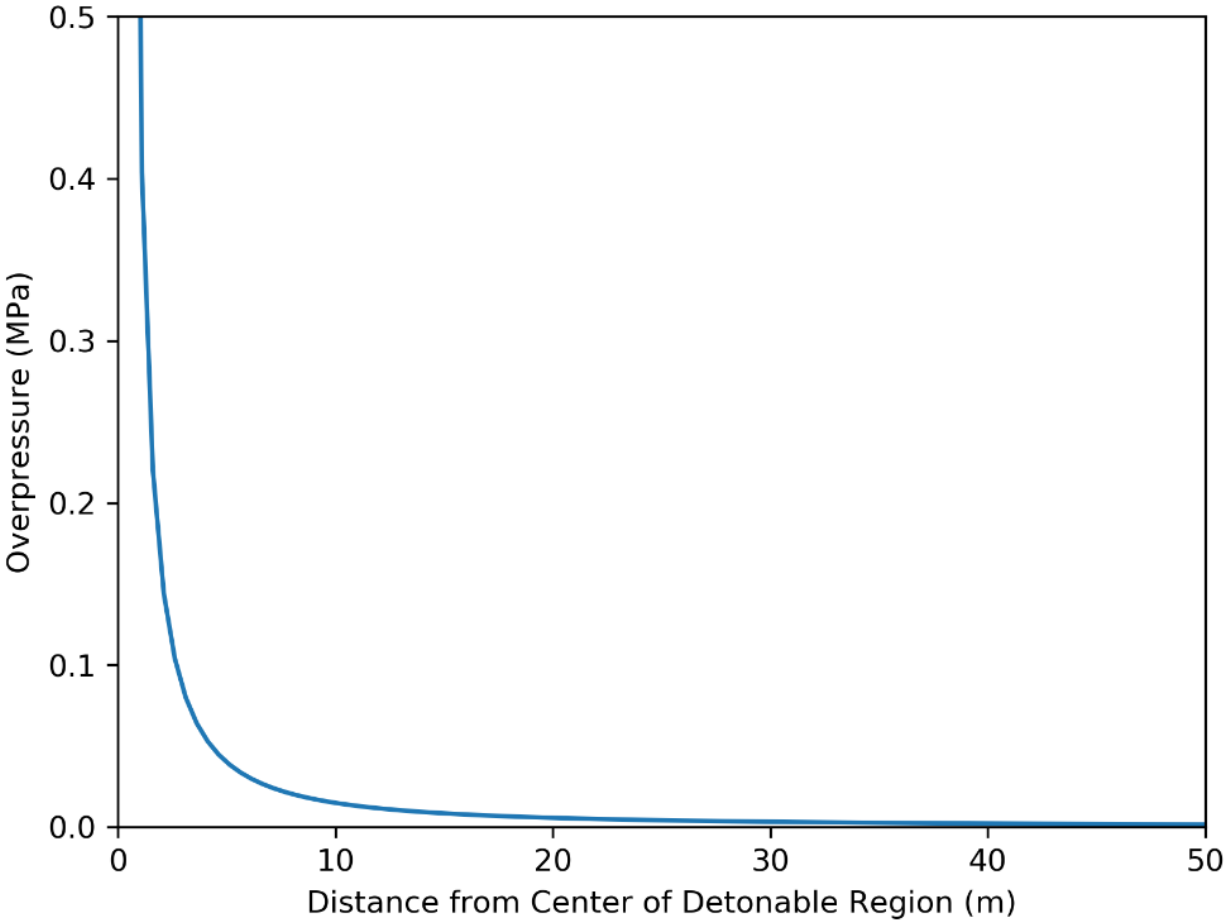

Figure D-8. Scenario 4 Overpressure Evaluation Results

Scenario 5

Scenario 5 is a 203.2 mm break with a temperature of 75°C and pressure of 0.48 MPa.

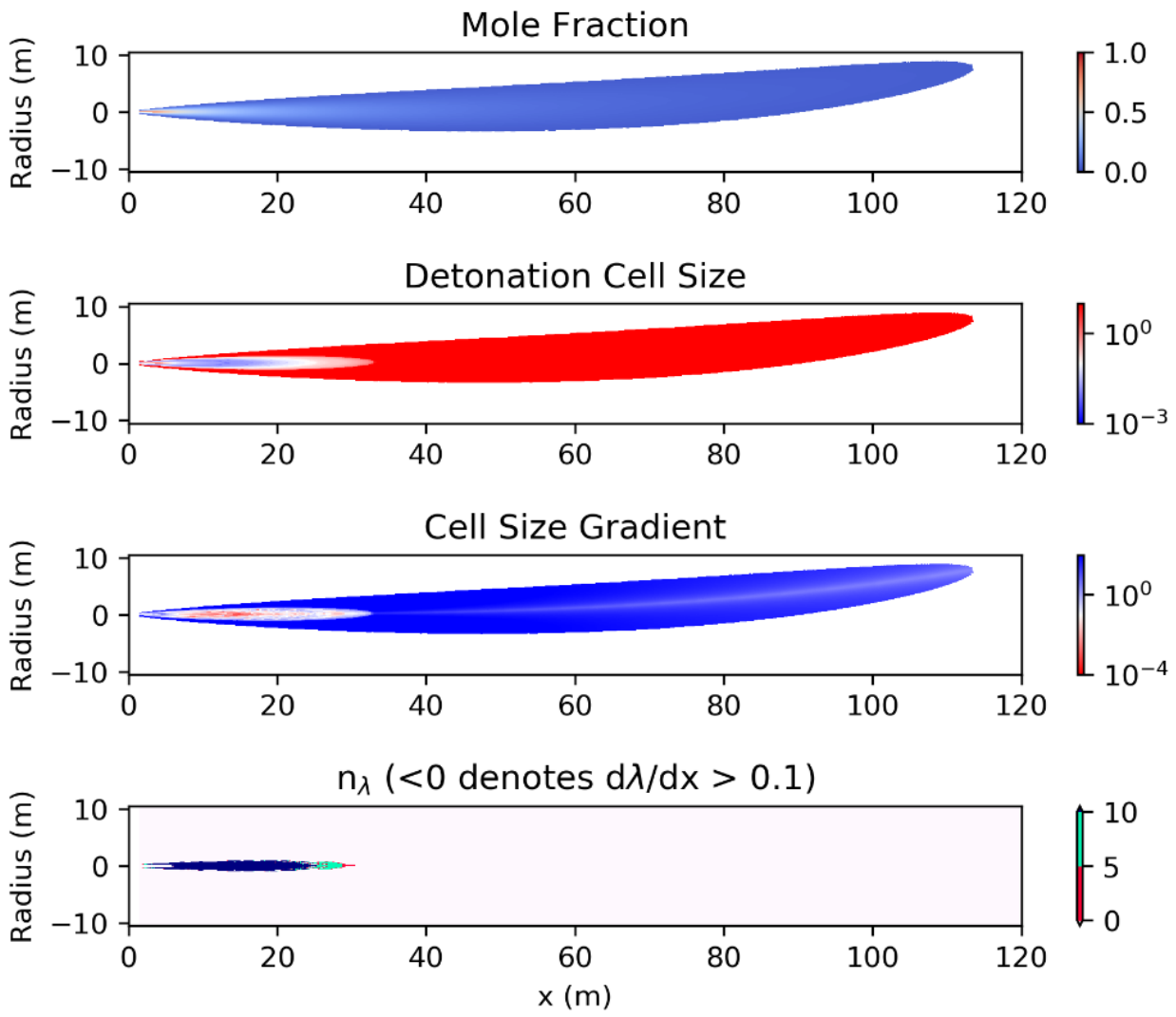

Figure D-9. Scenario 5 Consequence Evaluation Results

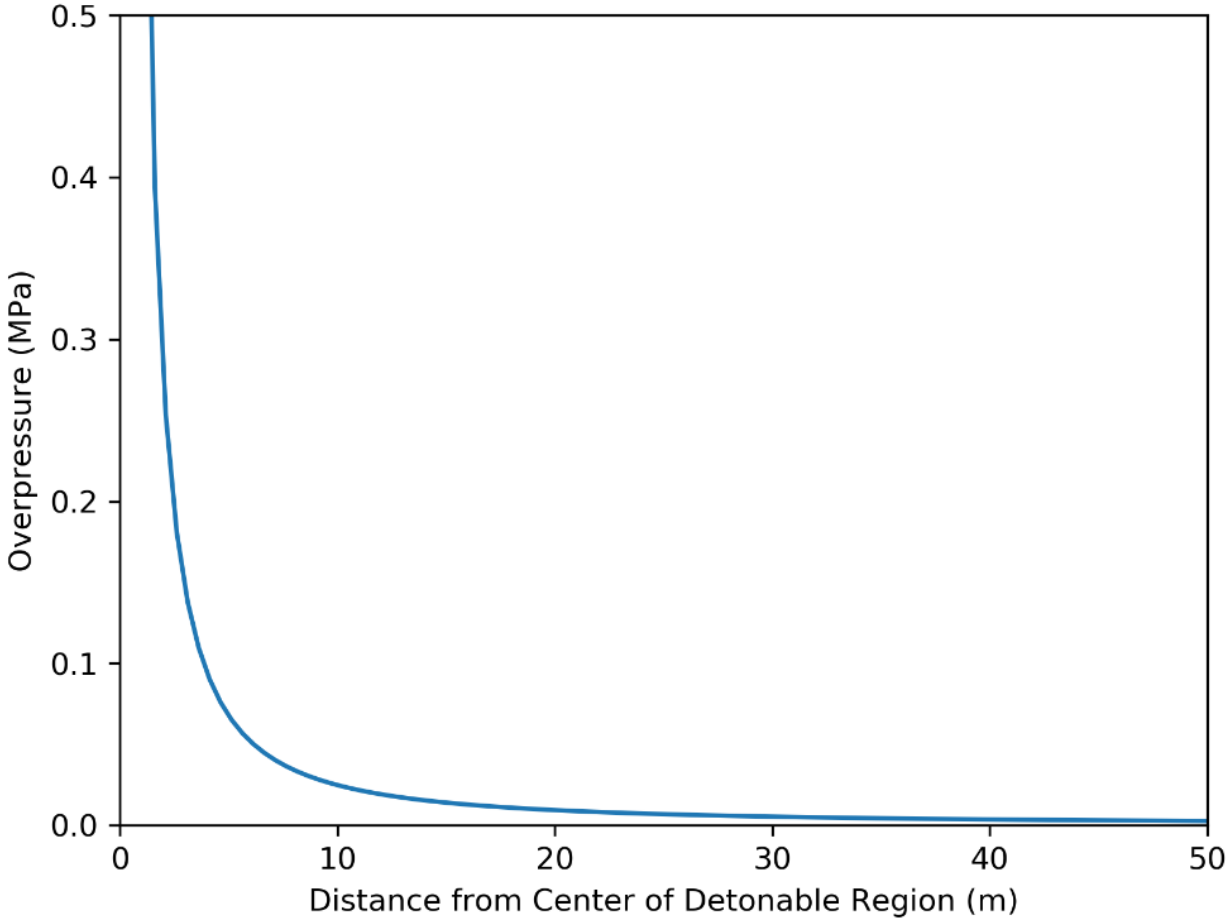

Figure D-10. Scenario 5 Overpressure Evaluation Results

Scenario 6

Scenario 6 is a 254.0 mm break with a temperature of 75°C and pressure of 0.48 MPa.

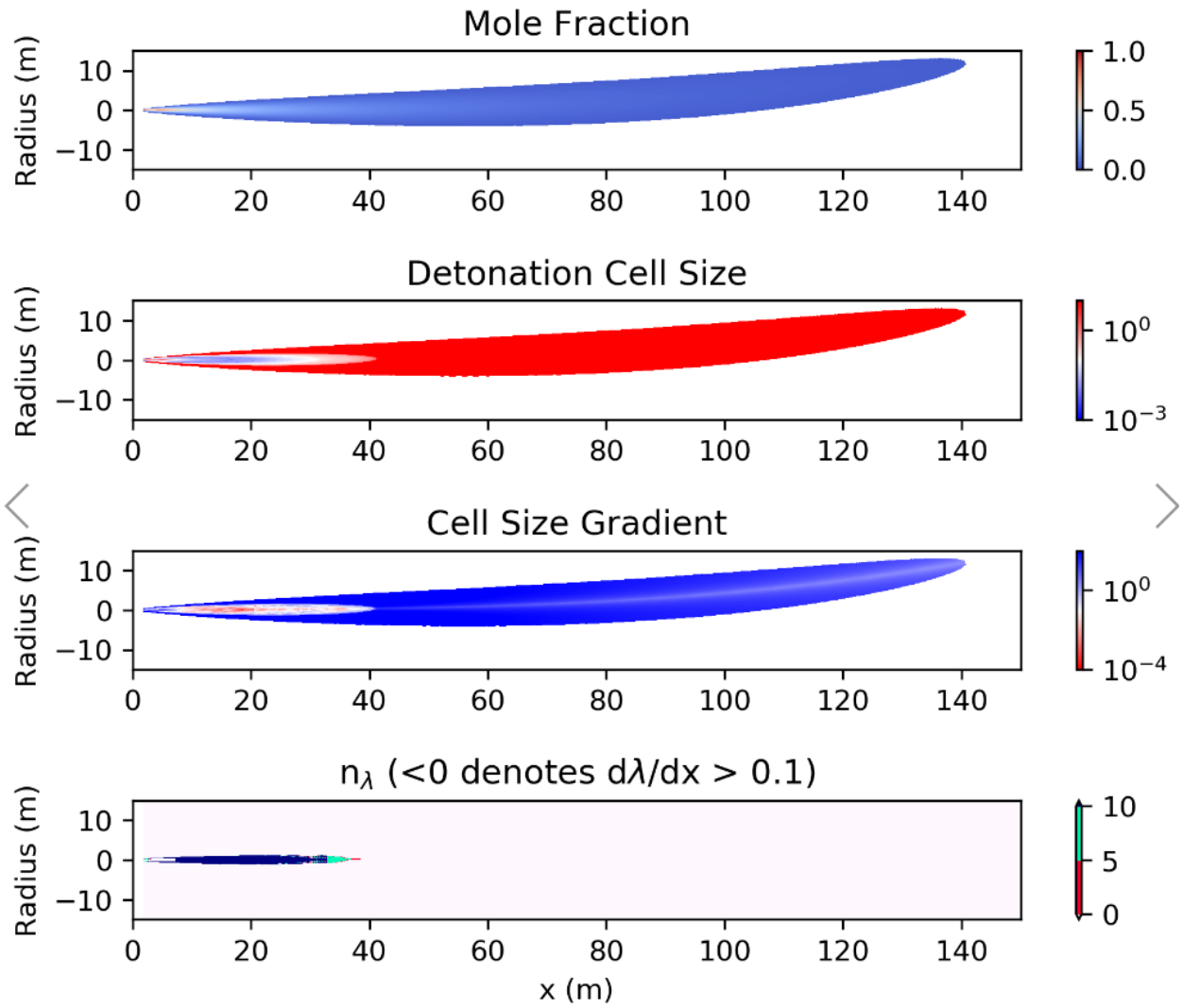

Figure D-11. Scenario 6 Consequence Evaluation Results

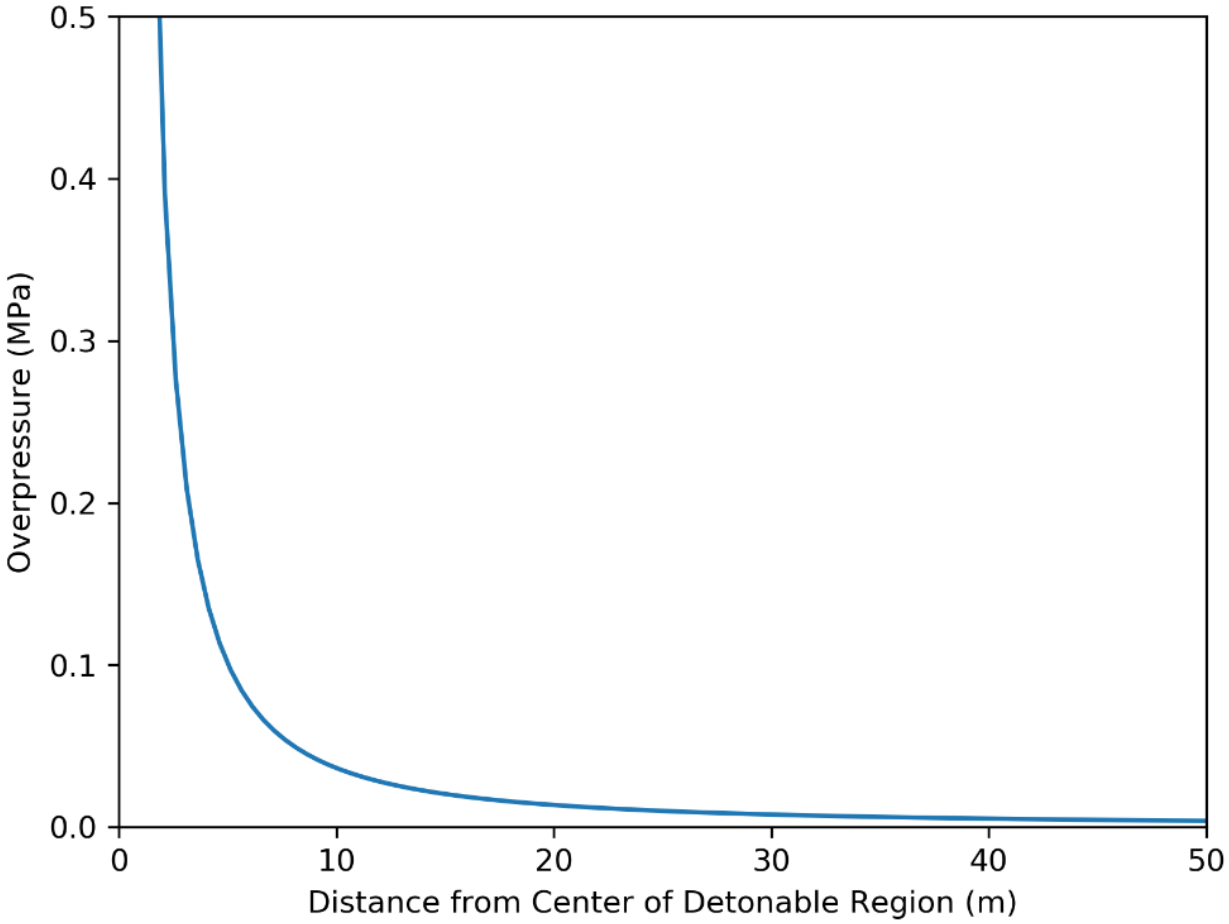

Figure D-12. Scenario 6 Overpressure Evaluation Results

Scenario 7

Scenario 7 is a 300.0 mm break with a temperature of 75°C and pressure of 0.48 MPa.

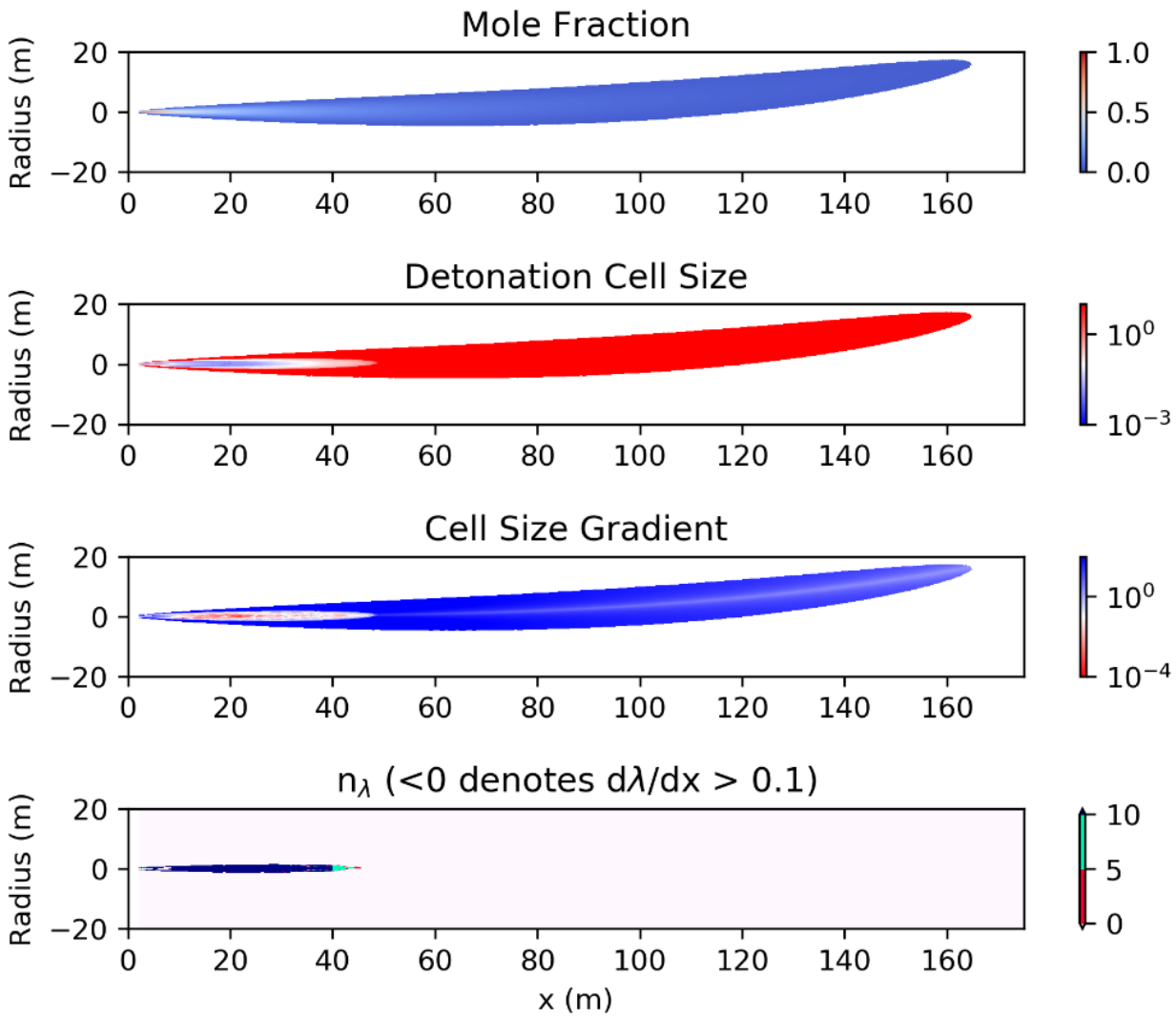

Figure D-13. Scenario 7 Consequence Evaluation Results

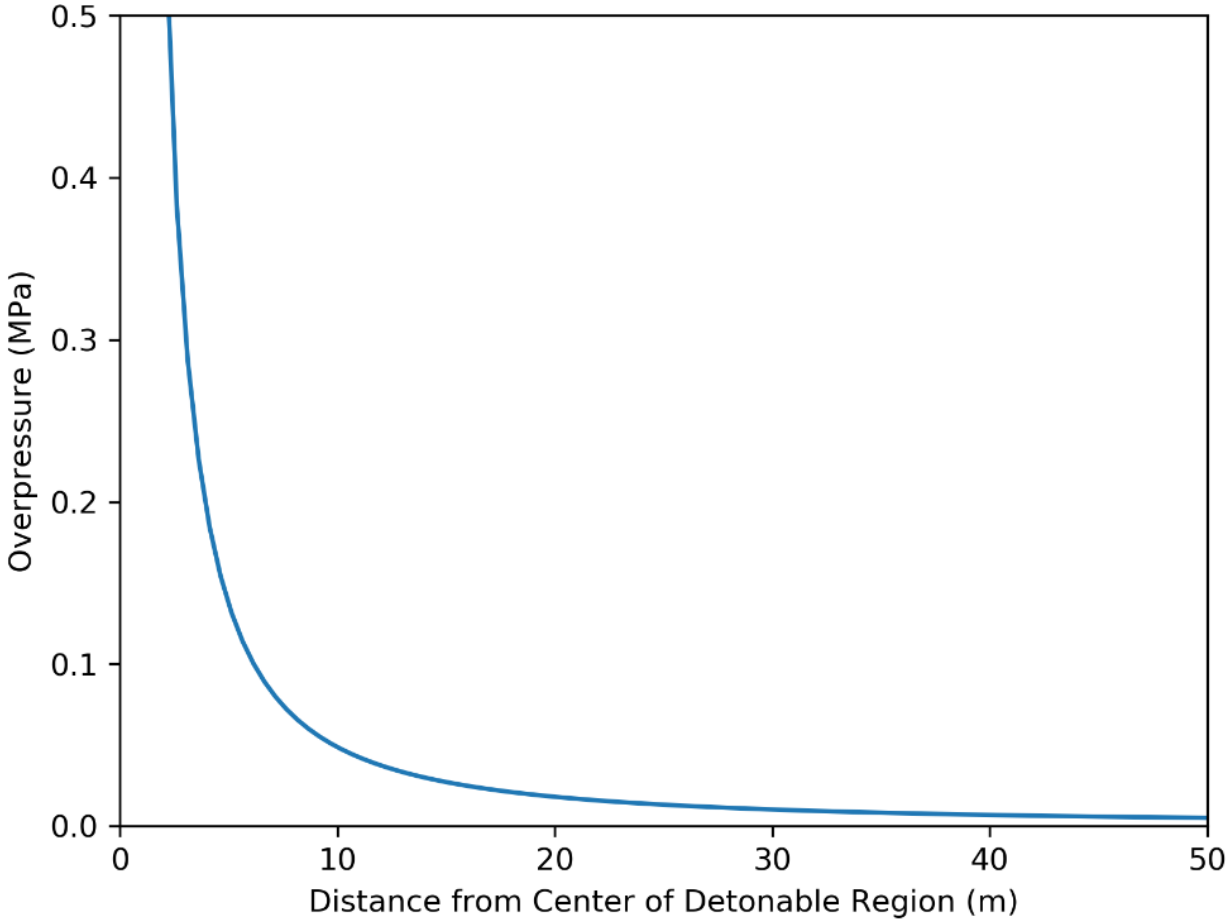

Figure D-14. Scenario 7 Overpressure Evaluation Results

Scenario 8

Scenario 8 is an 88.9 mm break with a temperature of 75°C and pressure of 1.01 MPa.

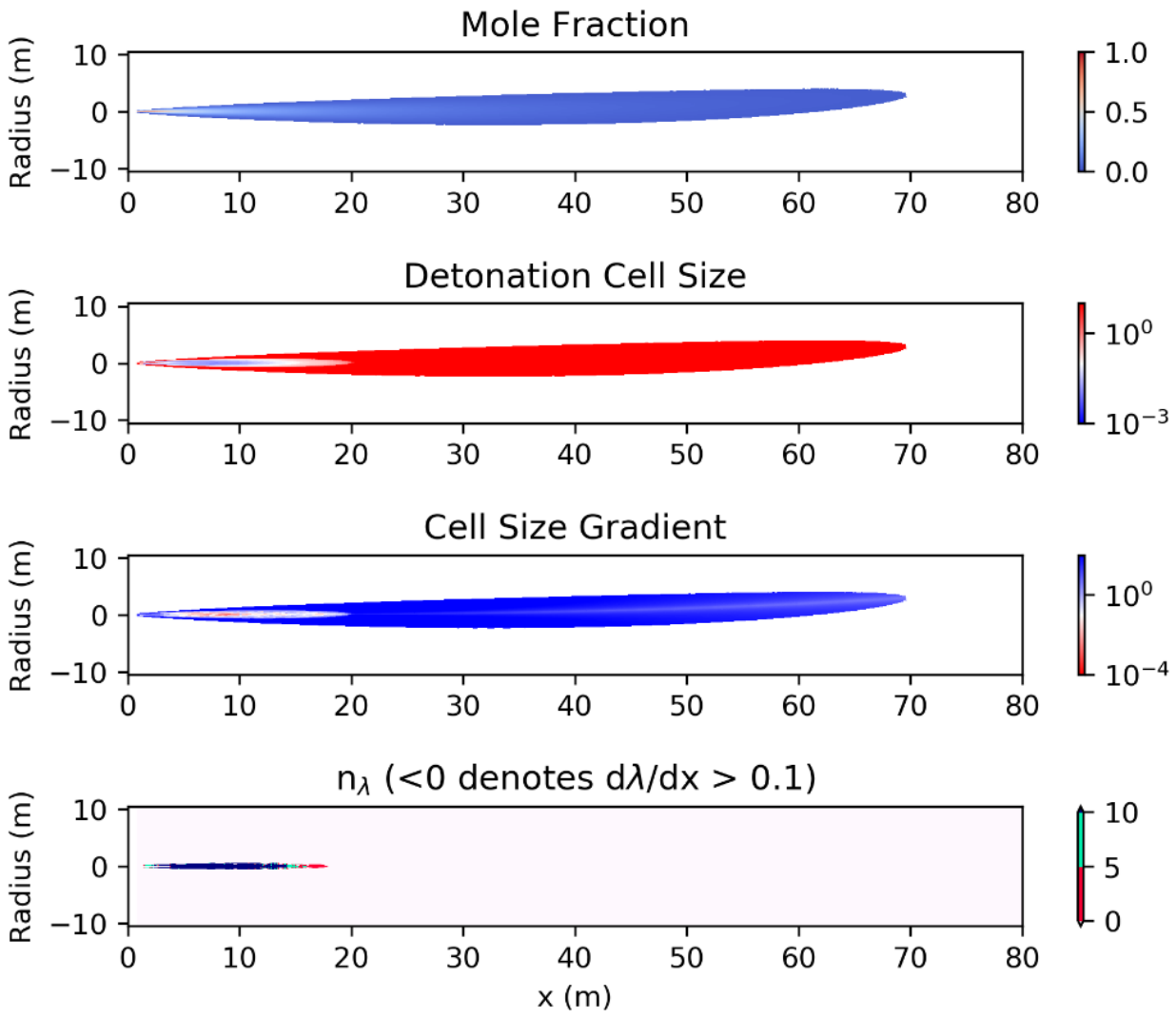

Figure D-15. Scenario 8 Consequence Evaluation Results

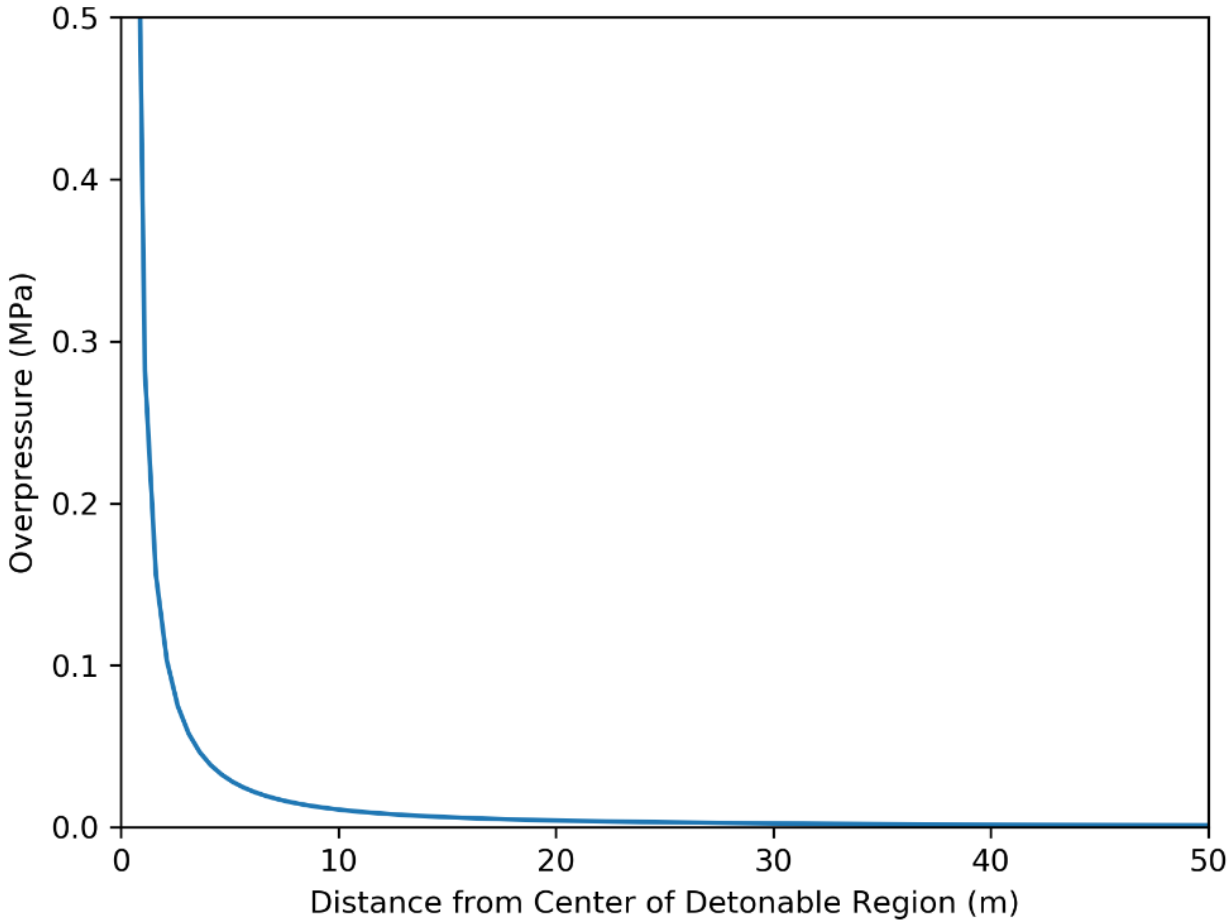

Figure D-16. Scenario 8 Overpressure Evaluation Results

Scenario 9

Scenario 9 is a 101.6 mm break with a temperature of 75°C and pressure of 1.01 MPa.

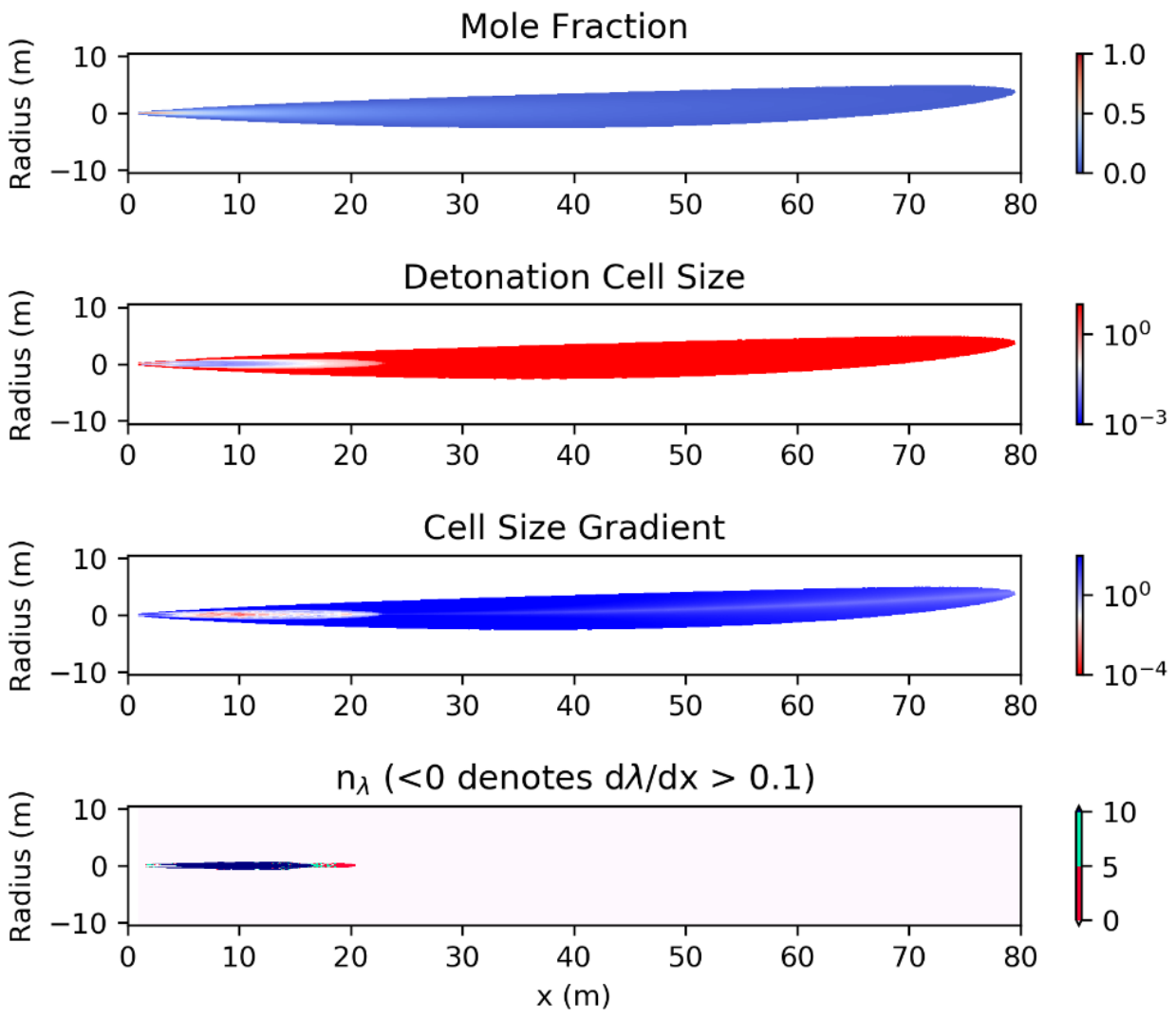

Figure D-17. Scenario 9 Consequence Evaluation Results

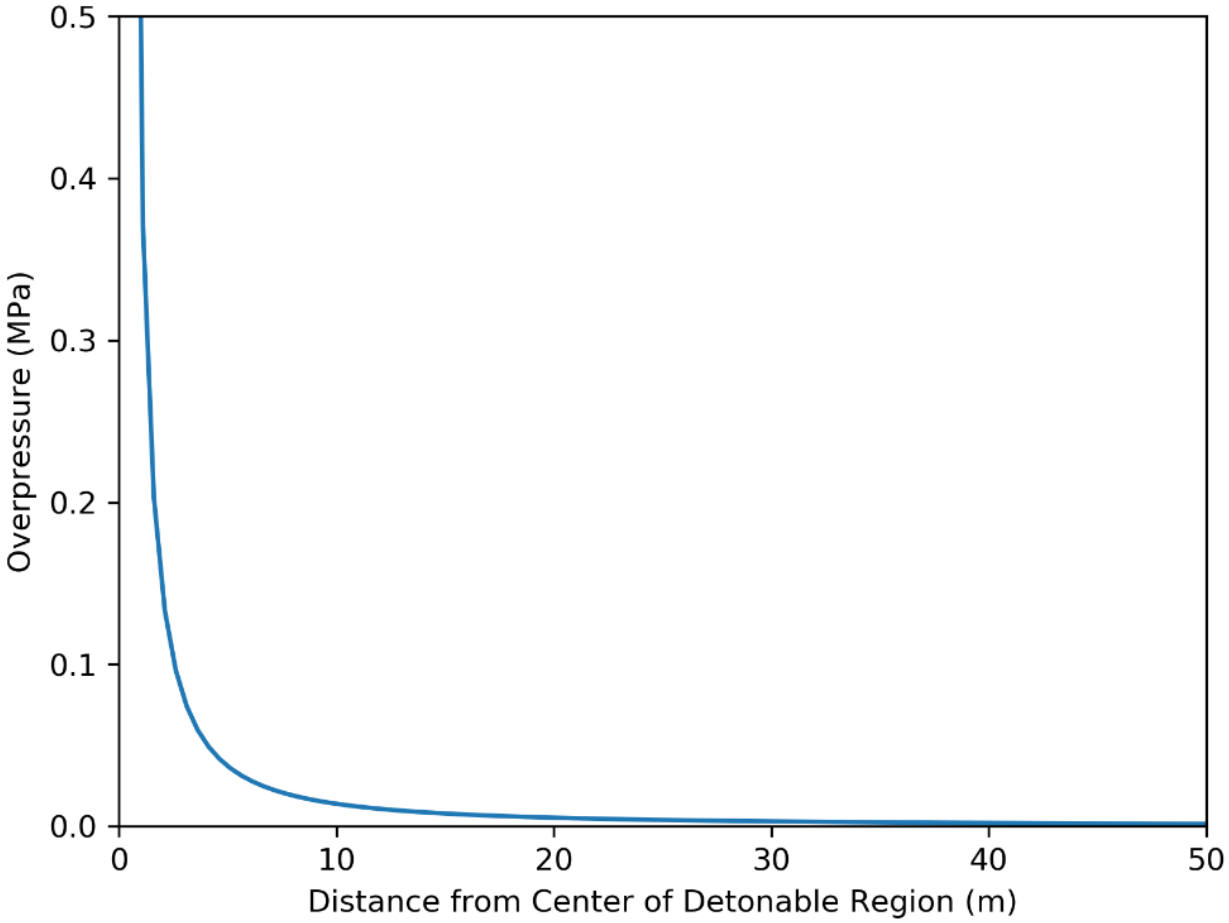

Figure D-18. Scenario 9 Overpressure Evaluation Results

Scenario 10

Scenario 10 is a 200.0 mm break with a temperature of 75°C and pressure of 1.01 MPa.

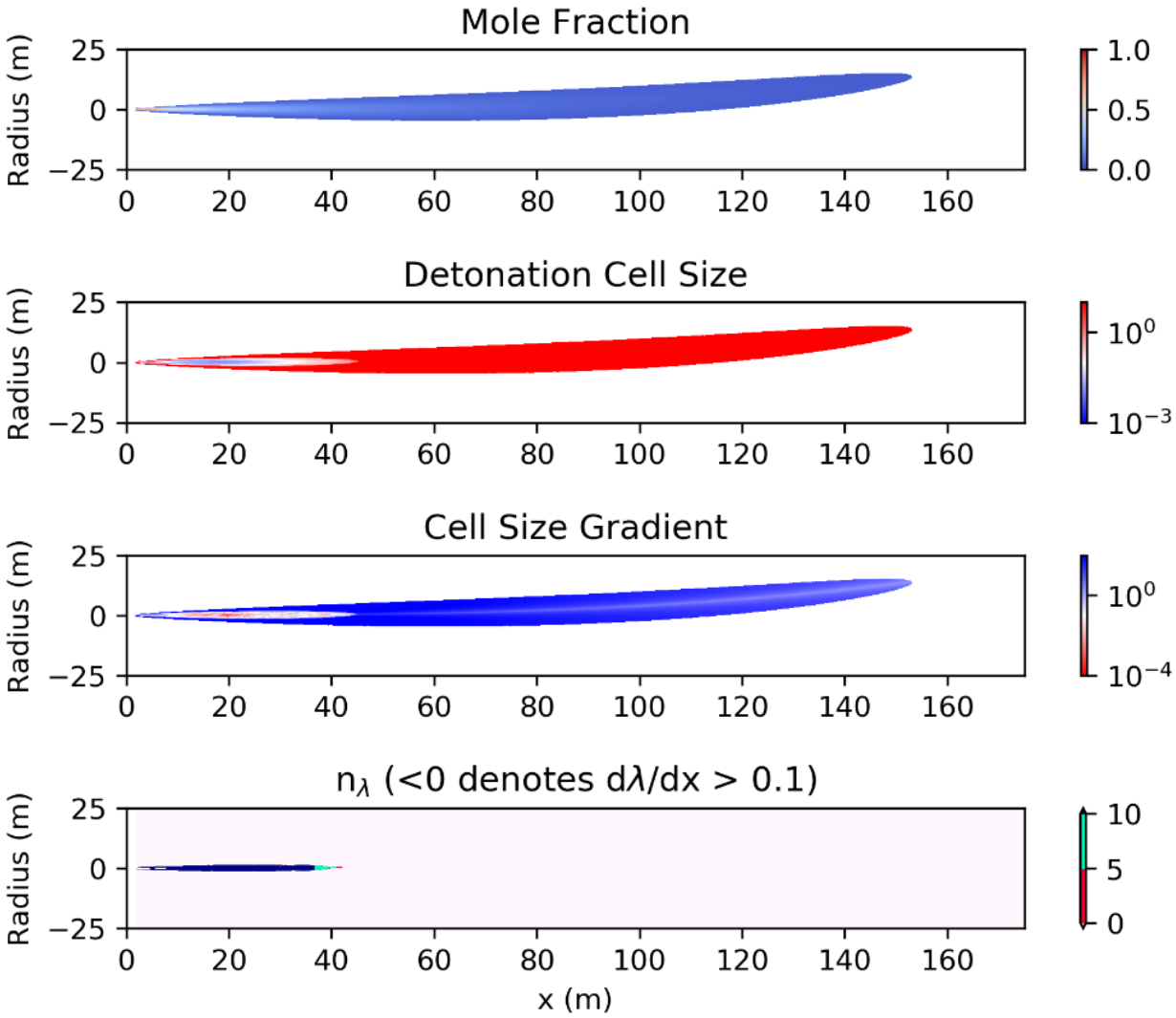

Figure D-19. Scenario 10 Consequence Evaluation Results

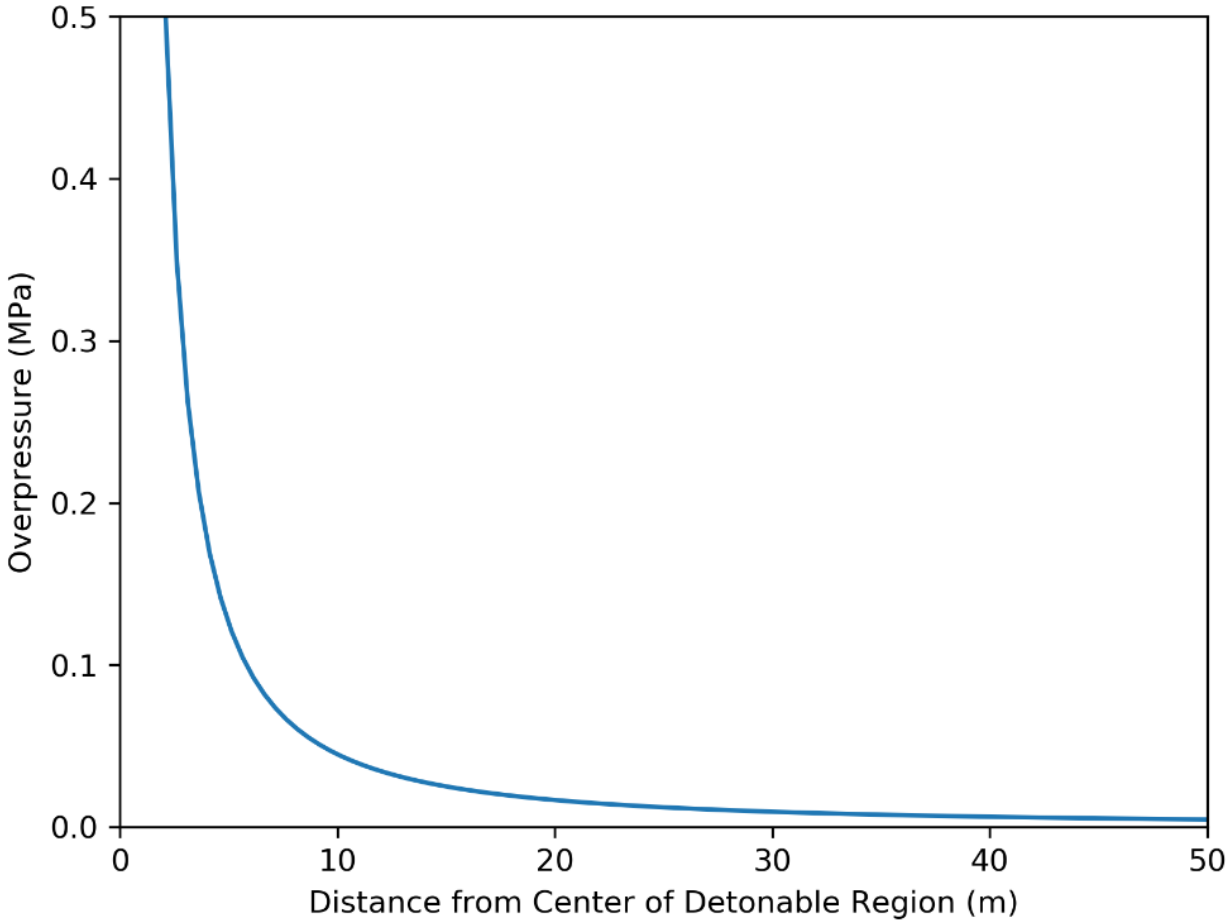

Figure D-20. Scenario 10 Overpressure Evaluation Results

Scenario 11

Scenario 11 is a 254.0 mm break with a temperature of 75°C and pressure of 1.01 MPa.

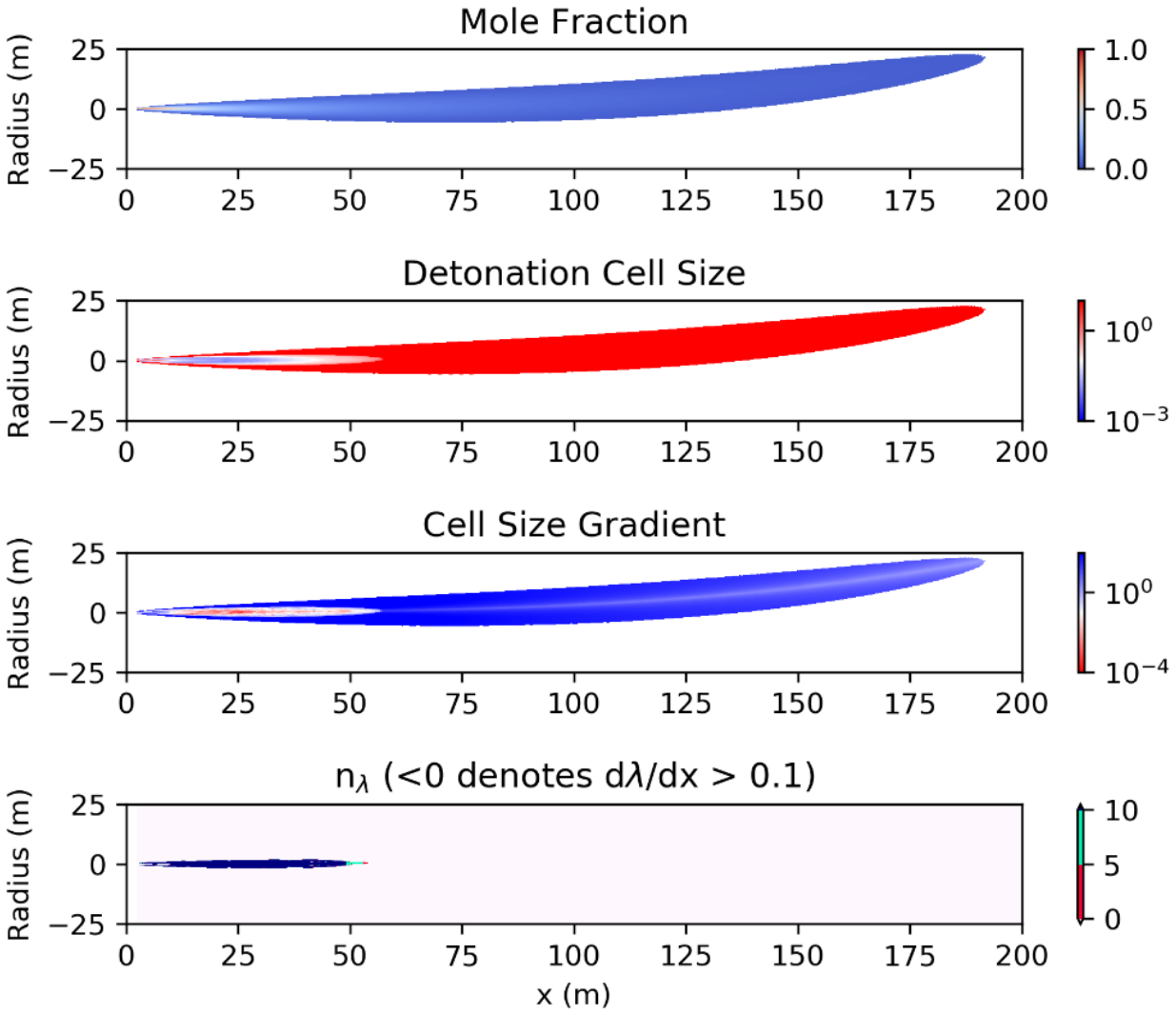

Figure D-21. Scenario 11 Consequence Evaluation Results

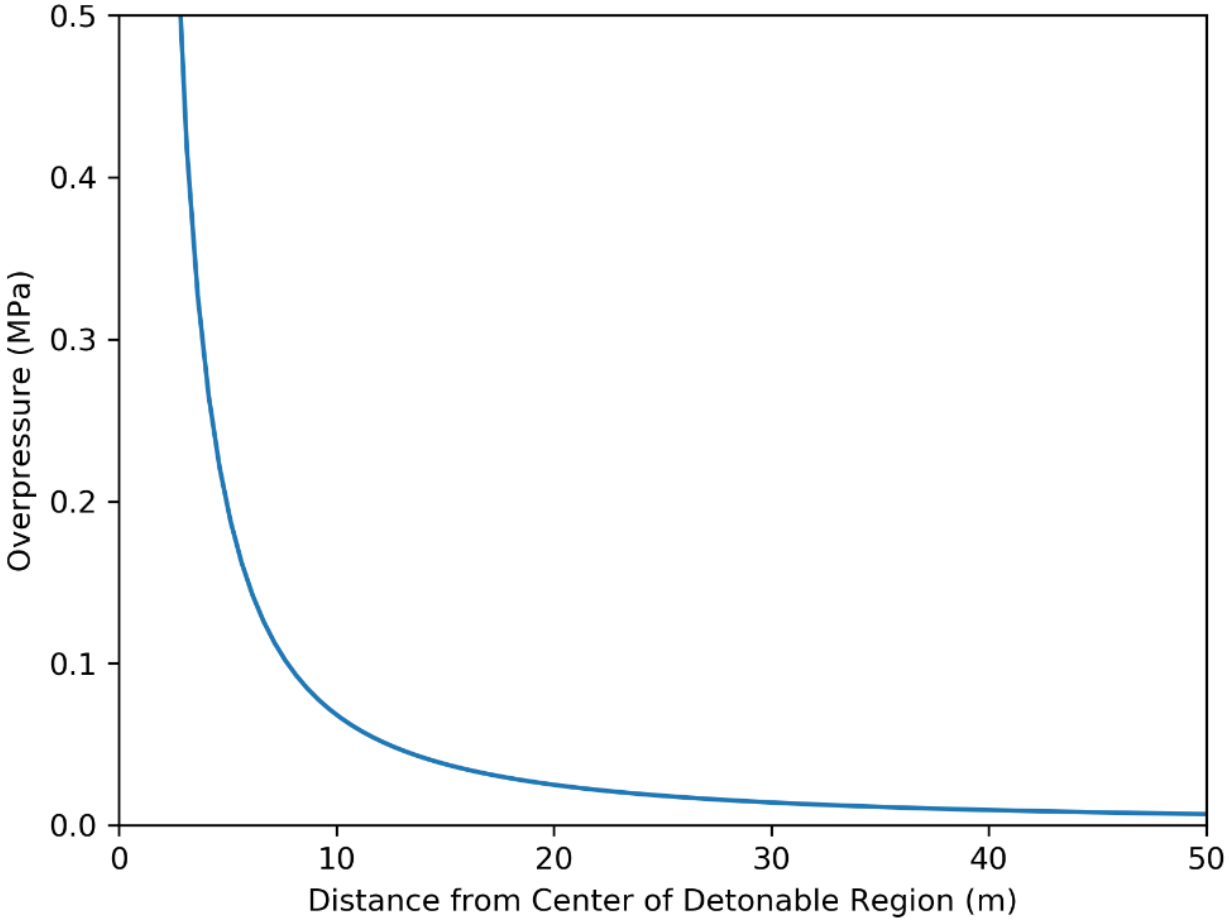

Figure D-22. Scenario 11 Overpressure Evaluation Results

Scenario 12

Scenario 12 is an 88.9 mm break with a temperature of 25°C and pressure of 2.23 MPa.

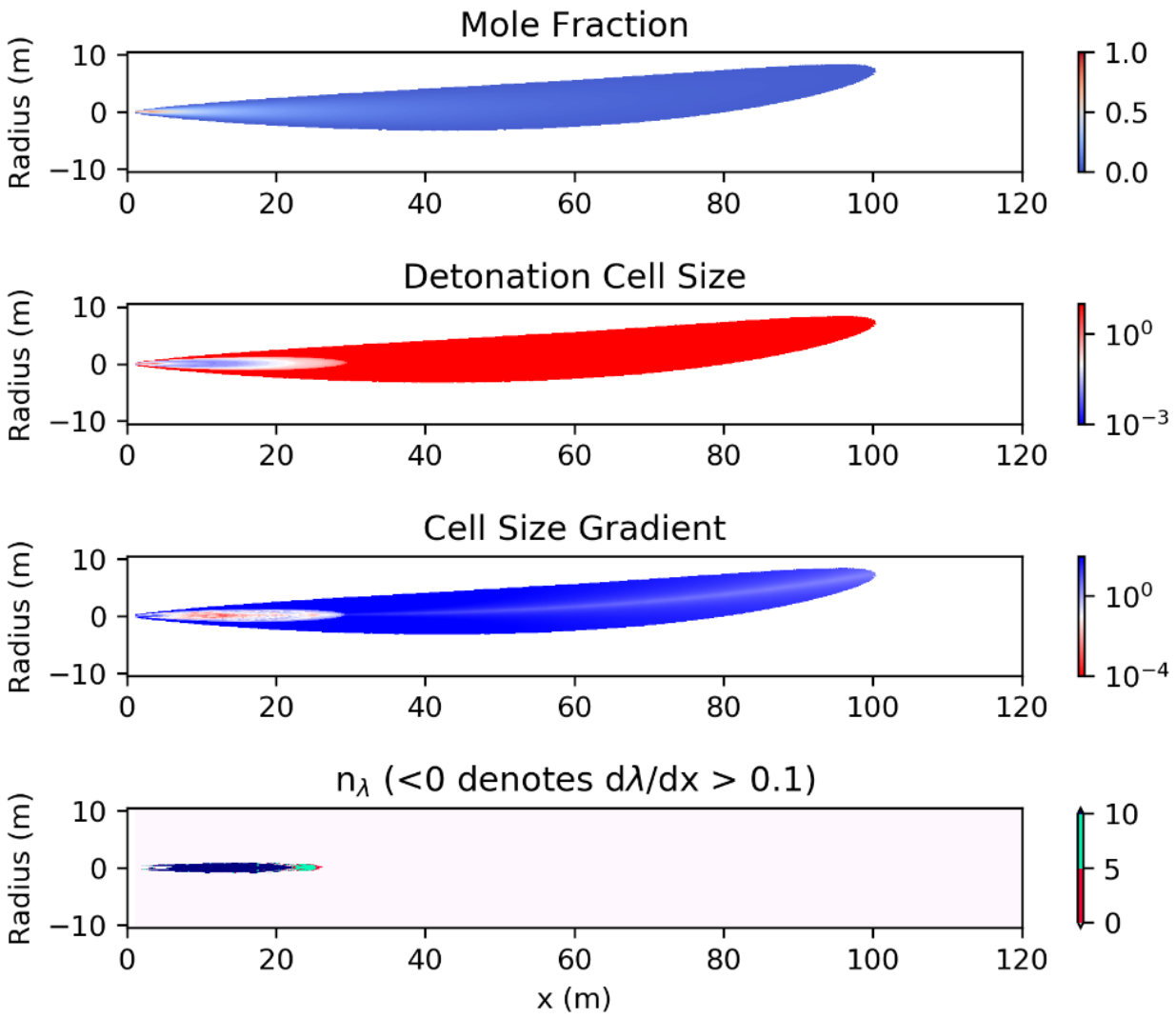

Figure D-23. Scenario 12 Consequence Evaluation Results

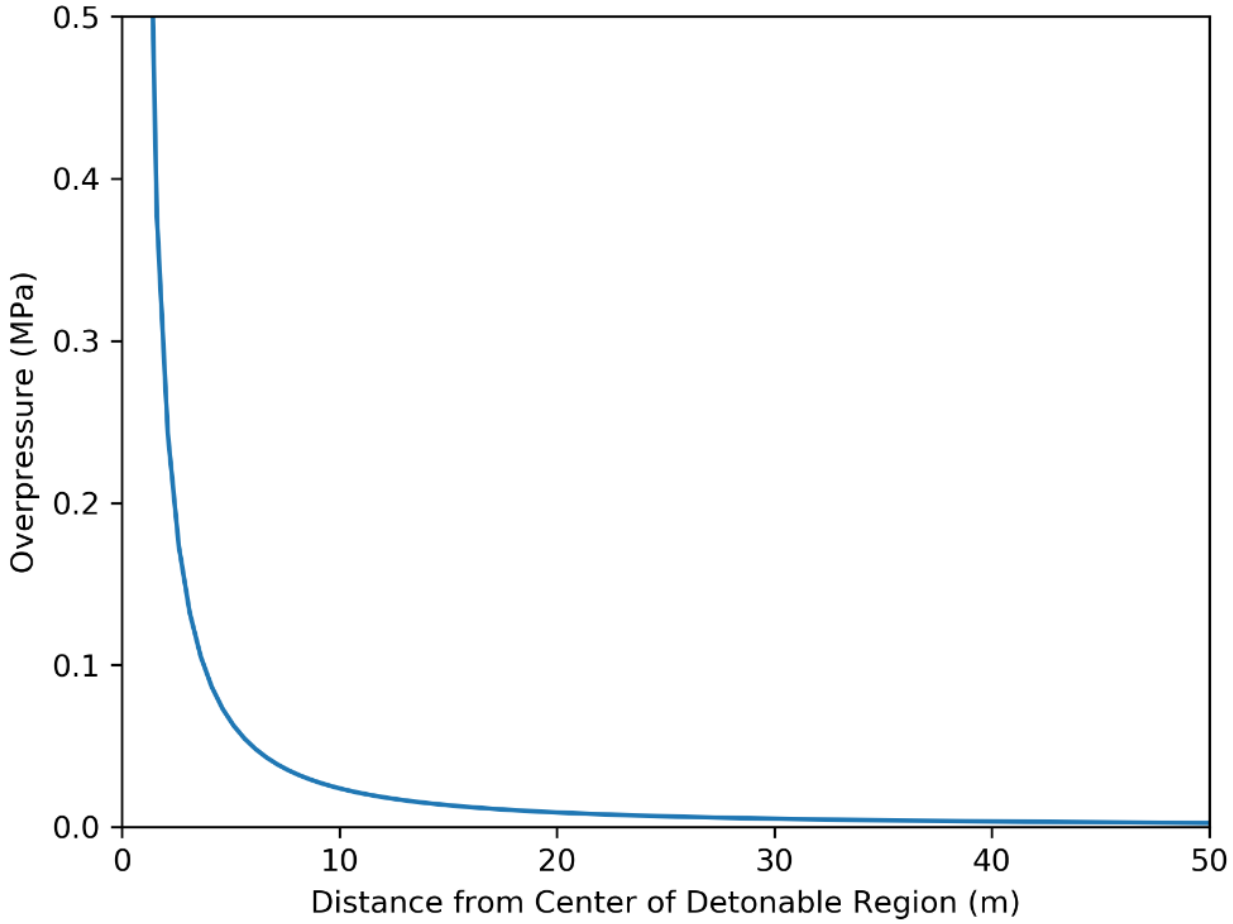

Figure D-24. Scenario 12 Overpressure Evaluation Results

Scenario 13

Scenario 13 is a 200.0 mm break with a temperature of 25°C and pressure of 2.23 MPa.

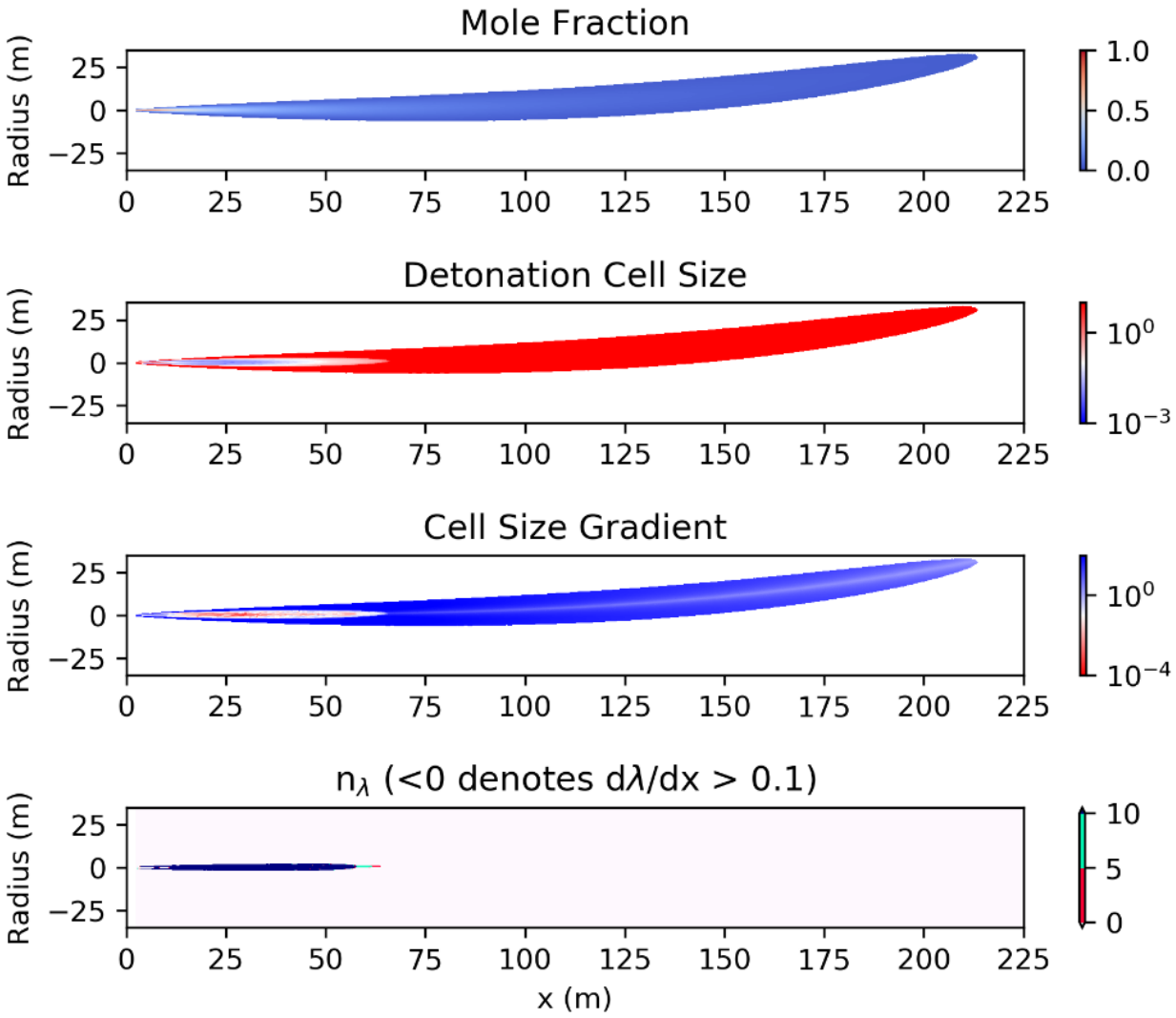

Figure D-25. Scenario 13 Consequence Evaluation Results

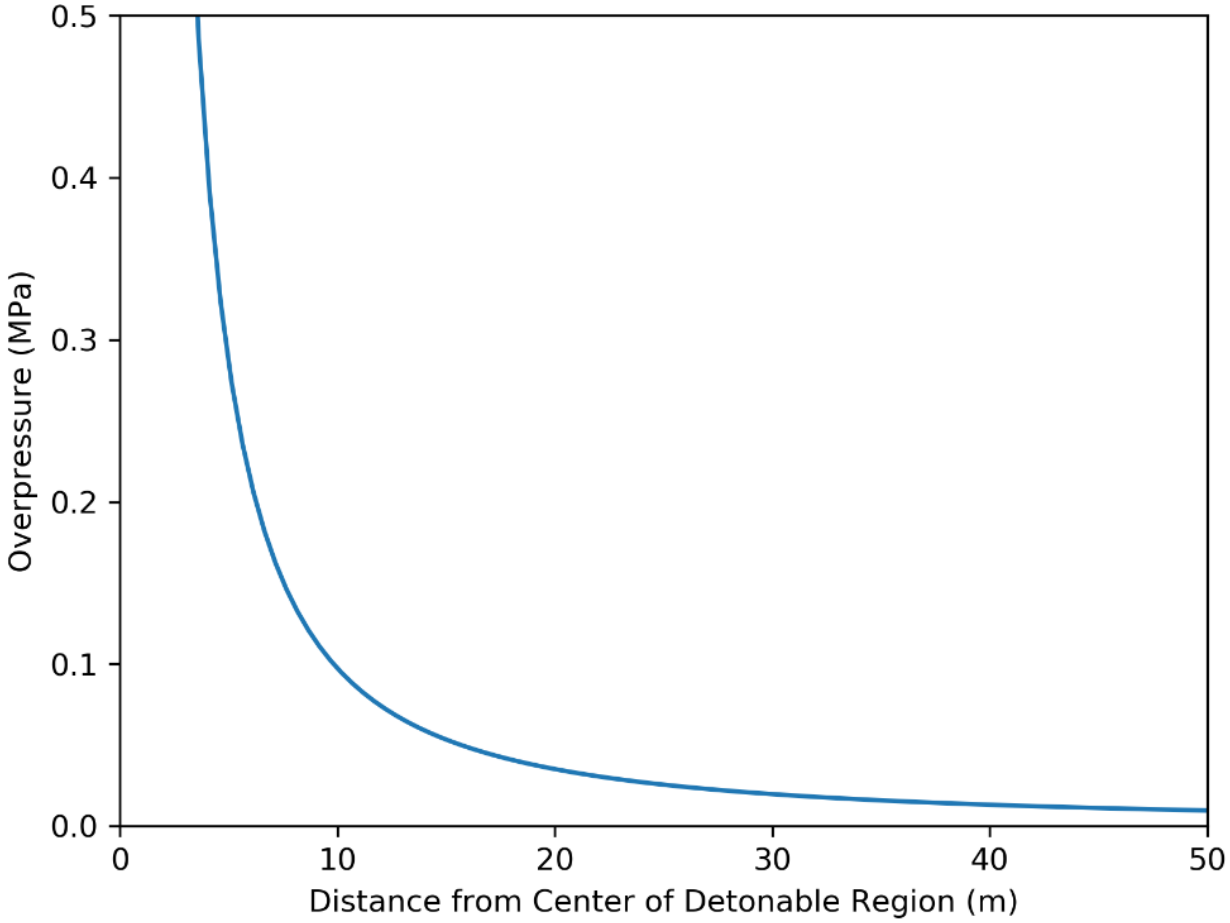

Figure D-26. Scenario 13 Overpressure Evaluation Results

Scenario 14

Scenario 14 is a 254.0 mm break with a temperature of 25°C and pressure of 2.23 MPa.

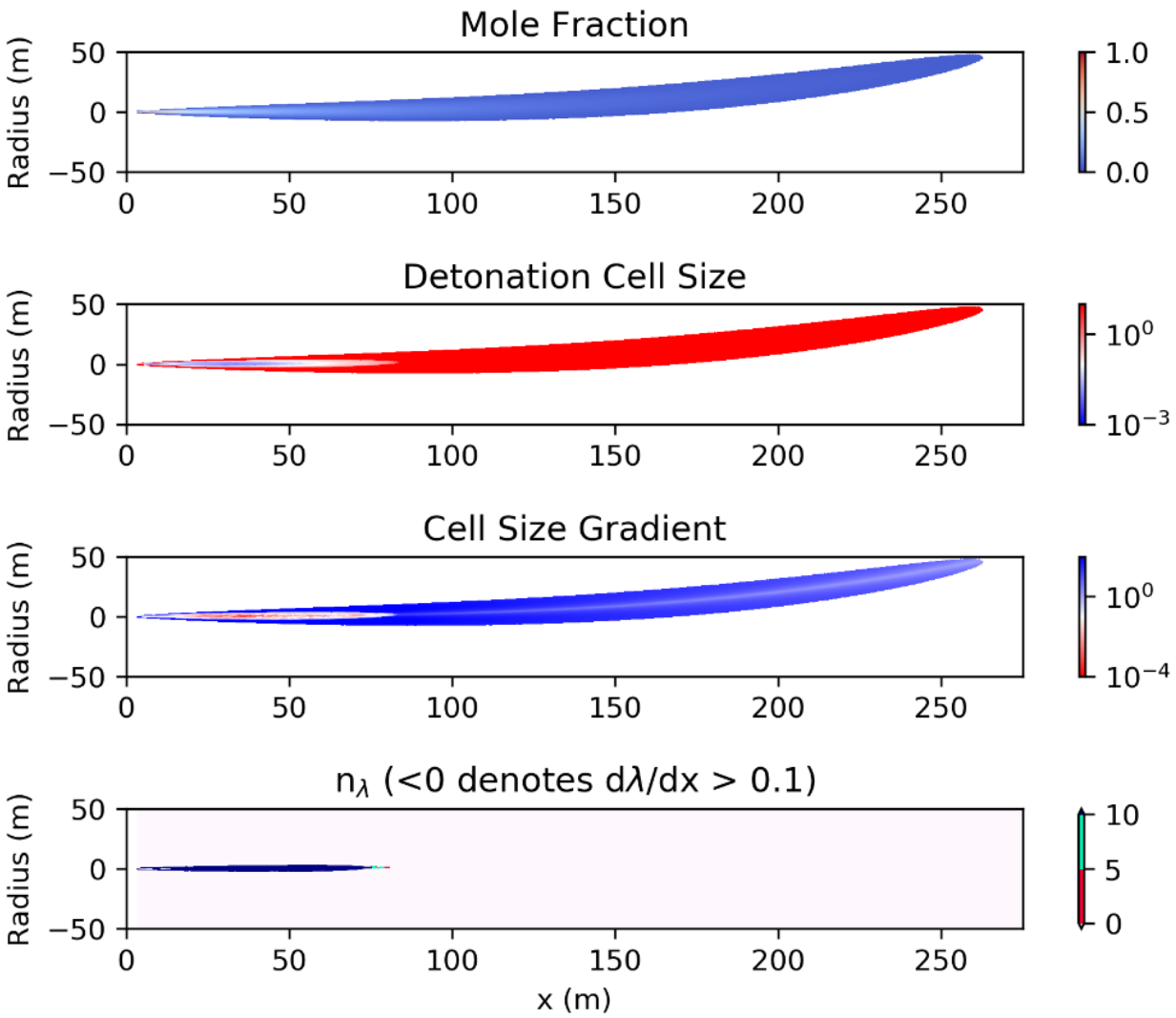

Figure D-27. Scenario 14 Consequence Evaluation Results

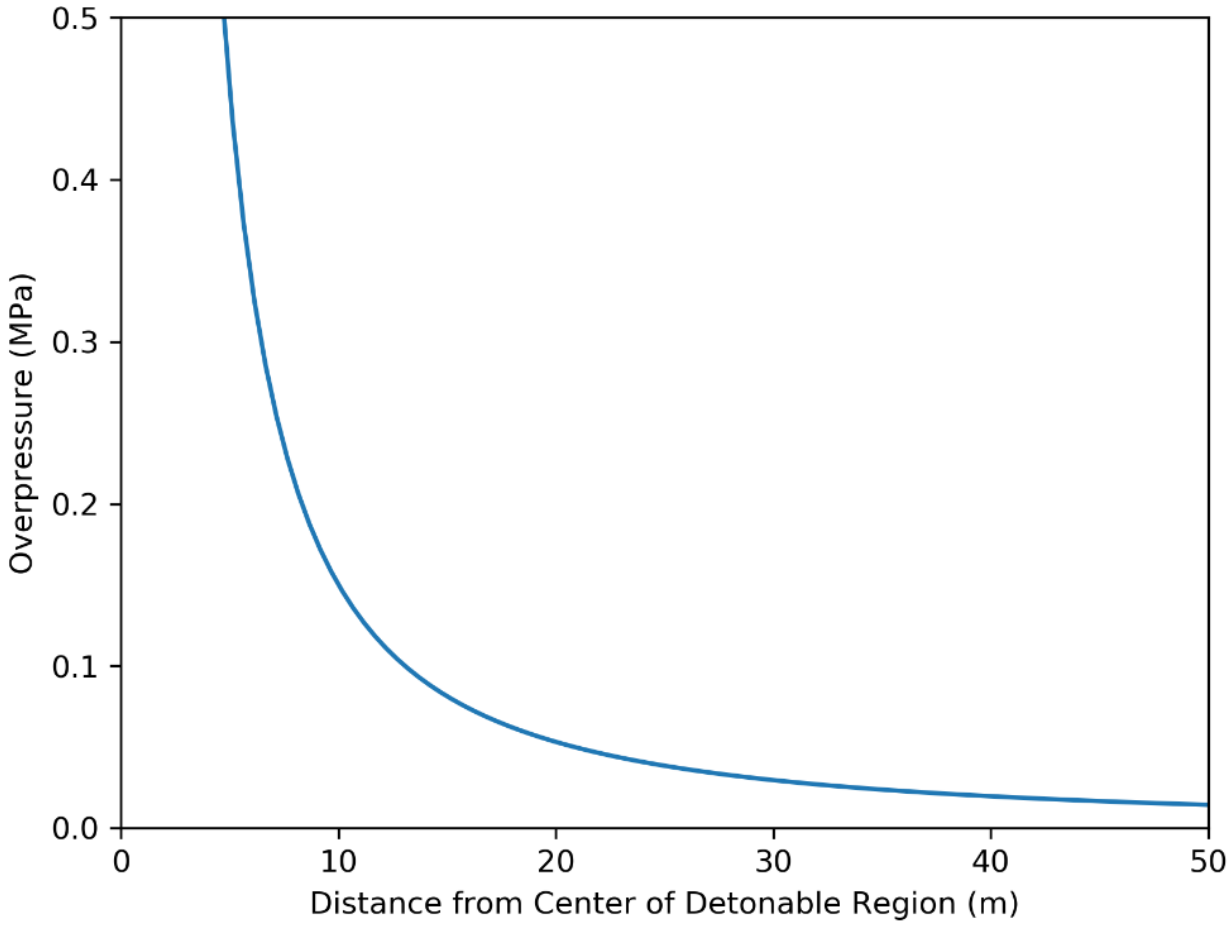

Figure D-28. Scenario 14 Overpressure Evaluation Results

Scenario 15

Scenario 15 is a 200.0 mm break with a temperature of 50°C and pressure of 7.0 MPa

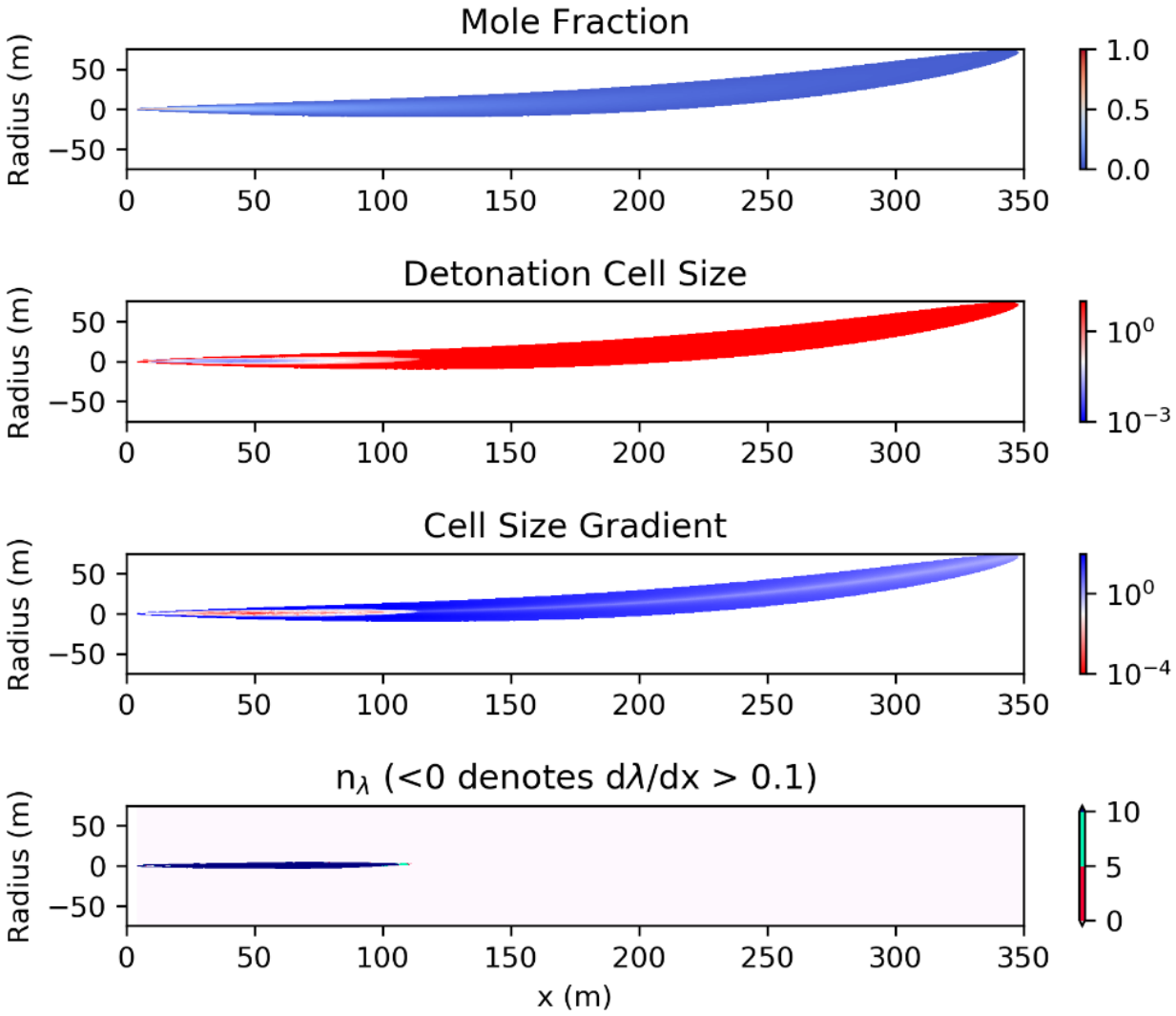

Figure D-29. Scenario 15 Consequence Evaluation Results

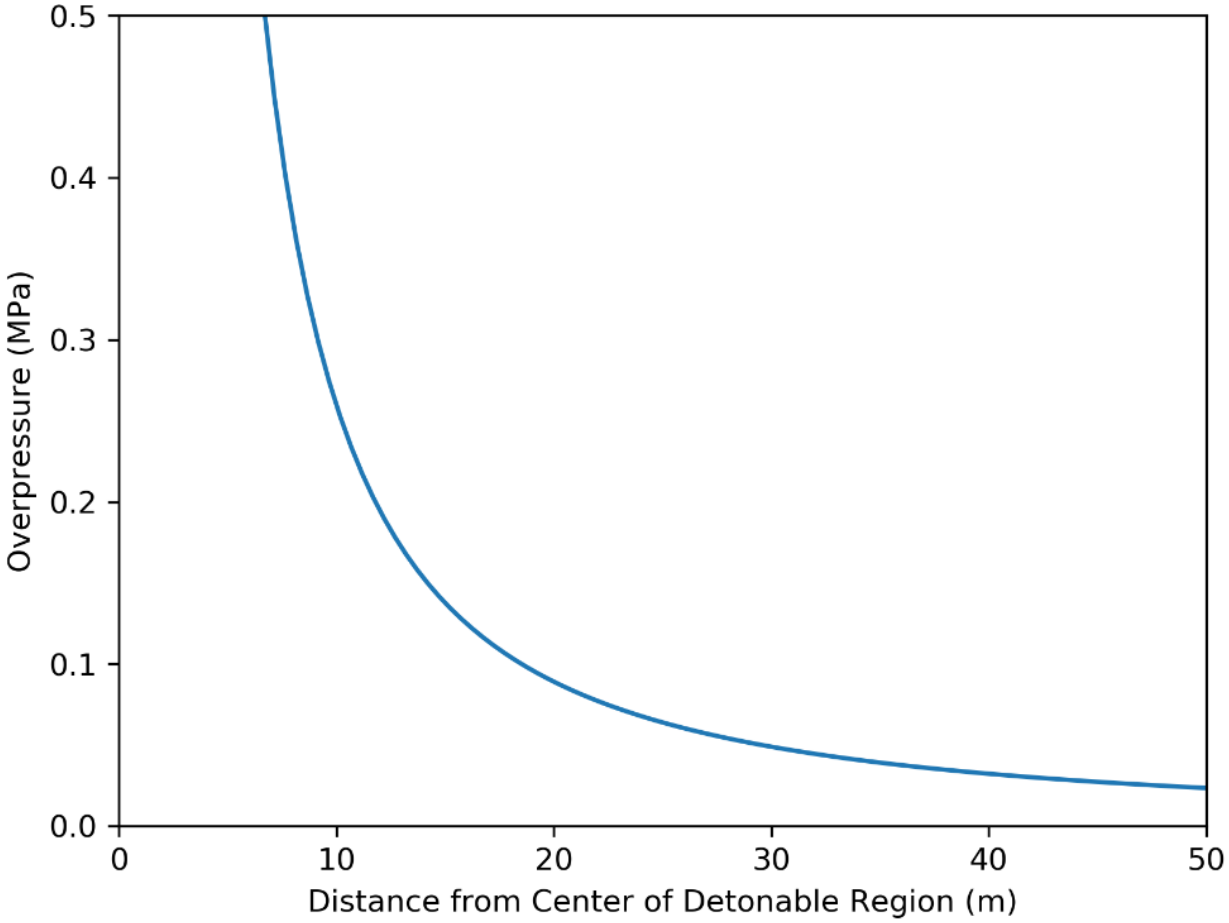

Figure D-30. Scenario 15 Overpressure Evaluation Results

APPENDIX E. HIGH-PRESSURE JET SEPARATION DISTANCE RESULTS

This appendix contains the detailed separation distance plots for each of the scenarios outlined in Table 3-3.

Scenario 1

Scenario 1 is a 203.2 mm break with a temperature of 735°C and pressure of 0.52 MPa.

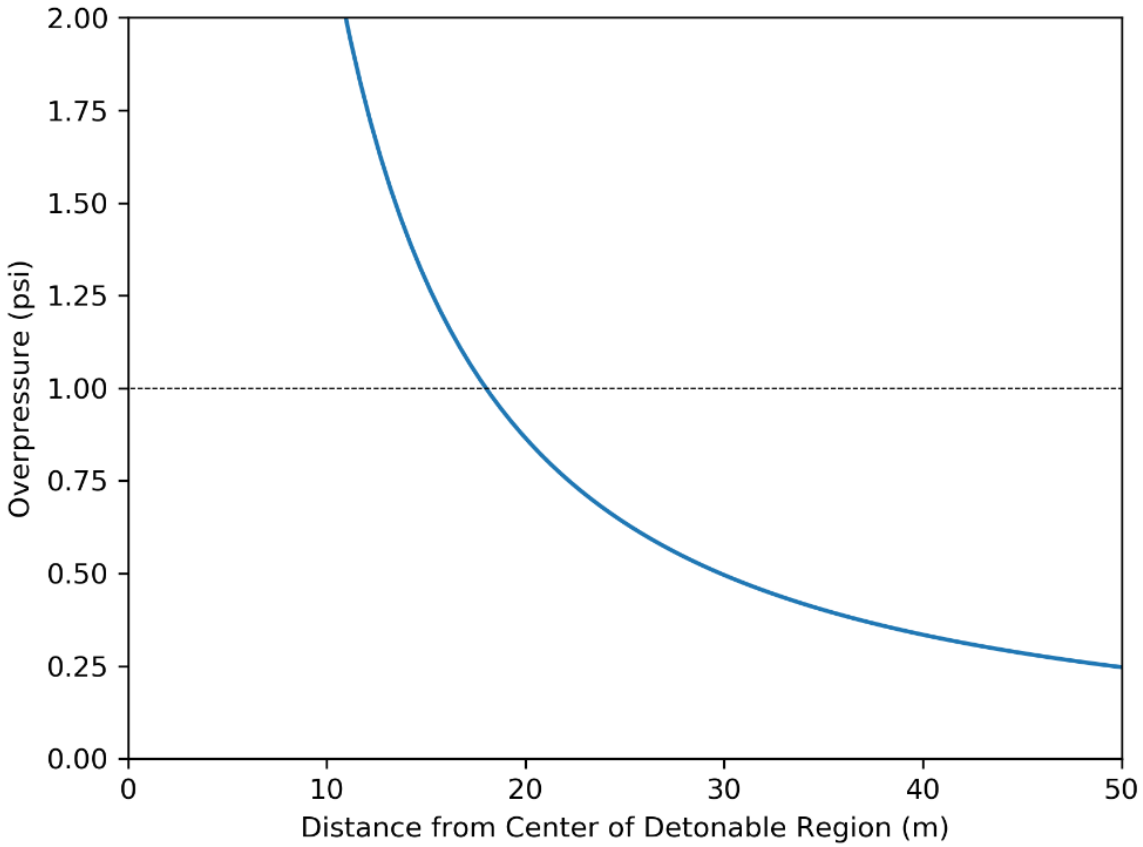

Figure E-1. Scenario 1 Separation Distance Results

Scenario 2

Scenario 2 is a 254.0 mm break with a temperature of 735°C and pressure of 0.52 MPa.

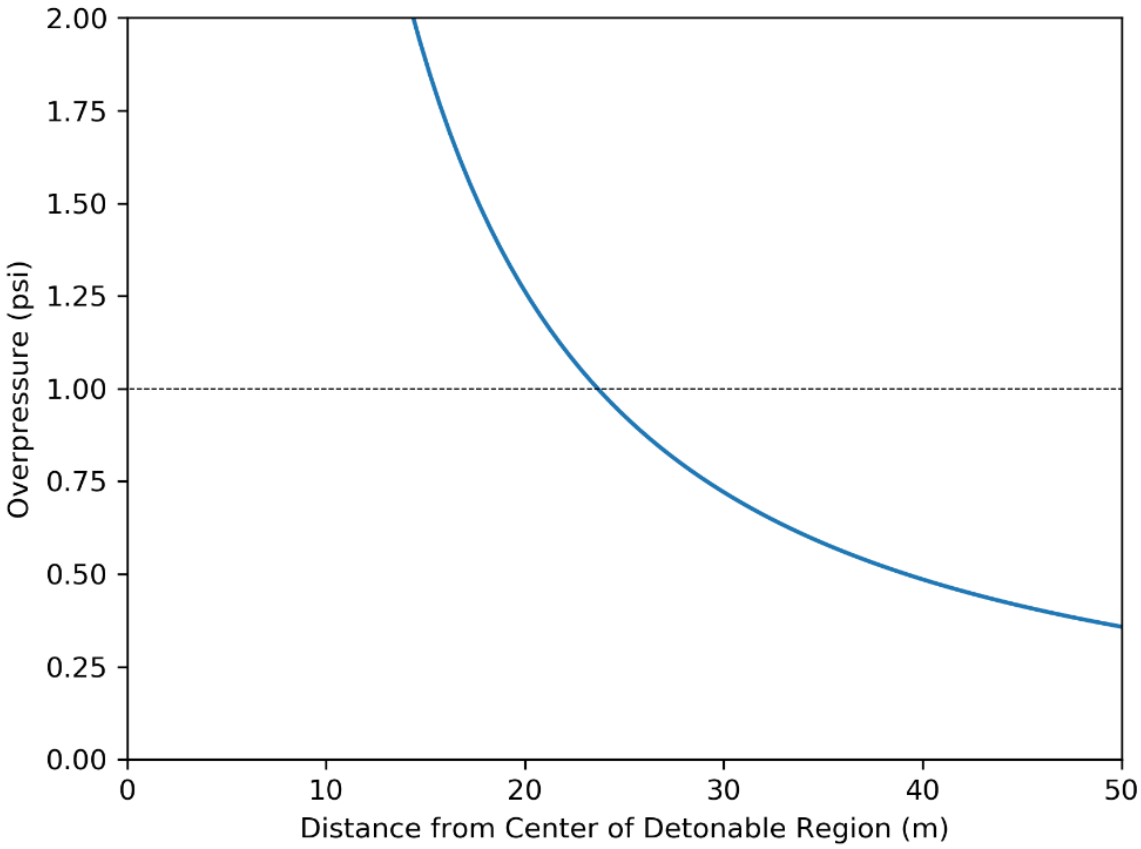

Figure E-2. Scenario 2 Separation Distance Results

Scenario 3

Scenario 3 is a 300.0 mm break with a temperature of 735°C and pressure of 0.52 MPa.

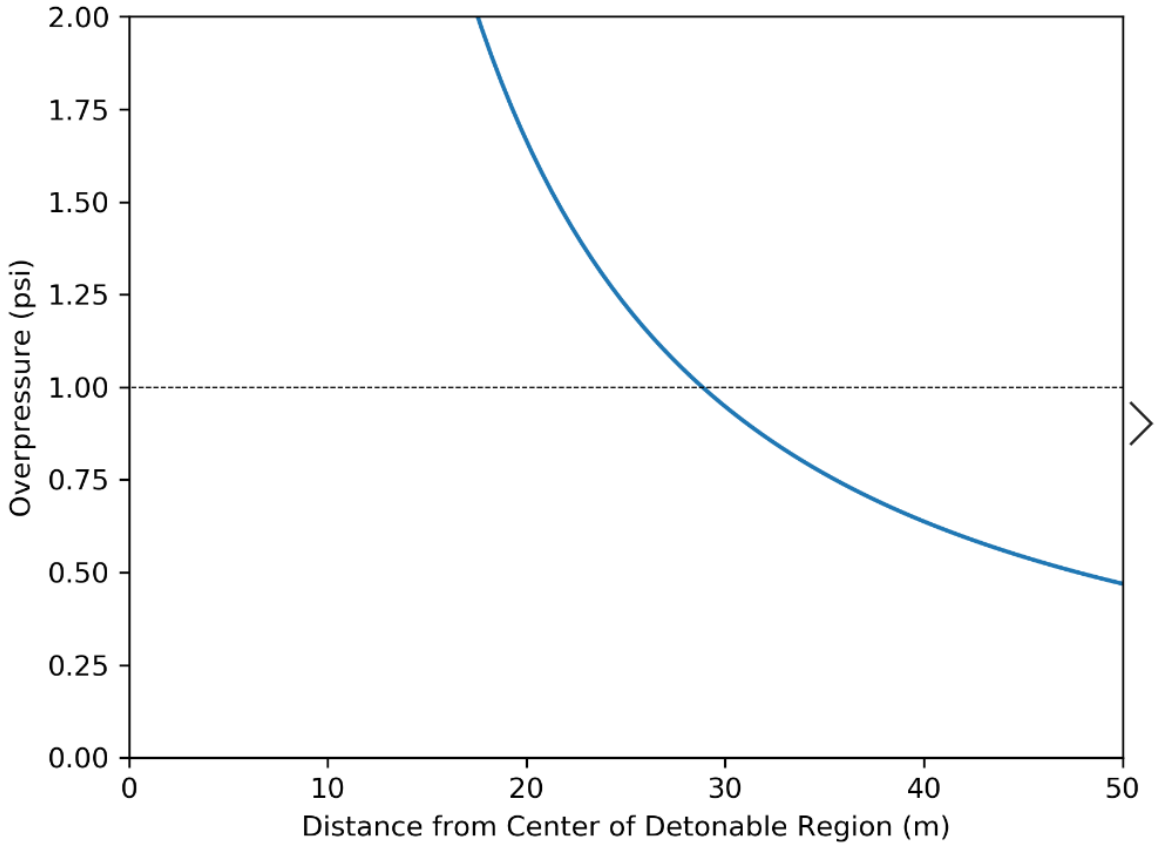

Figure E-3. Scenario 3 Separation Distance Results

Scenario 4

Scenario 4 is a 152.4 mm break with a temperature of 75°C and pressure of 0.48 MPa.

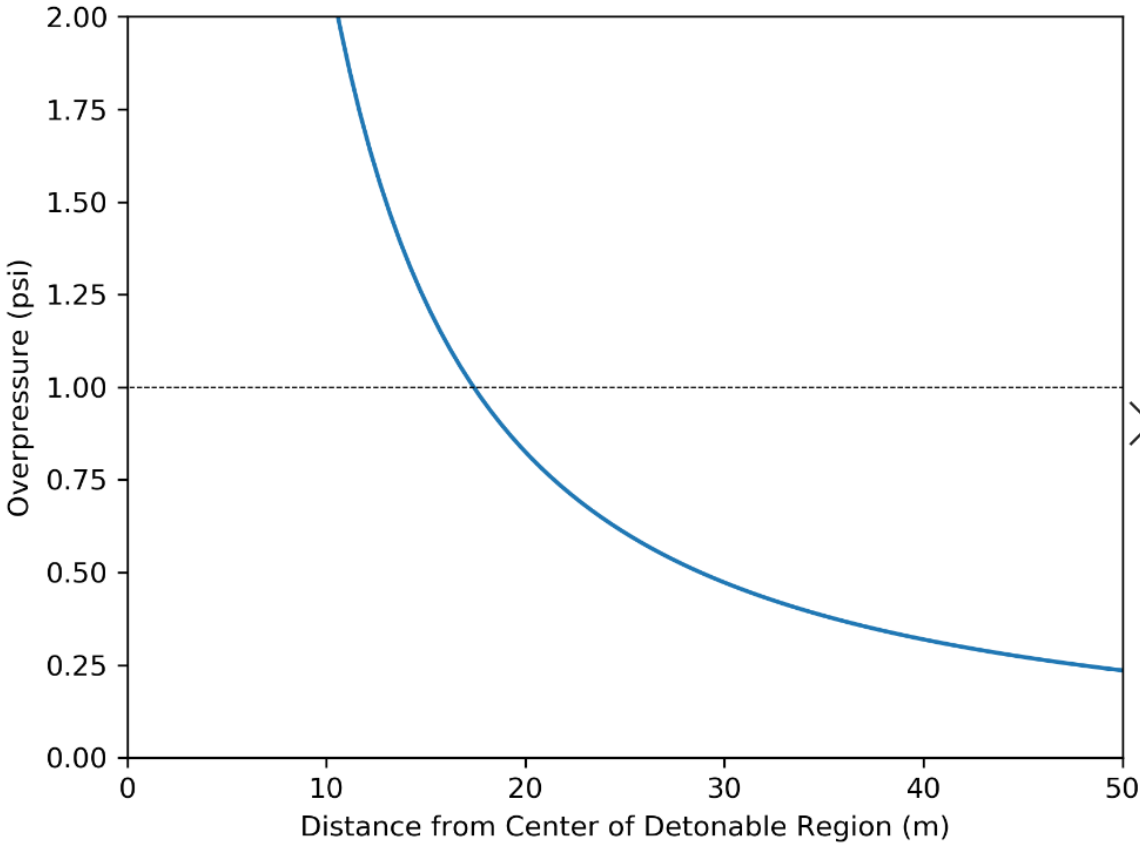

Figure E-4. Scenario 4 Separation Distance Results

Scenario 5

Scenario 5 is a 203.2 mm break with a temperature of 75°C and pressure of 0.48 MPa.

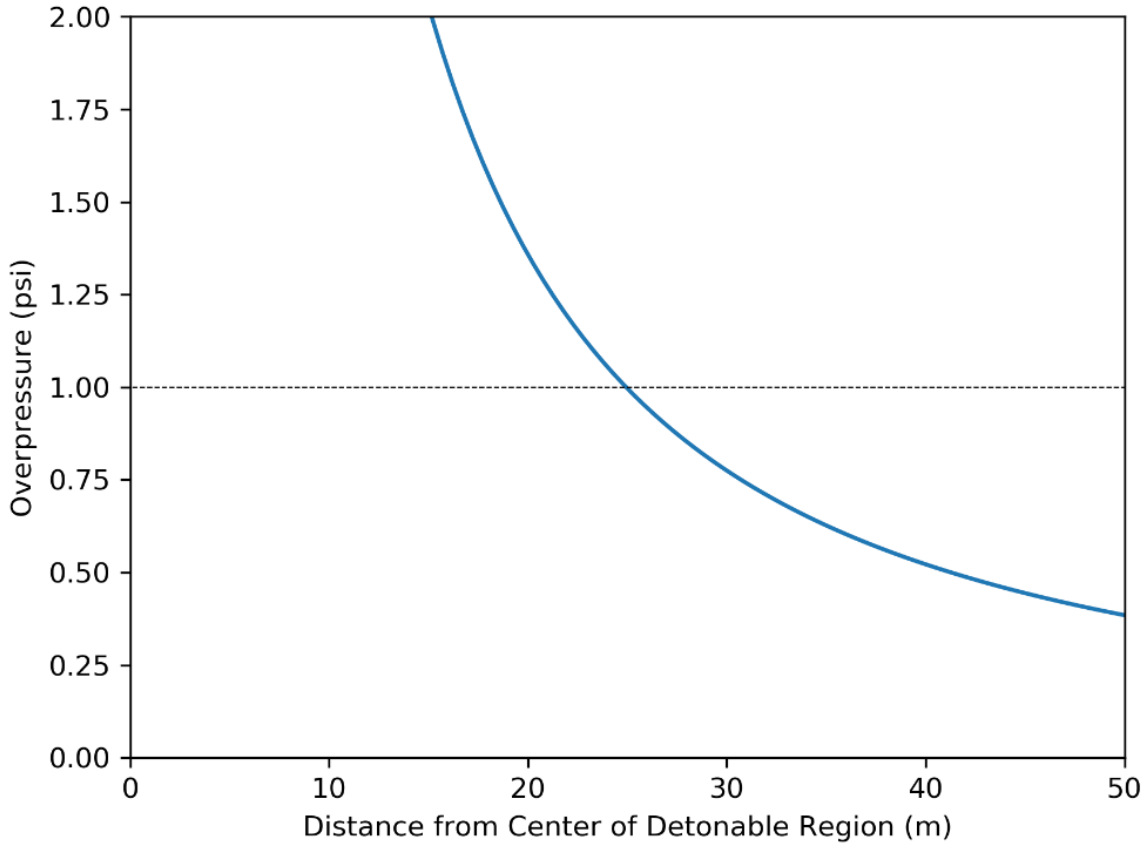

Figure E-5. Scenario 5 Separation Distance Results

Scenario 6

Scenario 6 is a 254.0 mm break with a temperature of 75°C and pressure of 0.48 MPa.

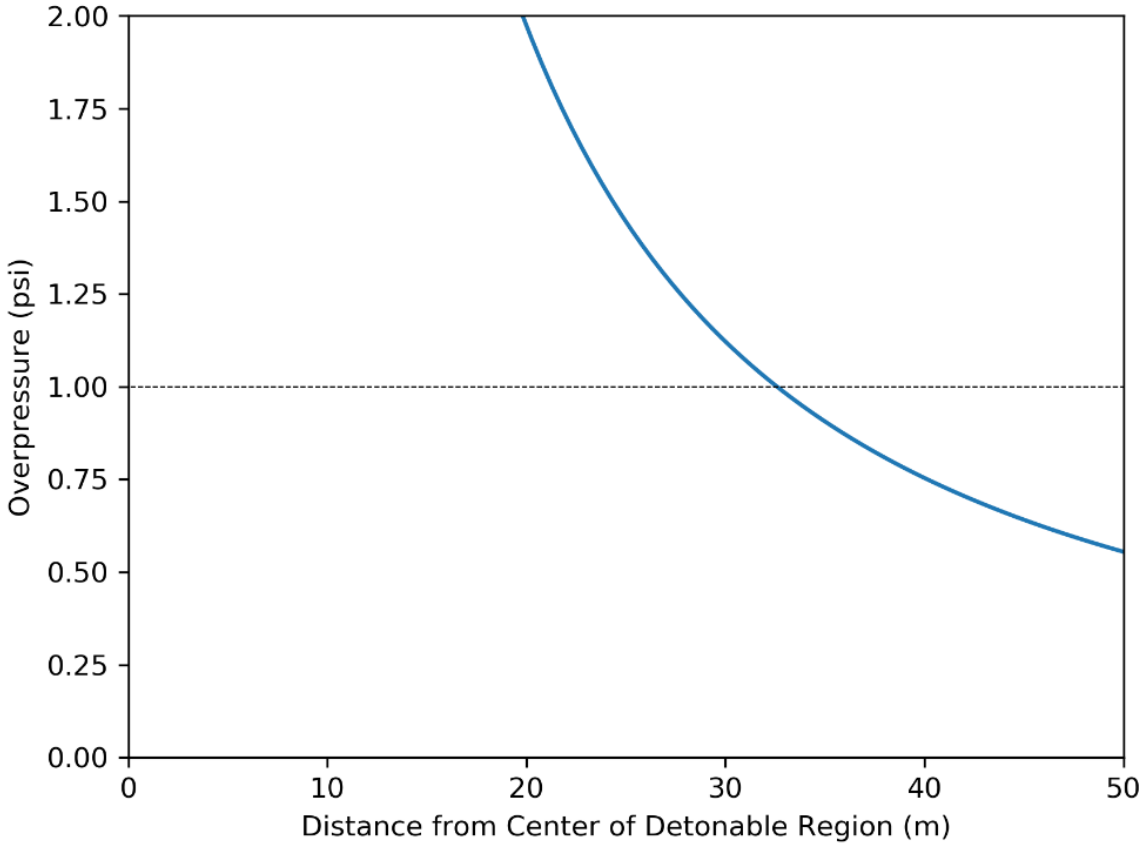

Figure E-6. Scenario 6 Separation Distance Results

Scenario 7

Scenario 7 is a 300.0 mm break with a temperature of 75°C and pressure of 0.48 MPa.

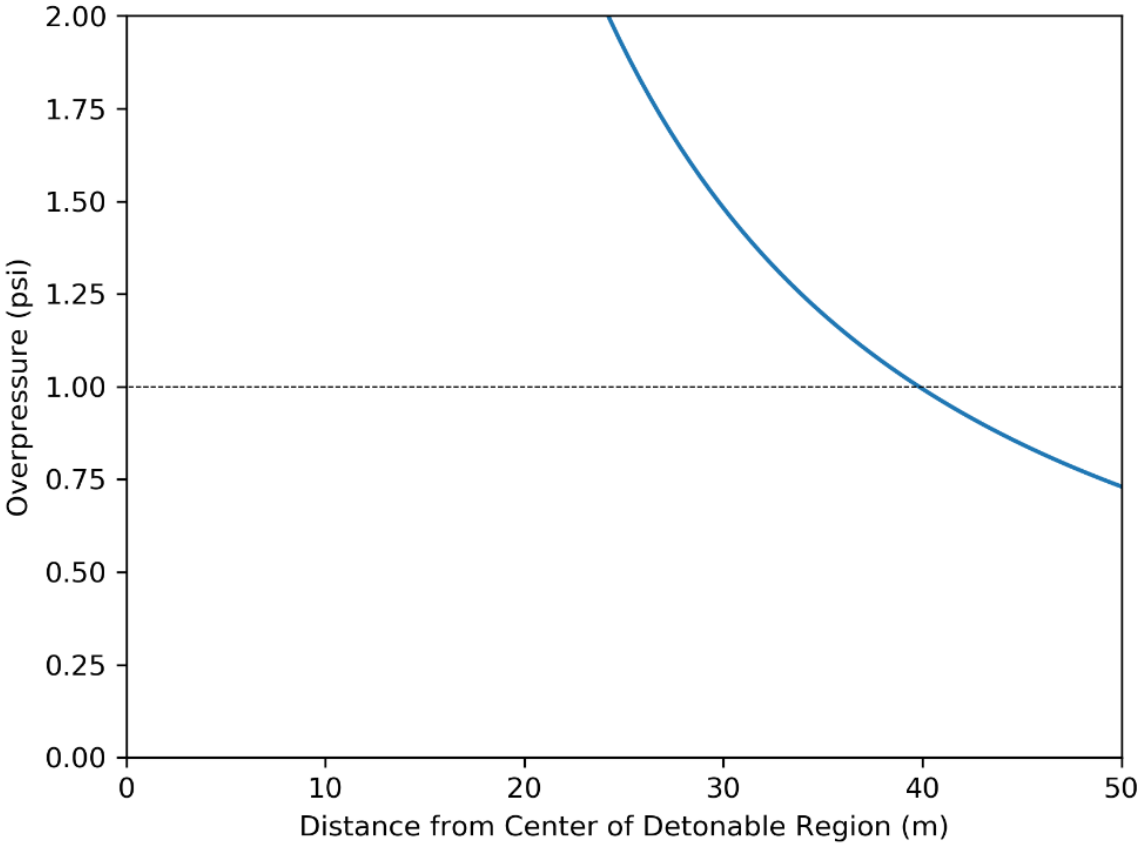

Figure E-7. Scenario 7 Separation Distance Results

Scenario 8

Scenario 8 is an 88.9 mm break with a temperature of 75°C and pressure of 1.01 MPa.

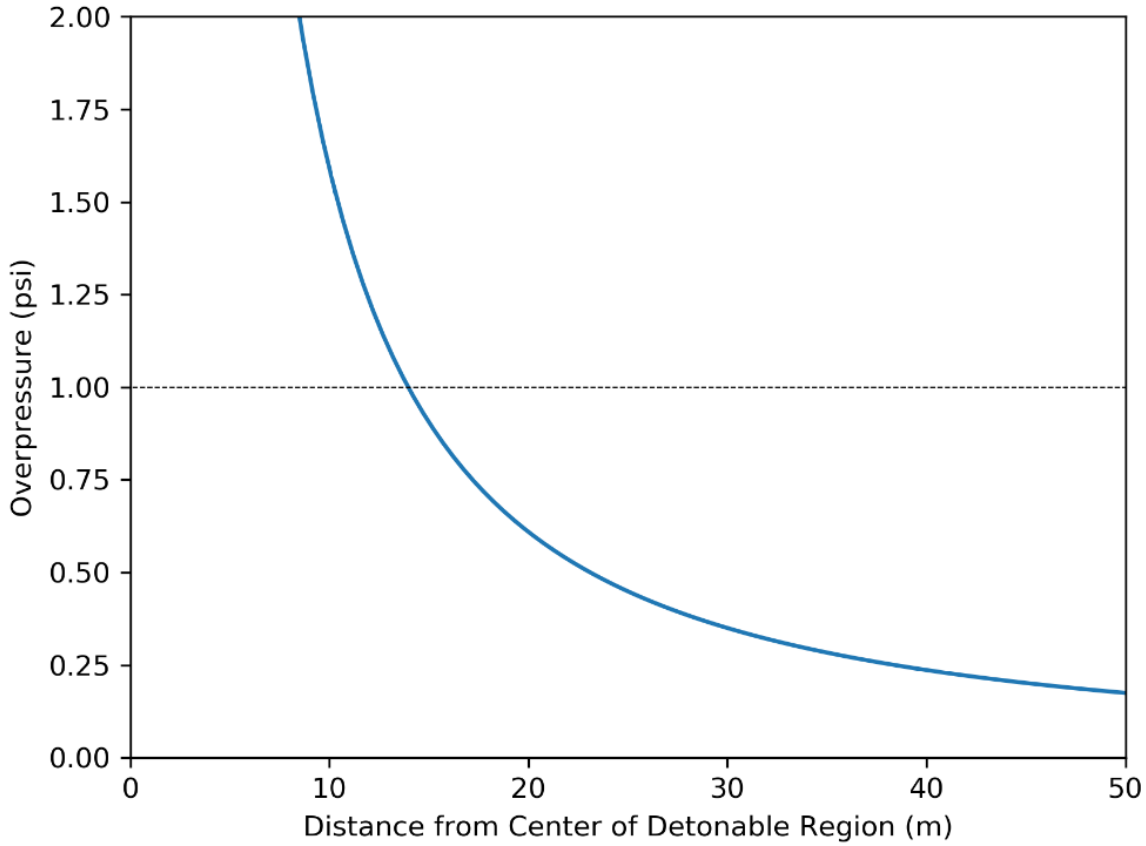

Figure E-8. Scenario 8 Separation Distance Results

Scenario 9

Scenario 9 is a 101.6 mm break with a temperature of 75°C and pressure of 1.01 MPa.

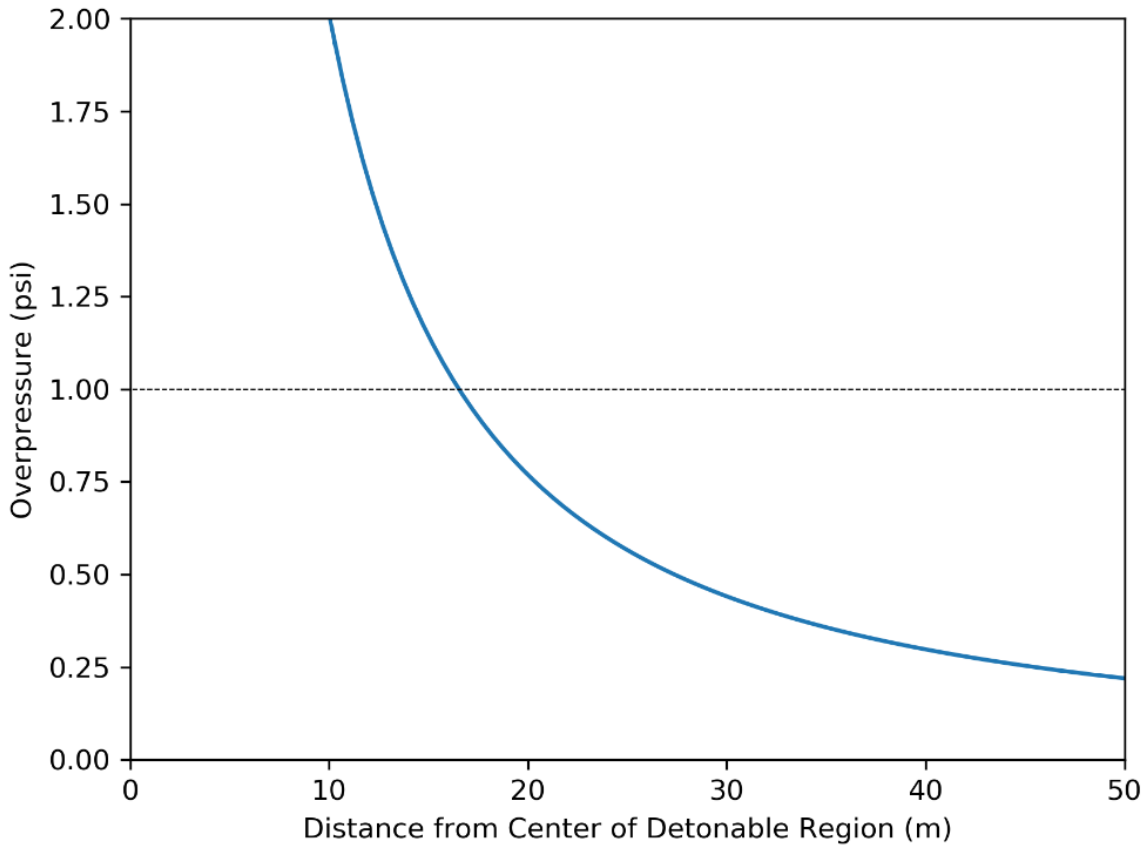

Figure E-9. Scenario 9 Separation Distance Results

Scenario 10

Scenario 10 is a 200.0 mm break with a temperature of 75°C and pressure of 1.01 MPa.

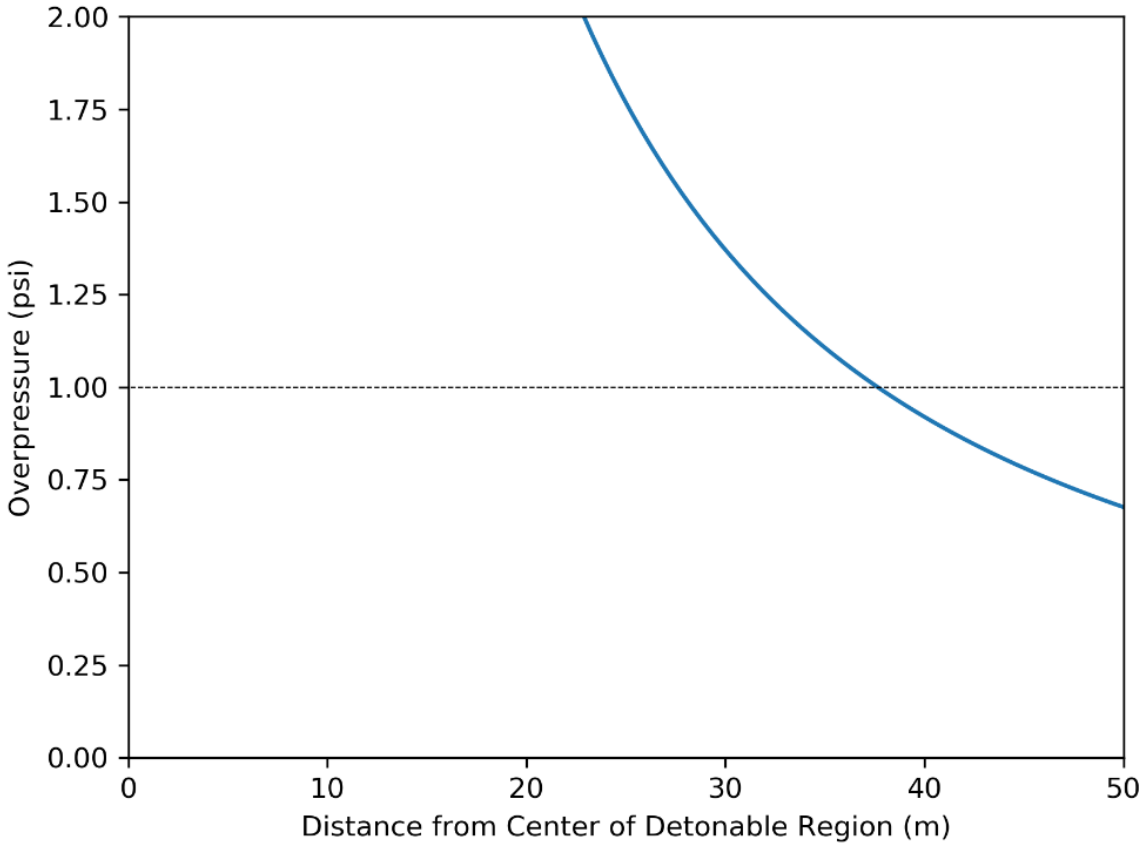

Figure E-10. Scenario 10 Separation Distance Results

Scenario 11

Scenario 11 is a 254.0 mm break with a temperature of 75°C and pressure of 1.01 MPa.

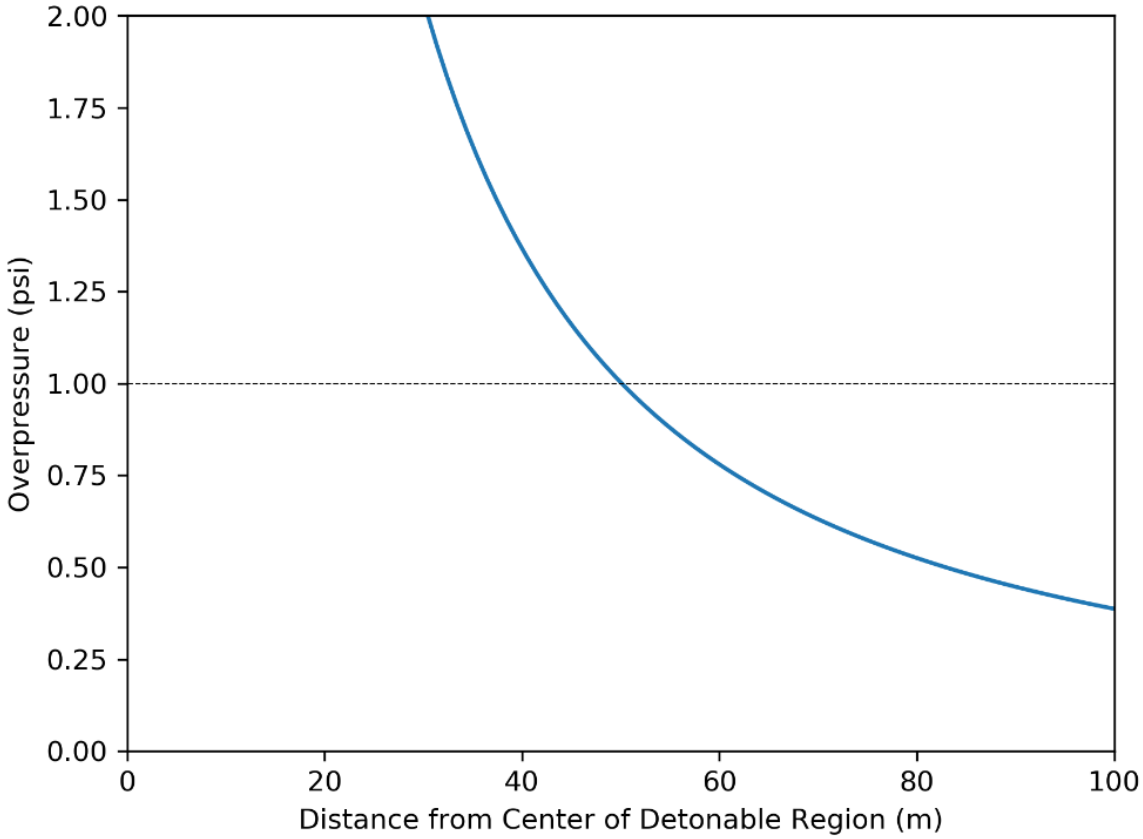

Figure E-11. Scenario 11 Separation Distance Results

Scenario 12

Scenario 12 is an 88.9 mm break with a temperature of 25°C and pressure of 2.23 MPa.

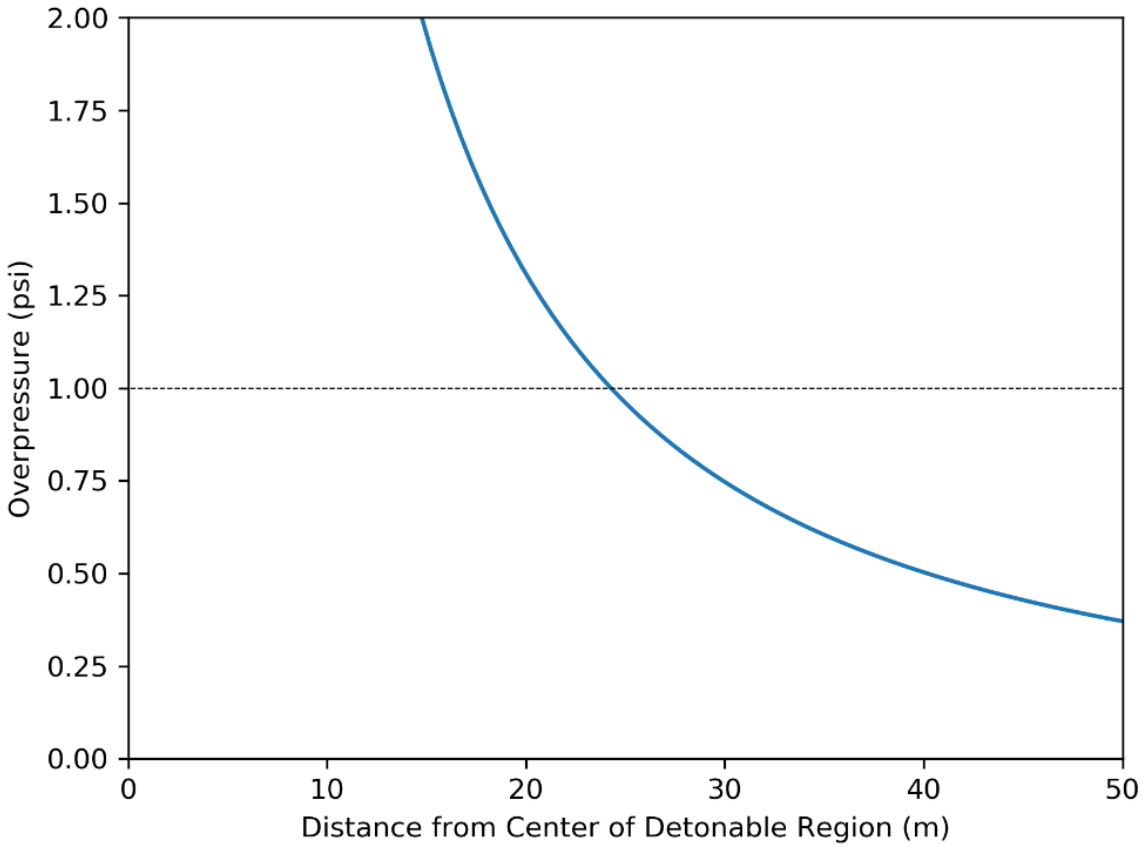

Figure E-12. Scenario 12 Separation Distance Results

Scenario 13

Scenario 13 is a 200.0 mm break with a temperature of 25°C and pressure of 2.23 MPa.

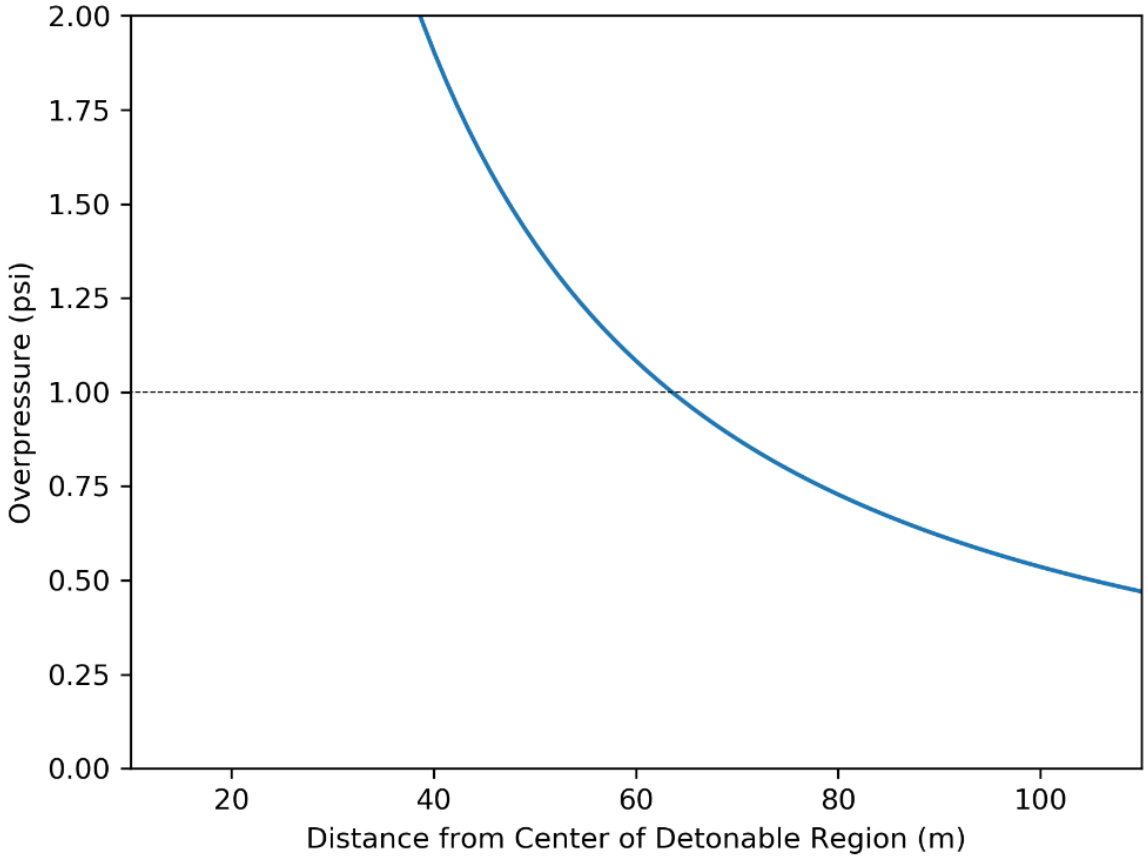

Figure E-13. Scenario 13 Separation Distance Results

Scenario 14

Scenario 14 is a 254.0 mm break with a temperature of 25°C and pressure of 2.23 MPa.

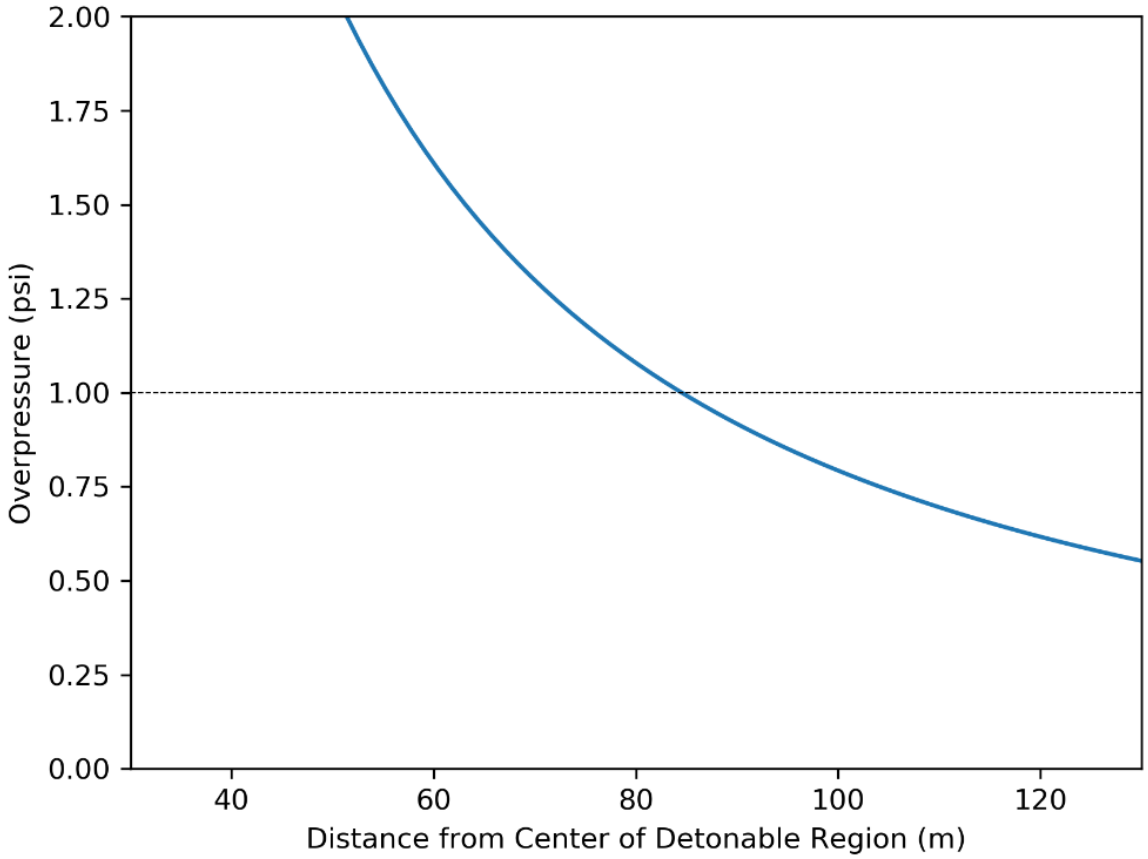

Figure E-14. Scenario 14 Separation Distance Results

Scenario 15

Scenario 15 is a 200.0 mm break with a temperature of 50°C and pressure of 7.0 MPa

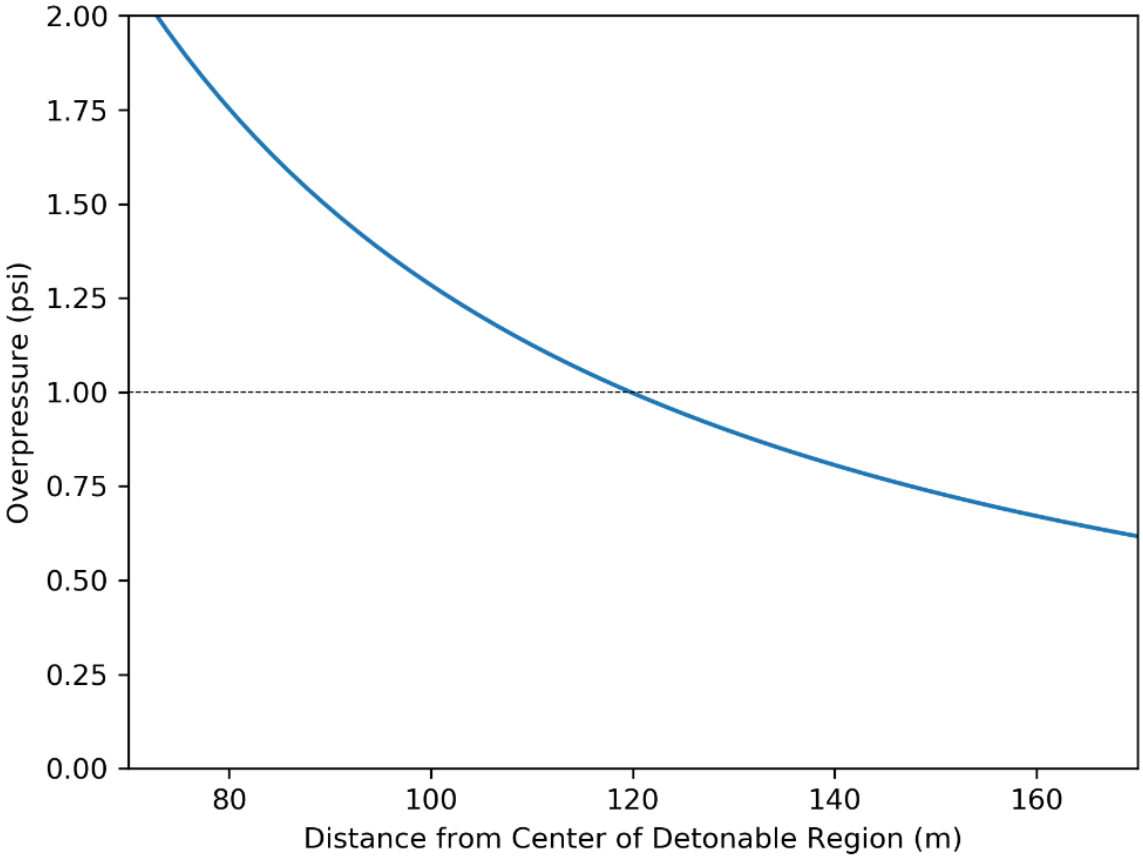

Figure E-15. Scenario 15 Separation Distance Results

APPENDIX F. HYDROGEN CLOUD SEPARATION DISTANCE RESULTS

This appendix contains the detailed separation distance plots for each of the scenarios outlined in Table 6-2.

Scenario 1

Scenario 1 evaluates the detonation of 0.3 kg of hydrogen resulting from a 5 minute leak at 750 nlpm.

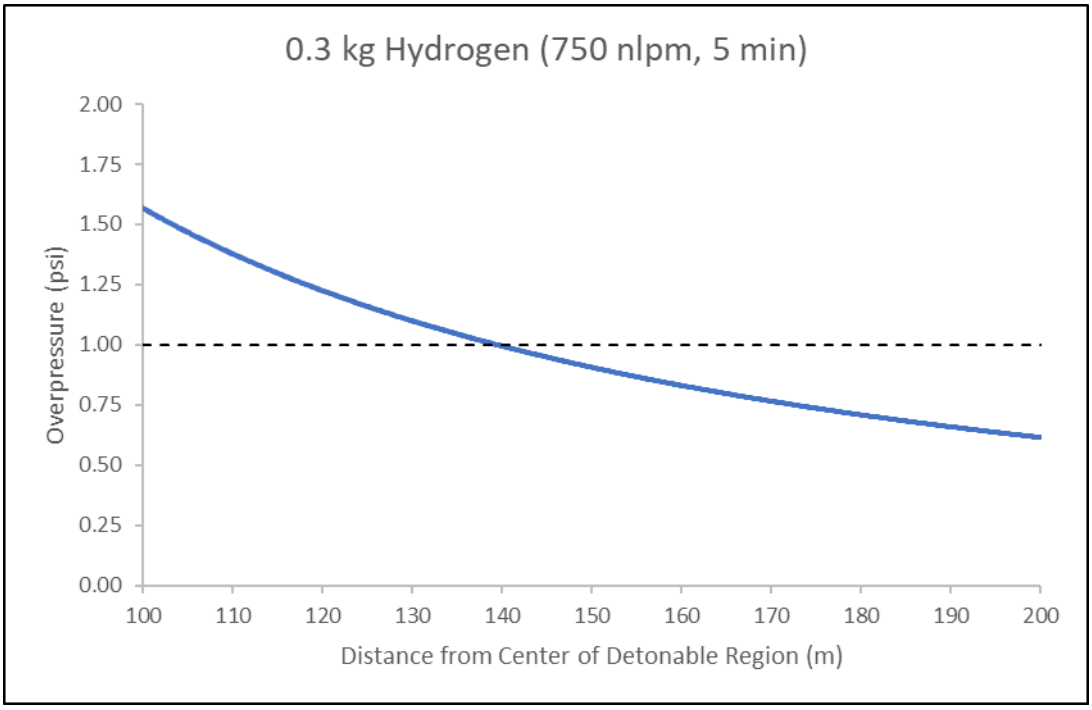

Figure F-1. Scenario 1 Separation Distance Results

Scenario 2

Scenario 2 evaluates the detonation of 0.7 kg of hydrogen resulting from a 10 minute leak at 750 nlpm.

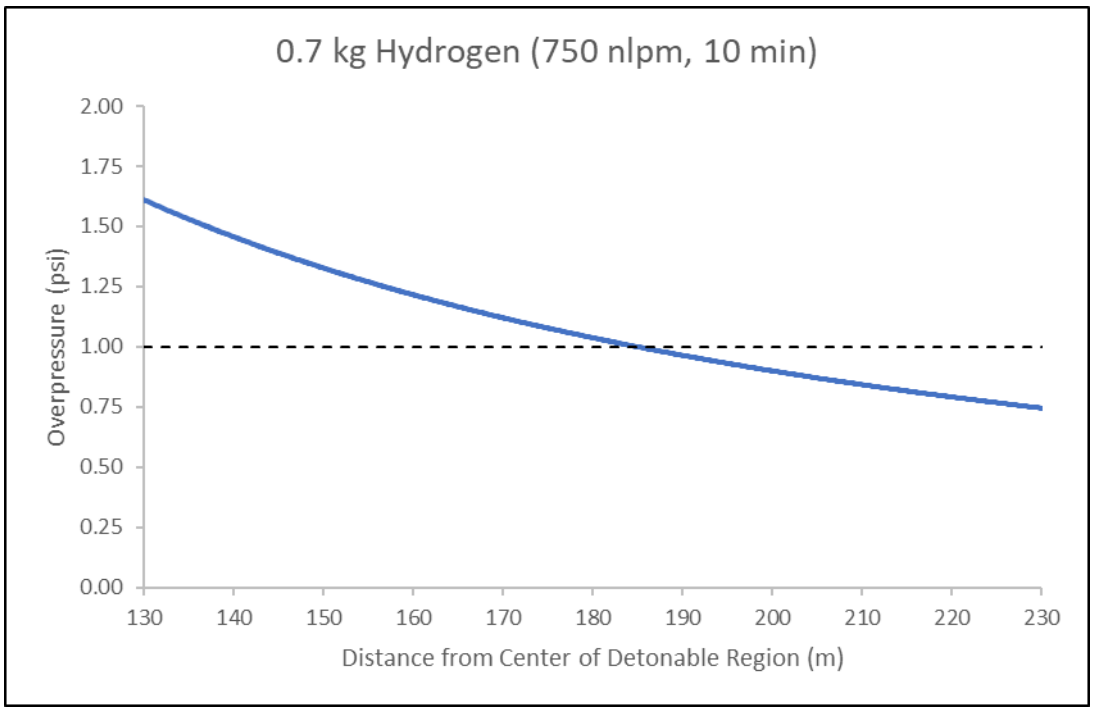

Figure F-2. Scenario 2 Separation Distance Results

Scenario 3

Scenario 3 evaluates the detonation of 1.3 kg of hydrogen resulting from a 20 minute leak at 750 nlpm.

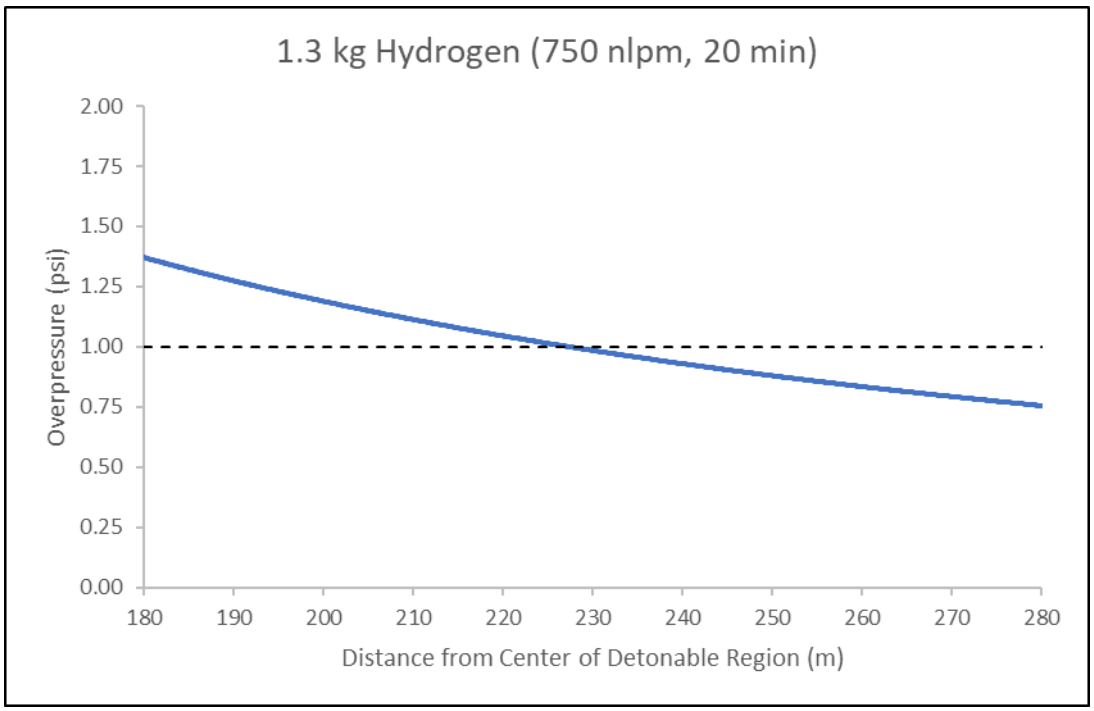

Figure F-3. Scenario 3 Separation Distance Results

Scenario 4

Scenario 4 evaluates the detonation of 2 kg of hydrogen resulting from a 30 minute leak at 750 nlpm.

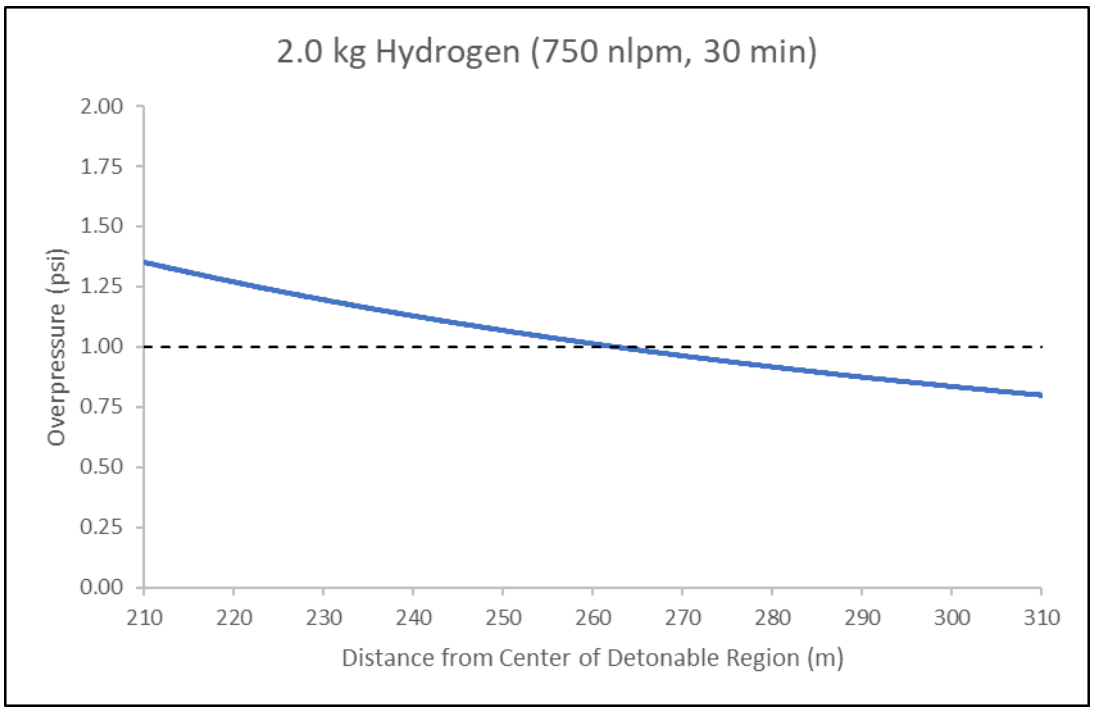

Figure F-4. Scenario 4 Separation Distance Results

Scenario 5

Scenario 5 evaluates the detonation of 4 kg of hydrogen resulting from a 60 minute leak at 750 nlpm.

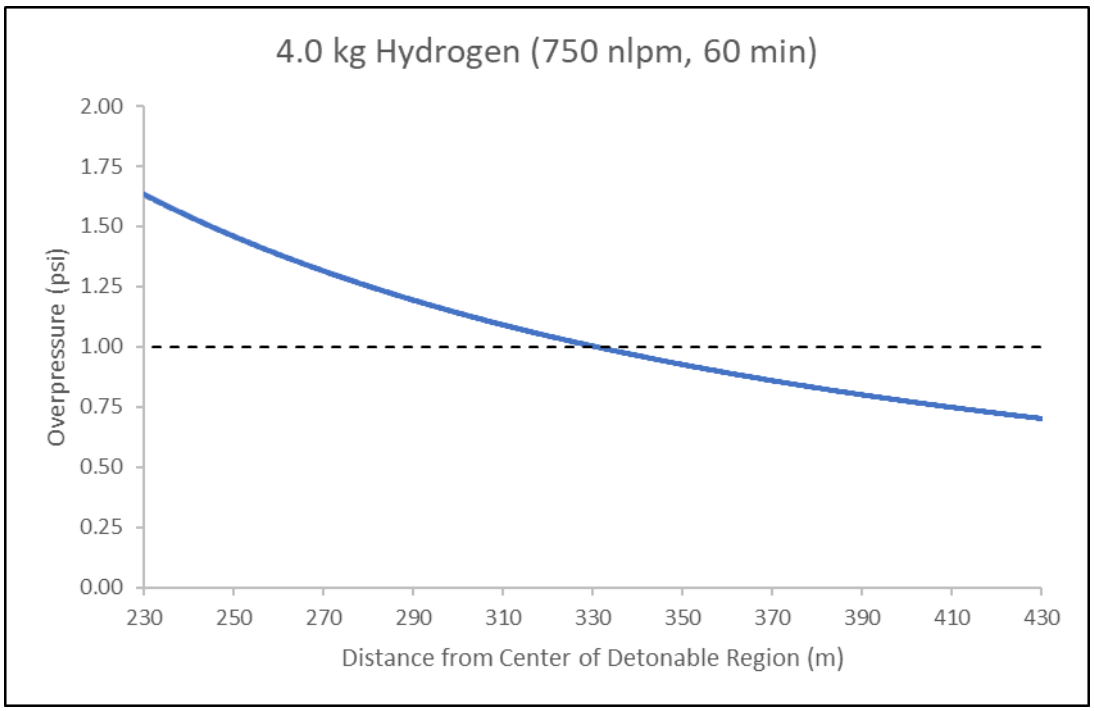

Figure F-5. Scenario 5 Separation Distance Results

Scenario 6

Scenario 6 evaluates the detonation of 8.1 kg of hydrogen resulting from a 120 minute leak at 750 nlpm.

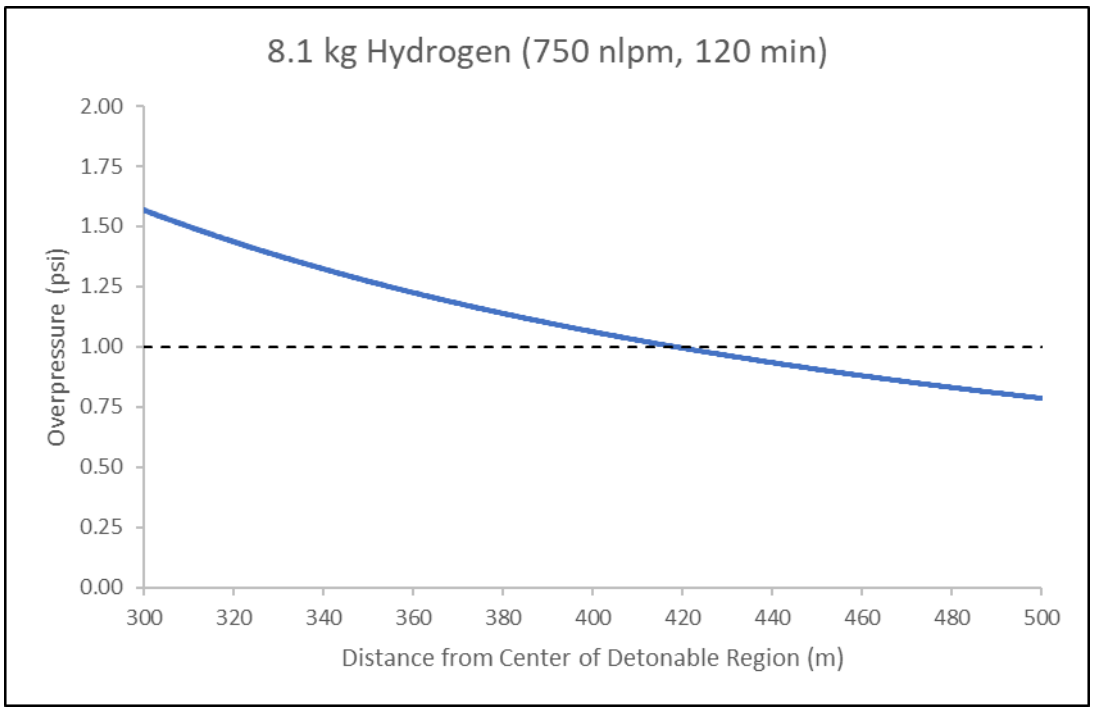

Figure F-6. Scenario 6 Separation Distance Results

Scenario 7

Scenario 7 evaluates the detonation of 0.5 kg of hydrogen resulting from a 5 minute leak at 1,223 nlpm.

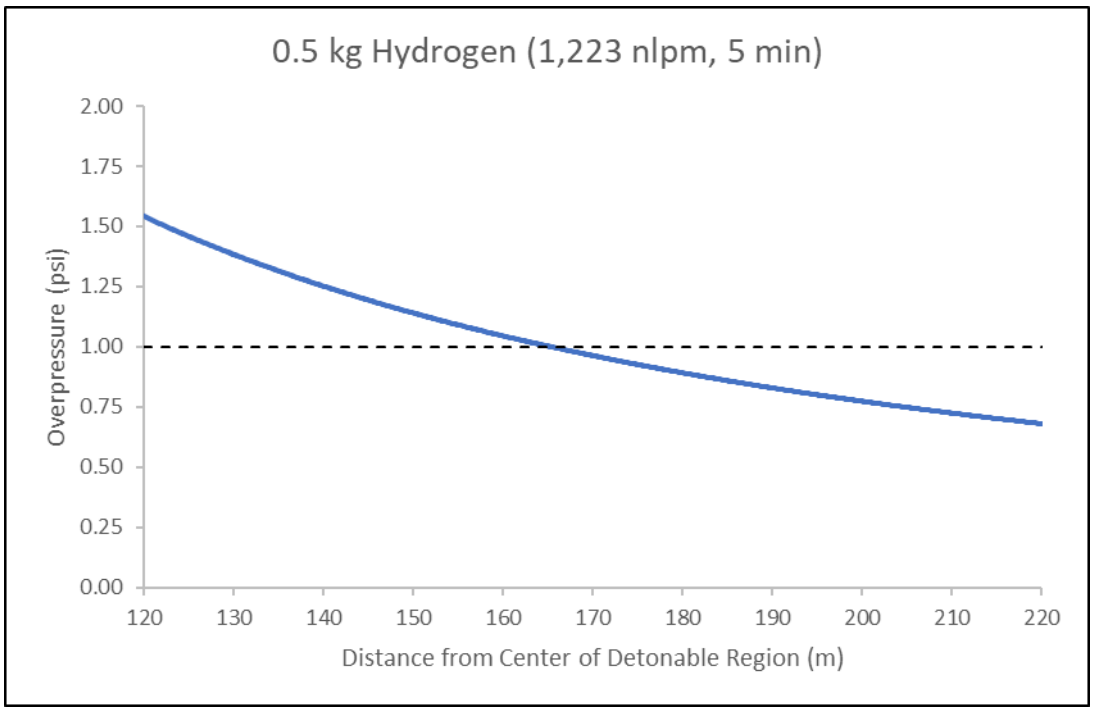

Figure F-7. Scenario 7 Separation Distance Results

Scenario 8

Scenario 8 evaluates the detonation of 1.1 kg of hydrogen resulting from a 10 minute leak at 1,223 nlpm.

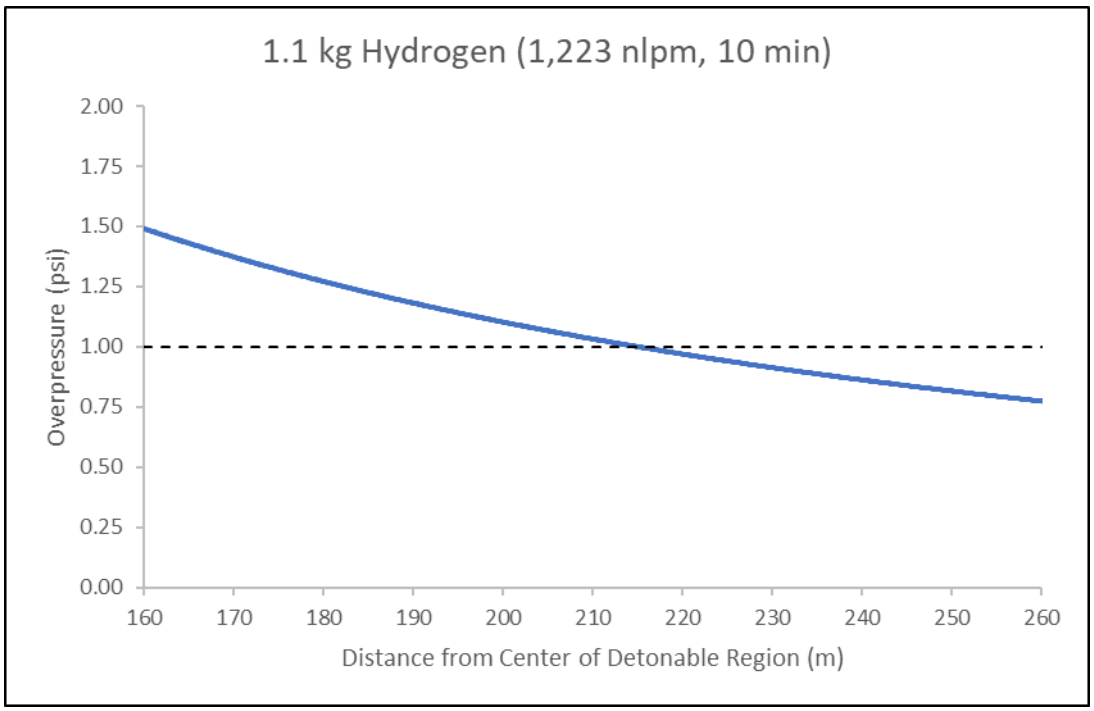

Figure F-8. Scenario 8 Separation Distance Results

Scenario 9

Scenario 9 evaluates the detonation of 2.2 kg of hydrogen resulting from a 20 minute leak at 1,223 nlpm.

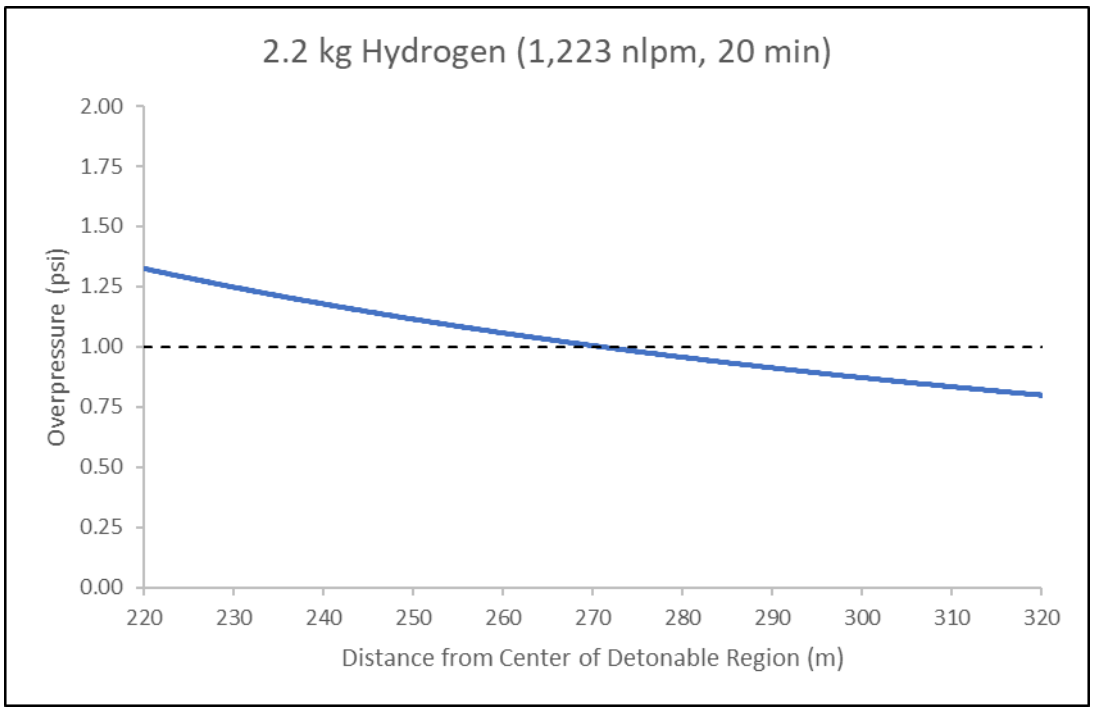

Figure F-9. Scenario 9 Separation Distance Results

Scenario 10

Scenario 10 evaluates the detonation of 3.3 kg of hydrogen resulting from a 30 minute leak at 1,223 nlpm.

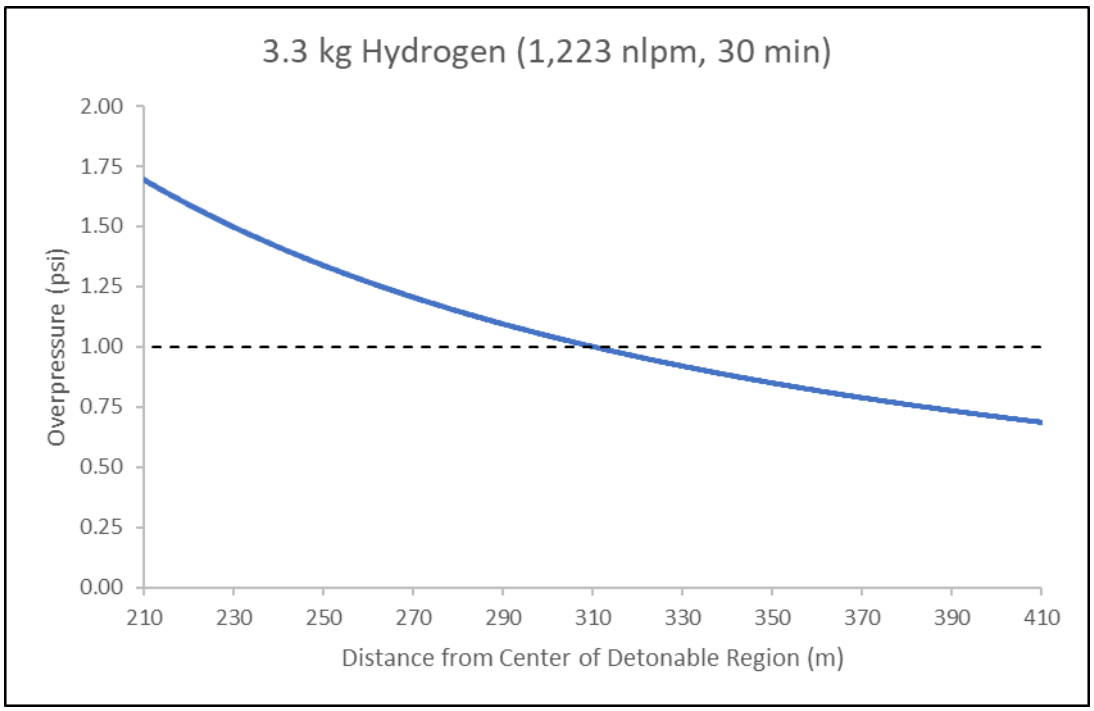

Figure F-10. Scenario 10 Separation Distance Results

Scenario 11

Scenario 11 evaluates the detonation of 6.6 kg of hydrogen resulting from a 60 minute leak at 1,223 nlpm.

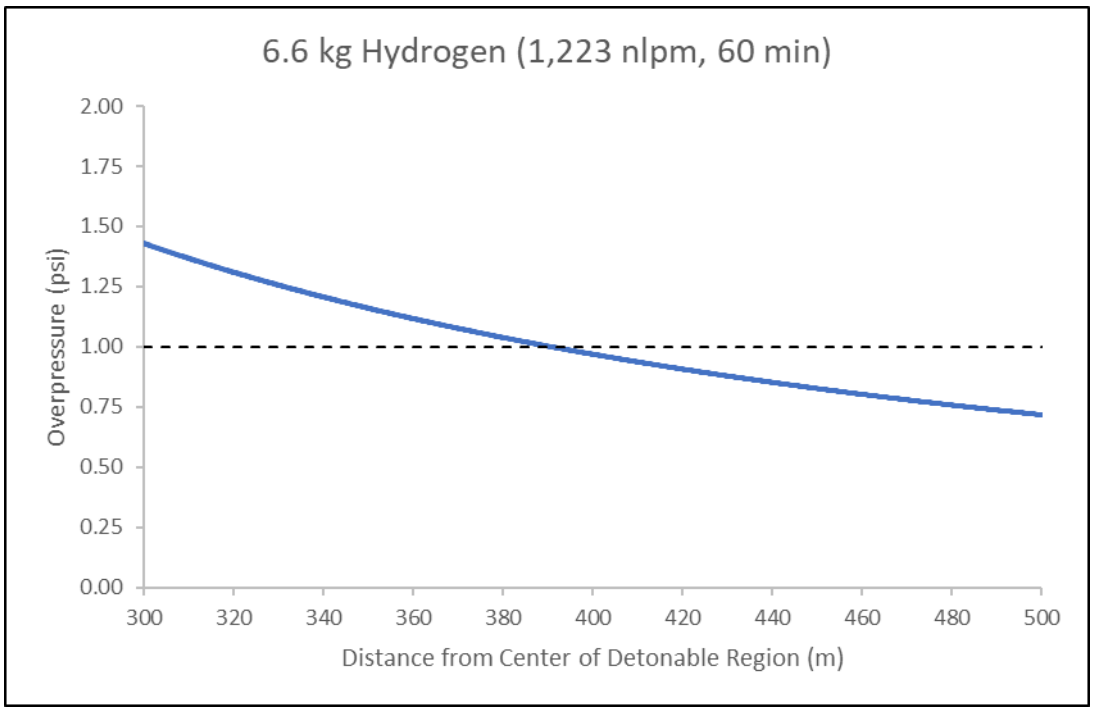

Figure F-11. Scenario 11 Separation Distance Results

Scenario 12

Scenario 12 evaluates the detonation of 13.2 kg of hydrogen resulting from a 120 minute leak at 1,223 nlpm.

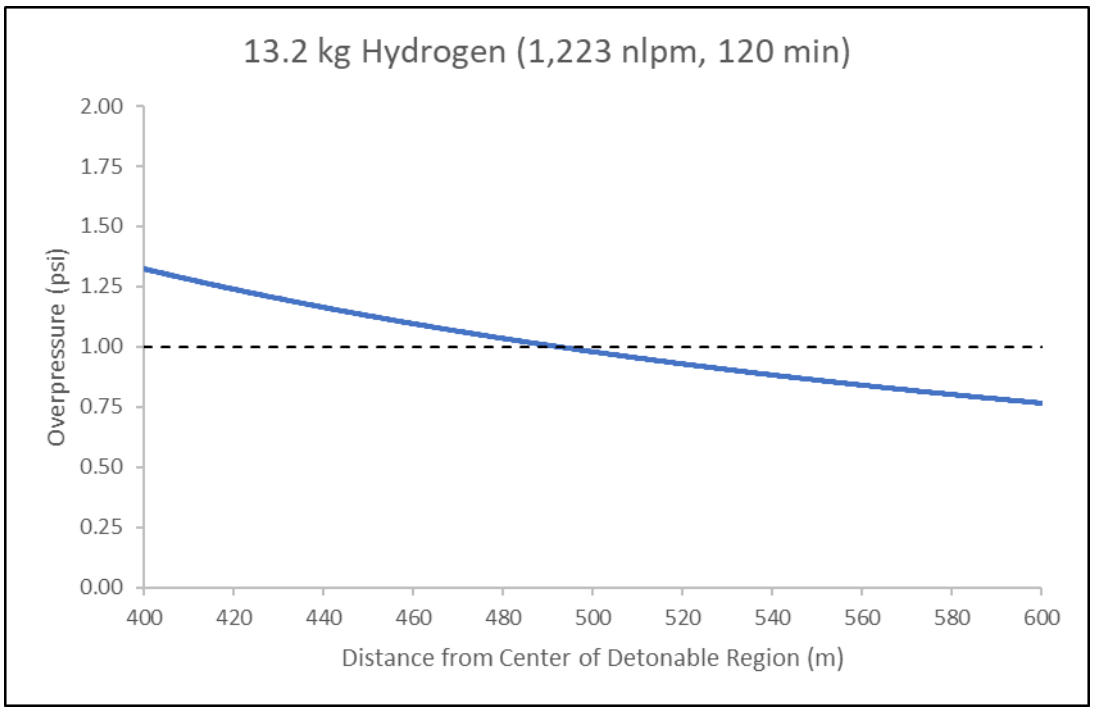

Figure F-12. Scenario 12 Separation Distance Results

This page left blank

DISTRIBUTION

Email—Internal

Name	Org.	Sandia Email Address
Dusty Brooks	08853	dbrooks@sandia.gov
Austin Baird	08854	arbaird@sandia.gov
Brian Ehrhart	08854	bdehrha@sandia.gov
Austin Glover	08854	amglove@sandia.gov
Chris LaFleur	08854	aclafle@sandia.gov
Scott Sanborn	08854	sesanbo@sandia.gov
Technical Library	01977	sanddocs@sandia.gov

Email—External (encrypt for OUO)

Name	Company Email Address	Company Name
Cristian Rabiti	cristian.rabiti@inl.gov	Idaho National Laboratory
Kurt Vedros	kurt.vedros@inl.gov	Idaho National Laboratory

This page left blank

This page left blank

Sandia National Laboratories is a multimission laboratory managed and operated by National Technology & Engineering Solutions of Sandia LLC, a wholly owned subsidiary of Honeywell International Inc. for the U.S. Department of Energy's National Nuclear Security Administration under contract DE-NA0003525.